

CONTINGENCY SEVERITY ANALYSIS USING LINEARIZED
FLOW BOUND ESTIMATES ; THEORY AND
NUMERICAL EXPERIENCE

by

John Wing Mao Cheng, B.Eng.(Sask.)

A thesis submitted to the Faculty of Graduate Studies and Research
in partial fulfillment of the requirements for the degree of
Master of Engineering.

Department of Electrical Engineering,

McGill University,

Montreal, Canada.

September, 1984..

© J.W.M. Cheng, 1984

ABSTRACT

This thesis is concentrated on the derivation and testing of a contingency severity analysis technique using bound estimates of the contingency real power flows. A series of 'contingency filters' are constructed based on different types of bound estimates, i.e. from conservative to tight bounds. Each filter classifies an incoming contingency as either 'critical', 'non-critical' or 'uncertain', depending on the relation of the bounds compared to the corresponding security limits of the real power flows. The 'critical' contingencies will be selected for detailed analysis and the 'non-critical' will be filtered out. Only the 'uncertain' contingencies are submitted to the next filter, where a set of tighter bounds are used to evaluate the status of the contingencies. The final filter is a DC load flow simulation which calculates the exact solutions.

The performance of each filter, in terms of their time efficiencies and classification efficiencies are investigated. Five IEEE testing systems are used to examine and demonstrate the performances of these filters when they are applied to different system sizes and different loading conditions. Some newly proposed contingency selection algorithms based on the results from the filtering process are also tested. It is shown that these algorithms perform very effectively and reliably.

RÉSUMÉ

Cette thèse présente une technique d'analyse de la sévérité des pannes sur un réseau électrique, et en fait l'essai. Au lieu de calculer au long les transits de puissance réelle d'après-défaut, on fournit très rapidement des intervalles contenant ces variables. Une chaîne de telles étapes, ou 'filtres', est construite, produisant des intervalles de plus en plus étroites. Chaque filtre fait le tri des pannes en trois catégories, d'après les positions des intervalles par rapport aux bornes dues aux limitations physiques. Les pannes 'critiques' sont retenues pour une analyse ultérieure, et l'on pourra négliger les pannes 'non-critiques'. Seulement les pannes 'incertaines' alimenteront le prochain filtre, plus sélectif. Le calcul exacte des puissances réelles constitue le dernier, mais n'est appelé que s'il est requis. Un modèle linéarise (DC load flow) est utilisé pour ce calcul.

Les critères de comparaison des filtres sont le temps de calcul et l'efficacité à détecter les états définitifs des pannes. Ces filtres sont testés sur différents modèles de réseaux, de différentes grandeurs et à différents niveaux de charge. Cinq systèmes d'essais de l'IEEE sont retenus pour ces fins. De nouveaux algorithmes de sélection des pannes, basés sur ces résultats, sont évalués ; l'étude démontre qu'ils sont très rapides et fiables.

ACKNOWLEDGEMENTS

I would like to express my utmost gratitude and appreciation to my supervisor, Dr. F.D. Galiana, for his initiative, expert guidance, continuous assistance and friendship throughout all stages in this research.

I am also thankful to Prof. B.J. Gevay and Mrs. P. Hyland from the Department of Electrical Engineering for their hospitality and kindness during my stay at McGill. Special thanks are extended to Mrs. Hyland for her superb job of typing the second half of the manuscript.

Special appreciations are extended to all my colleagues and friends at McGill, in particular Messrs. Ranendra Ponrajah, Maurice Huneault, Rodolfo Calderon-Giron and Danny Fok for their advices, encouragements and sincere friendships. Especially to Mr. R. Ponrajah, who has spent his valuable time in proof-reading the text and Mr. M. Huneault, who also has spent time in reading the manuscript and gracefully translating the abstract.

The financial support from NSERC, FCAC and the award of the McGill Summer Fellowship in 1984 are all gratefully acknowledged.

Finally, I would like to express my heartfelt thanks to my dear wife, Mable, for her faith, understanding and consistent encouragements during the past twenty months of my stay at McGill.

TABLE OF CONTENTS

	<u>Page</u>
ABSTRACT	1
RESUME	11
ACKNOWLEDGEMENTS	iii
TABLE OF CONTENTS	iv
LIST OF TABLES	viii
LIST OF FIGURES	x
LIST OF SYMBOLS	xiii
LIST OF ABBREVIATIONS	xix
CHAPTER I INTRODUCTION	1
1.1 Power System Security	1
1.2 Contingency Analysis, An Introduction	3
1.2.1 Definition of Contingency Analysis	3
1.2.2 Applications of Contingency Analysis in Security Evaluations	4
1.2.3 Requirements of Evaluation Methods	5
1.3 Automatic Contingency Selection	6
1.4 The Present Study : Contingency Filtering Using Linearized Flow Bound Estimates	8
1.5 Outline of the Thesis	9
CHAPTER II REVIEW OF STEADY STATE CONTINGENCY ANALYSIS AND AUTOMATIC CONTINGENCY SELECTION METHODS IN POWER SYSTEMS	12
2.0 Introductory Remark	12
2.1 Part I : Review of Steady State Contingency Analysis Methods	12
2.1.0 Focus of This Review	12
2.1.1 Classification of Steady State Contingency Analysis Methods	13
2.1.2 Point-Wise Approach	14
2.1.2.1 General Algorithm	14
2.1.2.2 Distribution and Shift Factors Methods	16

Page

2.1.2.3	Z-Matrix Methods	16
2.1.2.4	Decoupled Load Flow Methods	16
2.1.2.5	Compensation Methods	18
2.1.2.6	Sensitivity Matrix Methods	18
2.1.2.7	Concentric Relaxation Method	19
2.1.2.8	Discussion	19
2.1.3	Region-Wise Approach	21
2.1.3.1	Definition of the Secure Region	21
2.1.3.2	Set-Theoretic Approach Methods	21
2.1.3.3	Pattern Recognition Methods	26
2.1.3.4	Discussion	26
2.2	Part II : Review of Automatic Contingency Selection Methods	28
2.2.0	Introductory Remarks	28
2.2.1	Filtering Concept of ACS	29
2.2.1.1	Filtering Criteria	29
2.2.1.2	Filtering Strategies	30
2.2.2	ACS Methods Based on a Scalar Performance Index	33
2.2.2.1	General Concept	33
2.2.2.2	Defining a General Form of a Scalar Performance Index	35
2.2.2.3	Summary of ACS Methods Based on a SPI	37
2.2.2.4	Discussion	40
2.2.3	ACS Methods Based on a Vector Performance Index	44
2.2.3.1	General Concept	44
2.2.3.2	Summary of ACS Methods Based on a VPI	46
2.2.3.3	Discussion	47

CHAPTER	III	CONTINGENCY FILTERING BASED ON LINEARIZED FLOW BOUND ESTIMATES; THEORY AND COMPUTATIONAL CONSIDERATIONS	50
	3.0	Introductory Remarks	50
	3.1	Basic Concept	51
	3.1.1	Contingency Flows Calculated from Base Case Flows	51
	3.1.2	Bounding Contingency Flows by Bounding the LODF	52
	3.1.3	Safe, Unsafe and Uncertain Contingency Flows	53
	3.1.4	Critical, Non-critical and Uncertain Contingencies	55
	3.1.5	Contingency Filters	55
	3.2	Derivation of Bound Estimates on the LODF	57
	3.2.1	Derivation of the LODF	57
	3.2.2	Bounding the LODF in Terms of x_{jk} and $x_{lm/jk}$	61
	3.2.3	Resistive Network Interpretation of $x_{lm/jk}$ and x_{jk}	63

3.2.4	Extreme Bounds on $x_{lm/jk}$ and x_{jk}	68
3.2.5	Tighter Bounds on the Input Resistance (x_{jk})	72
3.2.6	Tighter Bounds on $x_{lm/jk}$, the 'Transfer Resistance'	82
3.2.6.1	Type 1 Bounds on $x_{lm/jk}$	82
3.2.6.2	Type 2 Bounds on $x_{lm/jk}$	101
3.3	Contingency Filter Arrangement	103
3.4	Ranking and Selection Algorithms	106
3.5	Computational Considerations	109
3.5.1	Usage of the 'Link List' and 'Sparspack'	109
3.5.2	Automatic Loop Searcher	111
3.5.3	Retained Network Builder	117
3.5.4	Computational Algorithm	119
 CHAPTER IV	 CONTINGENCY FILTERING USING LINEARIZED FLOW BOUND ESTIMATES; NUMERICAL EXPERIENCE	 121
4.0	Introductory Remarks	121
4.1	Numerical Results of Different Bound Estimates on x_{jk}	122
4.1.1	Results from the IEEE 24-Bus System. An Example	123
4.1.2	Results of the x_{jk} Bounds Based on One Closed Loop	127
4.1.3	Results of the x_{jk} Bounds Based on Two Closed Loops	129
4.1.4	Discussion	131
4.2	Numerical Results of Bound Estimates on $x_{lm/jk}$, LODF and Contingency Flows	132
4.2.0	Introductory Remarks	132
4.2.1	Example 1	134
4.2.2	Example 2	139
4.3	Filter Performances	141
4.3.0	Introductory Remarks	141
4.3.1	Identification Efficiencies of Filters	142
4.3.2	Computational Efficiency of Filters	151
4.3.3	Performances under Different Loading Conditions	154
4.4	Performance of the Proposed Selection and Ranking Algorithms	155
4.4.1	Method A : Selection Based on the Number of Uncertain Flows	155
4.4.2	Method B : Selection Based on the Relative Overload Expectation	157
4.4.3	Discussion	158
4.5	DC and AC Load Flow Simulations Comparison	160

CHAPTER	V	CONCLUSIONS AND RECOMMENDATIONS FOR FUTURE RESEARCH	161
	5.1	Conclusions	161
	5.2	Recommendations for Future Research	166
BIBLIOGRAPHY AND REFERENCES			169
APPENDIX	A	DERIVATION OF A DC LOAD FLOW	178
APPENDIX	B	DATA OF FIVE IEEE SYSTEMS	182

LIST OF TABLES

<u>Table</u>		<u>Page</u>
2.1	Summary of ACS Methods Based on SPI	38
3.1	$x_{lm/jk}^{lc}$ as Functions of the Common Node	96
3.2	Filtering Scheme # 1	104
3.3	Filtering Scheme # 2	105
3.4	Checking Procedures of the Automatic Loop Searcher, Example 1	113
3.5	Checking Procedures of the Automatic Loop Searcher, Example 2	115
4.1	Selected Results of the Calculated Bounds of x_{jk} on the IEEE 24-bus System	124
4.2	Results of x_{jk} Bounds for the IEEE Testing Systems with One Closed Loop	128
4.3	Results of x_{jk} Bounds for the IEEE Testing Systems with Two Closed Loops	130
4.4	Selected Results on the Bound Estimates of Example 1	136
4.5	Filter Performances of the Outage of Line # 7 in the 30-bus, 41-line System under Normal Load	138
4.6	Selected Results on the Bound Estimates of Example 2	139
4.7	Filter Performances of the Outage of Line # 7 in the 30-bus, 41-line System under Light Load	141
4.8	CPU Time (ms) of Different Filtering Schemes	152
4.9	Computational Efficiency of Selection Method A Based on the Total CPU Time (ms)	157

TablePage

4.10 Computational Efficiency of Selection Method B
Based on the Total CPU Time (ms)

158

4.11 Ranking of Contingencies According to Methods
A and B

159

LIST OF FIGURES

<u>Figure</u>		<u>Page</u>
1.1	Hierarchical Layout of Power System Security Study	2
2.1	General Algorithm of Contingency Analysis using Point-wise Approach	15
2.2	'Normal' Region	23
2.3	'Contingency' Region	23
2.4	'Secure' Region	23
2.5	One-stage Filtering Strategy	31
2.6	Multi-stage Filtering Strategy	32
2.7	General Algorithm of ACS Methods Based on a SPI	34
2.8	General Algorithm of ACS Methods Based on a VPI	45
3.1	Examples of Safe, Unsafe and Uncertain Contingency Flows	54
3.2	Two-port Resistive Network	66
3.3	Extreme Connection for $\hat{x}_{lm/jk}^0$	69
3.4	Extreme Connection for $\tilde{x}_{lm/jk}^0$	69
3.5	Extreme Connection for \tilde{x}_{jk}^0	71
3.6	Extreme Connection for \hat{x}_{jk}^0	71
3.7	Network Subdivision	73
3.8	N_1 with Tie-lines Opened	75
3.9	N_1 with Tie-lines Shorted	75
3.10	Islanding Line	81
3.11	Semi-independent Line	81
3.12	Network Subdivision for $x_{lm/jk}$ Bound Evaluations	84

<u>Figure</u>		<u>Page</u>
3.13	Extreme Connection Pattern for $\hat{x}_{lm/jk}^{1a}$	86
3.14	Extreme Connection Pattern for $\tilde{x}_{lm/jk}^{1a}$	86
3.15	Extreme Connection Pattern for $(x_{lm/jk}^{1b})_1$	91
3.16	Extreme Connection Pattern for $(x_{lm/jk}^{1b})_2$	92
3.17	Extreme Connection Pattern for $(x_{lm/jk}^{1b})_3$	93
3.18	Network Subdivision for the Triangular Case	95
3.19	Extreme Connection Pattern for $\tilde{x}_{lm/jk}^{1c}$	98
3.20	Extreme Connection Pattern for $(x_{lm/jk}^{1c})_1$	99
3.21	Extreme Connection Pattern for $(x_{lm/jk}^{1c})_2$	100
3.22	Network Subdivision for Type 2 Bounds of $x_{lm/jk}$	102
3.23	A 6-node Example Network	112
3.24	Connection Tree Structure of the 6-node Example Network	112
4.1	IEEE 24-Bus One-Line Diagram	126
4.2	Average \bar{x}_{jk} Values for the Five IEEE Systems Based on One and Two Closed Loops	133
4.3	Time Comparison of Evaluating x_{jk} Bound for the IEEE Systems Based on One and Two Closed Loops	133
4.4a	Filter Performances on IEEE 14-Bus System Using Type 1 Bound of x_{jk}	144
4.4b	Filter Performances on IEEE 14-Bus System Using Type 2 Bound of x_{jk}	144
4.5a	Filter Performances on IEEE 24-Bus System Using Type 1 Bound of x_{jk}	145
4.5b	Filter Performances on IEEE 24-Bus System Using Type 2 Bound of x_{jk}	145

<u>Figure</u>		<u>Page</u>
4.6a	Filter Performances on IEEE 30-Bus System Using Type 1 Bound of x_{jk}	146
4.6b	Filter Performances on IEEE 30-Bus System Using Type 2 Bound of x_{jk}	146
4.7a	Filter Performances on IEEE 57-Bus System Using Type 1 Bound of x_{jk}	147
4.7b	Filter Performances on IEEE 57-Bus System Using Type 2 Bound of x_{jk}	147
4.8a	Filter Performances on IEEE 118-Bus System Using Type 1 Bound of x_{jk}	148
4.8b	Filter Performances on IEEE 118-Bus System Using Type 2 Bound of x_{jk}	148
4.9	Filter Performances on IEEE 118-Bus System Under Medium Load	156
4.10	Filter Performances on IEEE 118-Bus System Under Light Load	156

LIST OF SYMBOLS

b	A number used to label different filters.
b_n	A number used to label different bound types.
\underline{B}	DC Jacobian matrix (nxn) .
$\hat{\underline{B}}_r$	Conductance matrix of N_1 where all tie-line conductances are neglected, (nrn-1) x (nrn-1) .
$\hat{\underline{B}}_r$	Conductance matrix of N_1 where all tie-line conductances are included, (nrn) x (nrn) .
CF^b	Type b contingency filter. \
\underline{e}_{jk}	A zero vector of dimension n by 1 with 1 and -1 at positions j and k respectively.
\underline{e}_{rjk}	A zero vector of dimension nrn by 1 with 1 and -1 at positions corresponding to nodes j and k of the original network.
$f_1(\cdot)$	A real value function of the system state variables.
i_{lm}	Current flow through branch (l,m) .
j,k	Ending nodes of the outaged branch (j,k) .
l,m	Ending nodes of any arbitrary branch (l,m) .
\underline{I}	Nodal current injection vector.
I_j, I_k	Nodal current injections at nodes j and k respectively.
J	Scalar performance index.

K_1^{lim}	Limits of the angle difference between the ending nodes of line 1 .
m	Total number of tie-line nodes in N_2 .
M_1	Retained network used to derive $x_{lm/jk}$ bounds (only contains nodes j, k, l, m) .
M_2	Remaining network, full network excluding M_1 .
$n+1$	Total number of buses.
n_{rn}	Total number of nodes in the retained network N_1 .
N_J	Total number of terms considered in a SPI evaluation.
N_1	Retained Network used to derive x_{jk} bounds.
N_2	Remainder Network, full network excluding N_1 .
NL	Total number of lines in the system.
NU	Total number of uncertain flows.
NTC	Total number of single line outage contingencies.
p	Exponent term.
\underline{P}	Real power injection vector.
P_1	Real power flow of line 1 .
P_{lm}, P_{jk}	Base case real power flows of branch (1,m) and branch (j,k) respectively.

$P_{lm/jk}$

Contingency real power flow of branch (1,m) while branch (j,k) is out of service.

 P_i

Same as P_1 .

 P_i^{lim}

Real power flow limit of line 1.

 r_1

Unit of capacity to be removed from line 1.

ROE

Relative Overload Expectation.

 TN_1

Tie-line node 1 in N_2 .

 \underline{V}

Nodal voltage vector.

V_1, V_m, V_j, V_k, V_c Voltage at nodes 1, m, j, k, c respectively.

 w_1

Weighting factor.

 w_m

Optimum weighting factor.

 w_{os}

Operation selected weighting factor.

 w_s

Element corresponding to line 1 in the sensitivity matrix.

 $x_{lm/jk}$

$e_{lm}^T B^{-1} e_{jk}$, the transfer resistance.

$(x_{lm/jk})^r$

A speculated extreme value of $x_{lm/jk}$, r is used to denote different speculated values.

 x_{lmjk}

Input resistance of the network while current injections are applied at both nodes j and k , and nodes l and m .

 x_{jk}

$\underline{e}_{jk}^T \underline{B}^{-1} \underline{e}_{jk}$, the input resistance.

 \bar{x}_{jk}

The interval of the x_{jk} bounds normalized by its line reactance.

 y_{rs}

Admittance value of branch (r,s) where r and s can be any two of the following nodes : j, k, l, m .

 y_{rs}^{new}

Adjusted value of y_{rs} .

 \underline{Y}

Conductance matrix of the resistive network.

yy_j, yy_k, yy_l, yy_m Equivalent connection elements from nodes j, k, l, m of M_1 to M_2 respectively.

 y_{eq}

Equivalent admittance of $yy_j, yy_l, y_{lm}, yy_m, yy_k$ connected in series.

 y_1, y_2, y_3

Diagonal elements of the conductance matrix used to evaluate $x_{lm/jk}$ bounds.

Δy_{jk}

Admittance value to be removed from the outaged branch (j,k) .

 \underline{z}

System state variable vector.

 $z_{lm/jk}, z_{jk/lm}$

Transfer resistance from port (l,m) to port (j,k) and vice versa.

 z_{jk}, z_{lm}

Input resistance looking in from port (j,k) and port (l,m) respectively.

 θ_1

Angle difference between the ending nodes of line 1 .

 $\rho_{lm/jk}$

LODF of branch (l,m) while branch (j,k) is out of service.

 $\underline{\delta}_{base}$

Base case bus phase angle vector.

 $\underline{\delta}_{cont}$

Contingency bus phase angle vector.

 Φ

The set of all the ending nodes of the 'tie-lines' in N_2 .

 α, β, μ, ν

The index sets of the nodes which nodes j,k,l,m are connected to in M_2 .

 \sim

A symbol denotes the minimum value of a variable.

A symbol denotes the maximum value of a variable.

$\cdot T$

Transpose of a vector.

∞

Denote the bound type where all nodes in the system are included in N_1 .

LIST OF ABBREVIATIONS

ACS	Automatic Contingency Selection.
ALS	Automatic Loop Searcher.
CA	Contingency Analysis.
CF	Contingency Filters.
CR	Capture Rate.
FR	False-alarm Rate.
LODF	Line Outage Distribution Factor.
RNB	Retained Network Builder.
ROE	Relative Overload Expectation.
SPI	Scalar Performance Index.
Δ SPI	Change of SPI.
VPI	Vector Performance Index.

CHAPTER I

INTRODUCTION

1.1 Power System Security

Power system operators are occasionally confronted with sudden disturbances, namely equipment malfunctions, line outages due to severe climatic disruptions or operator's switching errors etc. These disturbances upset the equilibrium of the system and sometimes cripple the normal state of operation causing permanent equipment damages and severe interruption of service. The chaotic 1977 New York City blackout was a classical example demonstrating how a series of lightning strokes on the transmission network can trigger such a large scale disruption [Elgerd 1982].

In order to ensure that the electric utility service to be consistent and reliable, a power system must be designed and operated in a 'secure' manner. In general, a power system is said to be 'secure' if it can withstand the occurrences of a set of postulated contingencies without violating any system constraints or causing instability. Otherwise, the system is in a 'vulnerable' or 'insecure' state [Debs et al. 1975]. To improve system performances under stresses and unexpected disturbances, contingencies are anticipated and their impacts are examined. Consequently, feasible and practical remedies are established to avoid or alleviate the damages which can

be caused by the contingencies. These are the objectives of Power System Security studies.

Power system security studies can be summarized in a hierarchical form as shown in Figure 1.1. Two major topics are of prime concern, namely security assessment and security enhancement.

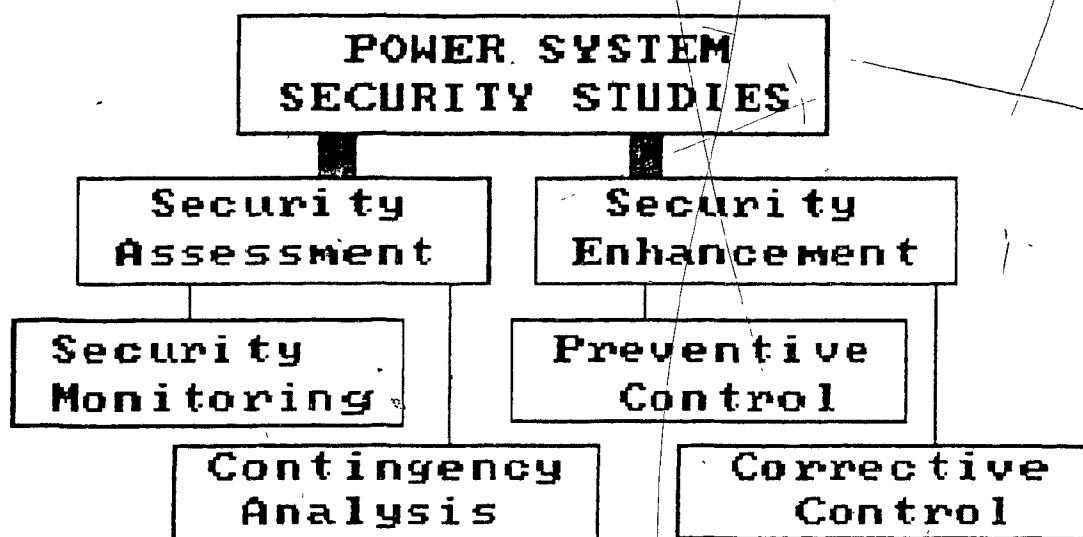


Figure 1.1 Hierarchical Layout of Power System

Security Studies

Security assessment consists of two major functions.

'Security Monitoring' serves to collect and process the system operation data, through telemetry systems and subsequently updating them through the state estimator. 'Contingency Analysis' utilizes the system information to simulate different contingencies in order to predict the post-contingency system conditions. Consequently, crucial events which will put the system in an 'insecure' state can be identified [Debs et al. 1975].

Security enhancement however investigates different control methods and operational strategies, preventive and corrective, to improve the system security, e.g. restoring the system from a 'vulnerable' state to a 'secure' state. Methods which have been commonly employed include security-constrained optimizations (e.g. secure economic dispatch, minimum load curtailment), system parameter adjustments (e.g. network adjustments) etc. [Dy-Liacco 1967, 1970; Hadju et al. 1975].

1.2 Contingency Analysis, an Introduction

1.2.1 Definition of Contingency Analysis

Contingency analysis, the principal topic of this thesis, is a vital evaluation procedure in power system security studies. It evaluates the impact of possible contingencies upon the normal operation of a power system. These contingencies usually include generator outage(s),

line outage(s), sudden loss or increase of load or any combinations of the above. Through the simulations of such contingencies, the post-contingency conditions (e.g. line flows or bus voltages) are checked to see whether any system constraints (e.g. thermal limits of transmission lines or minimum voltage levels) have been violated. The critical ones which will cause overloads, significant voltage degradations or infeasible operations are then identified for further investigations (e.g. security enhancement usages).

1.2.2 Applications of Contingency Analysis in Security Evaluations

In planning, contingency analysis serves as a valuable tool to evaluate all the viable alternatives in order to improve the reliability and security of the future system. In operations, contingency analysis assists the operators to identify potentially dangerous contingencies so that preventive control action(s) can be executed. The most significant contribution of this analysis is to assist planners and operators to systematically recognize some of the 'bottlenecks' in the system. For instance, if the loss of a certain line in the system can trigger a 'cascading outage' or an 'islanding effect', such a contingency will be identified as a 'structural bottleneck' in the system.

1.2.3 Requirements for Evaluation Methods

Contingency analysis is usually accomplished by executing a series of repeated load flow studies on different contingent events, based on one or a set of different operating points. The approach is deterministic (i.e. contingency classified as either secure or insecure), sequential (i.e. one contingent case to be evaluated at a time) and exhaustive (i.e. hundreds or thousands of cases to be examined). Hence, besides the accuracy, the speed requirement of evaluation methods is very crucial.

However, these two requirements are usually hard to be satisfied together. Because of the stringent time imposed on real-time evaluations and the inefficiency of exhaustive simulations for all possible contingencies, the following ideas are usually adopted in various evaluation methods in order to improve the speed performance and yet maintain an acceptable accuracy :

- (1) Using approximate system models, such as the fast decoupled model [Stott 1972,1974] and the DC model [Dhar 1982] instead of the exact AC full model [Tinney et al. 1976], where these simplified models offer acceptable results and require less computational effort.
- (2) Simulating contingencies using compensation methods or the matrix inversion lemma, where Tinney and others [Tinney 1972; Galiana et al. 1975; Alsac et al. 1983] have discussed how these methods

can be applied to simulate outages with better computational efficiency.

- (3) Selecting a small number of contingencies among all possibilities according to their expected severity and/or probability of occurrences, using either the operator's experience or some on-line automatic contingency selection schemes or both. Subsequently, only these selected contingencies will be investigated in detail [Irisarri et al. 1979].

1.3 Automatic Contingency Selection

In practice, the number of contingencies which can cause violations (e.g. overloadings) or serious interruptions (e.g. voltage collapse) in a power system are few. Therefore, if these 'critical' contingencies can be identified and put into a so-called 'contingency list', exhaustive runs of contingency simulations can then be reduced to a manageable number by only considering these 'critical' contingencies. This is particularly valuable to on-line evaluations.

Traditionally, a contingency list is constructed either from the operator's experience or some previous off-line study results. However, as power systems are growing and becoming more complex, even the most experienced operators may overlook some critical contingencies occasionally. Alternatively, a fixed list based on off-line studies fails to recognize the current system conditions which may be significantly different from the previously simulated conditions.

In order to eliminate the discrepancies of the manual and the non-updated types of selection, an adaptive and dynamic selection scheme of constructing the contingency list is desirable [Ejebe et al. 1979]. This new selection scheme is called the Automatic Contingency Selection (ACS) [Ibid]. In this thesis, various ACS methods are classified under two distinct approaches, namely Scalar Performance Index methods (SPI) and Vector Performance Index methods (VPI).

ACS can be thought of as a 'filtering' process. The SPI and VPI methods are basically differentiated by their 'filtering criteria'. SPI uses a scalar quantity as a criterion to rank contingencies according to their expected severity and subsequently selects the higher ranked events. However, VPI uses a vector to evaluate the severity of each contingency and subsequently labels the contingency as 'critical' or 'non-critical'. The 'non-critical' events are therefore filtered out.

Such filtering can be accomplished by a one-stage or a multi-stage strategy. For multi-stage strategy, contingencies are passed through a series of filters, where each one of which identifies the incoming events as either 'critical', 'non-critical' or 'uncertain'. Only the 'uncertain' contingencies are passed on to the next filter for more detailed studies in order to be classified as either 'critical' or 'non-critical'. A detailed description and discussion on these criteria and filtering strategies are presented in part II of the following chapter.

1.4 The Present Study : Contingency Filtering Using Linearized Flow Bound Estimates

This research adopts the contingency severity analysis approach proposed by Galiana [Galiana 1984]. It is basically a VPI based, multi-stage ACS method. Different bound estimates for the contingency flows are used to establish a series of 'contingency filters'. This technique assumes a DC model for the power system and derives the 'Line Outage Distribution Factor (LODF)' [Wood et al. 1984] using the matrix inversion lemma. Since each LODF is invariant with respect to the loading conditions but only depends on the topology and the parameters of the network, some simple topological characteristics are exploited to derive bound estimates for the LODF.

By bounding the LODF, the contingency real power flows (linearized due to the DC model) can also be bounded accordingly. The range of these bounds are gradually constricted in the subsequent filters by expanding the complexity of the filters. The final filter is an exact DC load flow simulation.

Using such bound estimates, contingencies are classified into the following three types at the output of each filter except the final one, namely critical, non-critical and uncertain¹. Only the

1 The definitions of these terms are explained in Chapter III.

uncertain contingencies are submitted to the subsequent filter for further analysis. Consequently, only a few remaining uncertain contingencies are required to be evaluated by a DC load flow simulation because the others are already identified by the previous filters.

The present study concentrates on the following :

- (1) Investigating the effectiveness of each filter, proposed by Galiana [Galiana 1984], in identifying critical contingencies.
- (2) Comparing the computational effort of each filter in terms of their processing speed.
- (3) Comparing the degree of trade-off between (1) and (2).
- (4) Investigating the efficiencies of two newly proposed selection schemes, using the results from the filtering procedures.

1.5 Outline of the Thesis

After reviewing the general background and objectives of this study, the following outlines the organization of the thesis :

CHAPTER II

This is a general review of various approaches used in contingency analysis. The point-wise and region-wise approaches are

presented and discussed. This chapter also reviews the state-of-the-art of the methods used in ACS. The SPI and VPI based methods are also presented and discussed.

CHAPTER III

The theory of contingency filtering using the linearized flow bound estimates is presented. The LODF is derived using the DC load flow model and the matrix inversion lemma. Different bound estimates on the LODF are then developed. Some newly proposed contingency selection algorithms will be introduced. Finally, the computational considerations in terms of programming on the filtering scheme and the selection algorithms are also discussed here.

CHAPTER IV

Numerical experience with the filters derived from the preceeding chapter are tested with the IEEE 14,24,30,57,118 bus systems. Observations on the numerical performances of these filters are presented and evaluated. Selection schemes based on the newly proposed scalar performance indices are also tested.

CHAPTER V

Conclusions and recommendations for future studies are drawn here. It is found that even the most conservative filter is able to identify most of the contingencies (i.e. 'critical' or 'non-critical')

Some filters are found to be not so computationally efficient. However, the proposed selection schemes are shown to be very effective in terms of speed and selection efficiency.

CHAPTER II

REVIEW OF STEADY STATE CONTINGENCY ANALYSIS AND AUTOMATIC CONTINGENCY SELECTION METHODS IN POWER SYSTEMS

2.0 Introductory Remarks

This chapter is divided into two parts. The first part reviews various evaluation methods proposed for Contingency Analysis (CA) over the past two decades. The second part reviews the state-of-the-art of Automatic Contingency Selection (ACS) methods.

2.1 Part I : Review of Steady State Contingency Analysis Methods

2.1.0 Focus of this Review

There are basically two kinds of contingency studies used by system planners and engineers, namely deterministic and probabilistic studies. Deterministic studies are widely employed for both planning investigations and operational applications, where the uncertainties of the system variables (e.g. load deviations) are ignored. Probabilistic studies however have mainly been applied to reliability and stochastic studies in planning evaluations only [Billinton 1970; Aboytes 1978], where probabilistic and statistical methods are implemented to account for the system uncertainties. The focus of this review is concentrated on the deterministic studies.

Due to different impacts caused by different stages of a contingency, contingency analysis can further be divided into three distinct modes, namely 'transient', 'dynamic' and 'steady state' analyses [Debs et al. 1975]. In the perspective of the present review, attention is focused on the 'steady state' analysis methods only. Such an analysis assumes that the power system has survived the transient and dynamic states and the concern is to check for any violations in the steady state condition.

2.1.1 Classification of Steady State Contingency Analysis Methods

Over the past two decades, many deterministic evaluation techniques for steady state contingency analysis have been proposed. In general, all of these different techniques can be classified under two distinct approaches : point-wise and region-wise.

Point-wise approach evaluates the system security at one operating point, the so-called 'base case', for each one of a list of contingencies one at a time. Should the condition of this base case change (e.g. load deviation), the system security will have to be evaluated at the new base case again. Examples include the distribution factors methods [MacArthur 1961; Limmer 1969], the decoupled load flow methods [Uemura 1972,1973; Stott et al. 1974] and the concentric relaxation methods [Zaborszky et al. 1980] etc.

Region-wise approach utilizes the system constraints, e.g. the load flow equations and the system functional inequalities, to identify a 'secure' region for one or more contingencies. The system security under different operating points can thus be evaluated by checking whether such operating points are within the corresponding 'secure' region. Examples include the pattern recognition methods [Pang et al. 1974], the set-theoretic approach [Hnyilicza et al. 1975], the security corridors concept [Banakar et al. 1981] etc.

2.1.2 Point-wise Approach

2.1.2.1 General Algorithm

The general algorithm of this approach is explained with Figure 2.1. System data are read from the beginning. These include the system structure, parameters, operation limits, a contingency list and the base case(s). In operations, the base case is the current operating condition which may be obtained from the state estimation program. In planning, a number of postulated discrete base cases (e.g. light loads and heavy loads) are given. Beginning with the first base case, a post-contingency load flow is carried out. All monitored variables are checked with their corresponding limits. Should violations occur, the contingency will be recorded. Otherwise, it will proceed to the next contingency on the list until all contingencies are studied. The process then returns to the first contingency in the list to perform the next base case if there is any, e.g. in planning studies.

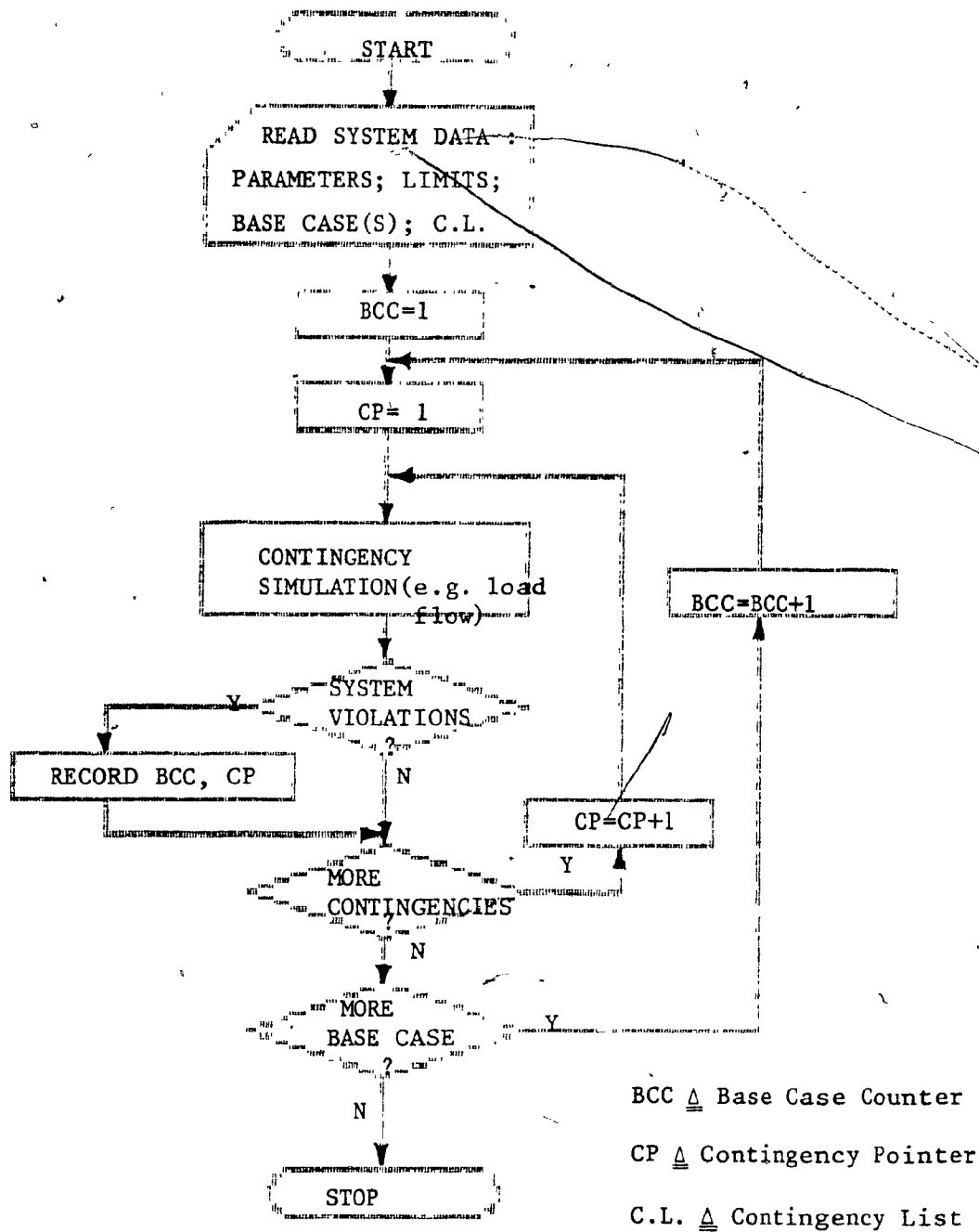


Fig. 2.1 General Algorithm of Contingency Analysis
Using Point-wise Approach

2.1.2.2 Distribution and Shift Factors Methods

A DC load flow model is used and the post-contingency conditions, i.e. real power line flows and real power generations, are calculated using their pre-contingency values with the corresponding Line Outage Distribution Factors (LODF) or the Generator Shift Factors (GSF) for line and generator outages respectively [MacArthur 1961; Limmer 1969; Wood et al. 1984]. These factors can be calculated off-line because they are invariant to the loading conditions but depend on the system structure and parameters only [Wood et al. 1984].

2.1.2.3 Z-matrix Methods

The nodal equations are used to solve for the post-contingency voltage deviations and line flows. The bus impedance matrix, the so-called Z-matrix, is presumably already constructed from the basic system data using either a direct inversion from the admittance matrix or the well-known Z-matrix algorithm [Stagg et al. 1969]. The pre-contingency Z-matrix elements are adjusted to reflect network changes [El-Abiad et al. 1962; Sullivan 1977]. Changes in line flows and voltages are then calculated from the base case values (i.e. voltages) and the newly adjusted Z-matrix [Ibid; Brown 1969, 1972].

2.1.2.4 Decoupled Load Flow Methods

Uemura used the Newton-type AC decoupled load flow

solution model for contingency analysis. The decoupled Jacobian, real and reactive parts, are treated as constant matrices and inverted using the Z-matrix algorithm [El-Abiad 1960]. These inverted matrices are then adjusted by the Kron's correction formula to reflect changes in the network due to an outage [Uemura 1972, 1974].

Stott and Alsac also proposed the use of the Newton-type AC decoupled load flow solution model to study outages. However, the outages were simulated using the matrix inversion lemma [Stott et al. 1974]. Also, the iterative linear AC power flow solution method for outage studies, proposed by Peterson, Tinney and Bree should also be mentioned [Peterson et al. 1972].

All of the above are basically iterative numerical methods used to solve the load flow equations with network changes (i.e. temporary changes). The accuracy of the solution to the problem therefore strongly depends on the number of iterations (e.g. more iteration cycles give more accurate results). Since approximate results are acceptable for contingency analysis, the number of iterations for the above mentioned methods are generally limited to 1 or $1\frac{1}{2}$ cycle only in order to increase the processing speed (one cycle means to solve the real and reactive parts separately once; an additional solution for the real power part with updating is called a half cycle).

2.1.2.5 Compensation Methods

Changes in the network due to outages can be simulated by appropriate injections (e.g. current or power injections) at the nodes of the outages using a linear system model. A Thevenin [Tinney 1972] or a Norton [Enns et al. 1982] equivalent (looking in from the outage ports) is necessary to be established to represent the original network. The correct amount of injections required to simulate the outage at the ports are thus calculated using such an equivalent network. The post-contingency changes are therefore solved by using the proportional properties between the above mentioned injections and the original system states, i.e. voltages and line flows [Tinney 1972; Enns et al. 1982; Alsac et al. 1983].

2.1.2.6 Sensitivity Matrix Methods

Sachdev and Ibrahim [Sachdev et al. 1974] proposed that the inverse of the Jacobian matrix in the Newton-type load flow formulation can be viewed as the first order sensitivity matrix of the state variables (e.g. bus voltage angles and magnitudes) with respect to the control variables (e.g. power injections). The post-contingency conditions can therefore be simulated by correct modifications of the bus injections, real and reactive, using such a sensitivity relationship and the base case conditions [Sachdev et al. 1974; Manandur et al. 1982]. This method needs no augmentation of the Jacobian and only a few elements (i.e. at most 16 (4x4) [Sachdev et al. 1974]) of the sensitivity matrix are required to be calculated for each contingency study.

2.1.2.7 Concentric Relaxation Method

Zaborszky and others recently introduced the so-called 'concentric relaxation' method for contingency analysis [Zaborszky et al. 1980]. This method assumes that the changes caused by the contingencies are mostly within the neighborhood area of the contingencies. The method first identifies a group of concentric 'tiers' around the contingency spot. Each of these tiers is composed of a number of buses and these tiers expand concentrically outward (i.e. each outer tier contains buses which are directly connected to the inner tier buses but farther away from the fault). The post-contingency conditions are thus calculated by systematically relaxing the voltages and angles, tier by tier, starting from the innermost to the outermost.

2.1.2.8 Discussion

The distribution factors methods are by far the fastest [Debs et al. 1975] but the voltage and reactive power aspects are neglected. For those systems without strong reactive power support, this technique is not quite adequate. A distribution factors method using complex coefficients has been proposed by Arafah [Arafah 1977], which may shed new light to overcome the voltage and reactive power problems. The Z-matrix methods have been outrun by other methods because of the cumbersome construction procedures of the Z-matrix. On the other hand, the compensation methods and the matrix inversion lemma offer two very effective techniques to simulate outages in the network

and they are widely employed for temporary outage studies (e.g. contingency analysis).

For AC simulations, among the decoupled load flow methods, Stott's formulation has been widely employed and gives good performance. According to Debs [Debs et al. 1975], the sensitivity matrix methods, the Stott's method and the Peterson's method mentioned above however all have a similar accuracy, storage requirements and speed performances. The novel concentric relaxation method has just been developed and its future still remains to be explored.

With a large number of contingencies to be evaluated, even with the efficient techniques mentioned above, the AC simulations are still prohibitive especially for on-line evaluations. In current practice, linear contingency analysis methods like the distribution factors methods or the compensation methods [Limmer 1969; Enns et al. 1982] have been used [Hinkel et al. 1977; Subramanian 1983] as a screening tool and the identified critical contingencies are submitted to more detailed AC simulations, e.g. Stott's method [Stott et al. 1974].

This point-wise approach is by far the most popular because the necessary and efficient tools (i.e. load flow solution models and effective simulation techniques) are well established. With extremely fast methods like the distribution factors methods, contingency analysis using such a discrete approach (i.e. solving

'one base case at a time)' is regarded as acceptable even though many simulations are required for different operating conditions or for different contingencies.

2.1.3 Region-wise Approach

2.1.3.1 Definition of the Secure Region

The 'secure' region of a system is defined as a closed region in the operating space, e.g. generation or load spaces [Hnyilicza et al. 1975], such that any point inside such a region is guaranteed to be able to withstand a set of postulated contingencies without causing any violations in the system.

2.1.3.2 Set-theoretic Approach Methods

For a given operating state, e.g. normal or contingent, a set of hyperplanes in the operating space can be used to define a closed region (or a group of closed regions) such that all points inside the region are free from any violations in any state. These hyperplanes are defined by the system structure, limits, flow patterns etc. The shape of the region is unique to each operating state. If all regions representing the normal state and all the postulated contingent states are superimposed on each other in the operating space, the intersection, if it exists, is indeed the so-called 'secure' region. Any point inside such a 'secure' region is thus guaranteed to be able to withstand any one of the postulated contingencies.

A graphical interpretation of the assembly of such a 'secure' region is shown in Figure 2.2 to 2.4. The operating space (e.g. the generation space) is depicted in each figure. For simplicity, a two-dimensional space, defined by the generations U_1 and U_2 , is used. The square in each figure represents the limits imposed upon the operating variables U_1 and U_2 (e.g. minimum and maximum generation levels). The curves cutting through the squares represent different functional constraints (e.g. line flow limits or voltage magnitude limits) expressed in the operating space.

In Figure 2.2, the system is in the normal operating state. The shaded area represents a 'normal' region that any points inside will not cause any violations providing no contingency is imposed. In Figure 2.3, the system is subjected to a contingency and the functional constraints are therefore altered, e.g. a line outage. The so-called 'contingency' region is thus bounded by the new positions of the curves as shown in the shaded area. Apparently this 'contingency' region is quite different from the previous 'normal' region. In Figure 2.4, the darkened area within the square is the intersection of the 'normal' region and the 'contingency' region. This is indeed the 'secure' region for the system subjected to such a contingency because any operating condition within this region is guaranteed to be able to withstand that contingency.

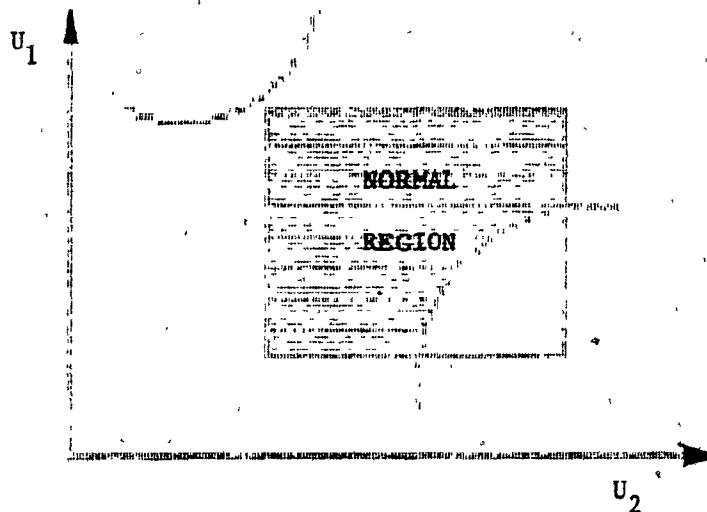


Fig. 2.2 'Normal' Region

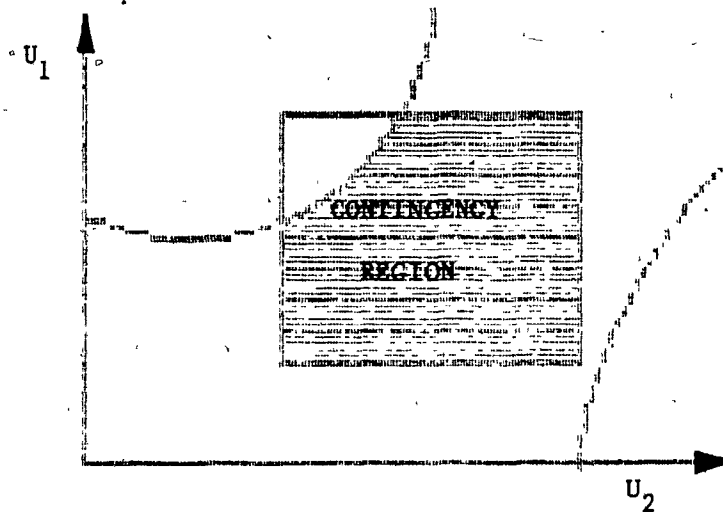


Fig. 2.3 'Contingency' Region

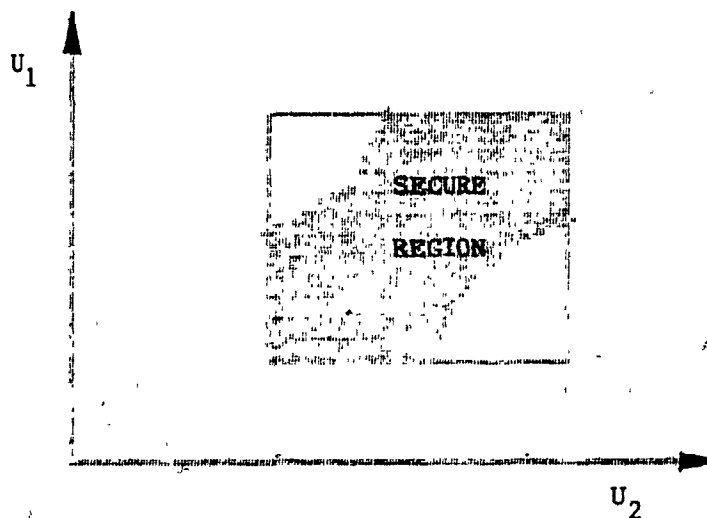


Fig. 2.4 'Secure' Region

To consider the system security against any other additional contingencies, their 'contingency' regions can simply be superimposed upon the previous regions (e.g. the above described region) and the final intersection will be the 'secure' region for all the contingencies considered.

A DC model and the thermal line flow limits were used by Hnyilicza, Lee and Schweppe [Hnyilicza et al. 1975] to derive a set of hyperplanes bounding each region of concerns in the generation space. Redundant hyperplanes, i.e. hyperplanes which will not affect the form of the region, are first identified and then discarded. The remaining constraints are thus used to define a minimal bounding hyperbox [Ibid] using Linear Programming methods.

With the consideration of load uncertainties, the 'secure' region in the generation space is found to be reduced according to Fischl and others [Fischl et al. 1976]. A 'maximum secure' operating point, defined as the point farthest from any bounding hyperplanes inside the 'secure' region, is also introduced [Ibid]. Such a point can thus be used as a quantitative measure for the degree of security. Furthermore, in case that no 'secure' region exists, i.e. infeasible condition, the 'insecurity margin' technique [Ibid] is also proposed such that this margin can be used as a reference to identify operation bottlenecks and to enhance the 'secure' region with a minimal amount of relaxation of the limits [Ibid].

Mescua and Fischl also used a similar technique and a linearized voltage-reactive power relationship to identify a 'secure voltage profile' for the system [Mescua et al. 1980].

Dersin and Levis employed the DC model to derive a feasibility set which is a convex/polyhedron in the space of the loads [Dersin et al. 1982]. As a result, a global view of all feasible load combinations and a probabilistic supply reliability measure can be obtained [Ibid].

Banakar and Galiana used a quadratic system model and considered that the load uncertainties are only limited to the neighborhood of a predicted or nominal load trajectory [Banakar et al. 1981]. A series of overlapping ellipsoids constructed on this trajectory define a 'security corridor' [Ibid]. Points falling within such a corridor therefore are guaranteed to be secure. In this method, the whole security region need not be evaluated completely but rather only the neighborhood area around the predicted or nominal load trajectory are required to be studied. Hence, the complexity of the bounding hyperplanes and the computational effort can be greatly reduced [Ibid].

2.1.3.3 Pattern Recognition Methods

This approach attempts to learn the 'secure' region directly using pattern recognition methods. A training set composed of a large number of 'patterns', i.e. different operating conditions, are collected and tested off-line to label whether there are 'secure' or 'insecure' patterns. Since the number of variables in each pattern is generally very large, it is desirable to extract only a small group of variables to be used for evaluation [Pang et al. 1974]. This is called the 'feature extraction', and the selected variables are called the 'features'. These features are selected on the basis that they can yield the best decision for the status of their pattern (i.e. secure or insecure). After selecting the features, the training procedures will construct a set of security functions using the features such that the functions will all be greater than or equal to zero if and only if the pattern is 'secure'. Otherwise the pattern is 'insecure'. Hence, the 'secure' region is expressed in the form of these 'security functions'. Using such functions prepared from off-line studies, on-line evaluation process thus only requires the solution of these functions which are usually few.

2.1.3.4 Discussion

The set-theoretic approach has received wide attention ever since it was first introduced [Hnyilicza et al. 1975]. However, most of the methods derived from this approach are still limited to

linear or decoupled system model. For the full AC model, such a 'secure' region is generally not well behaved like the DC or decoupled models, i.e. non-convex nor non-connected. If an empty 'secure' region results, the method of identifying the contingency(s) causing the region to disappear still remains to be solved using the full AC model [Halpin 1982].

Pattern recognition methods are also confronted with complex mathematical problems. For instance, techniques used for the two-dimensional problems in pattern recognition are well established. However, for multi-dimensional problems, especially in the case of power system applications, techniques like the decision making methods still remains to be explored. Another obstacle for this approach is the excessive amount of off-line training and simulations required, e.g. the system has to be retrained every time the system structure or parameters change.

At the present moment, current practices are mostly point-wise approach methods. Since the operations of power systems are continuously varying, point-wise approach can easily become inefficient when many base cases are required to be evaluated. However, region-wise approach overcome such a problem by defining a secure region. Deviations can be more easily evaluated by examining such a region. Furthermore, the by-products of region-wise approach, namely secure margins [Fischl et al. 1976] and detection of possible bottlenecks [Ibid] , provide broader perspectives and constructive information to system planners and operators.

2.2 Part II : Review of Automatic Contingency Selection Methods

2.2.0 Introductory Remarks

Even though efficient contingency evaluation techniques have been well established, as shown in the preceeding part of this chapter, exhaustive studies of all conceivable outages are still prohibitive for on-line evaluations or too expensive to perform for off-line studies on large systems. Current practices have commonly adopted the idea of assembling a 'contingency list' such that only a few 'critical' contingencies are selected for detailed investigations.

Traditionally, the selection relies on either the operator's experience or the off-line simulation results. However, such selection schemes are not always reliable because of operator's mistakes (e.g. omitting serious contingencies) or the inadequacy of a fixed contingency list obtained from off-line studies (e.g. a safe contingency in the off-line studies may be insecure under the current operating conditions). It is therefore desirable to have an adaptive and dynamic selection scheme, the so-called Automatic Contingency Selection (ACS) [Ejebe et al. 1979], such that the contingency list can be assembled systematically and automatically based upon the current operating conditions.

2.2.1 Filtering Concept of ACS

Automatic Contingency Selection (ACS) can be viewed as a 'contingency filtering' process [Mikolinnas et al. 1981; Wasley et al. 1983; Galiana 1974, 1984]. Instead of running exhaustive simulation studies, one or more 'contingency filter(s)' are used to select a small number of the postulated contingencies. These selected events are considered to be more 'severe' than the others according to the filter(s). Therefore, the selection assures that the most 'critical' contingencies will be considered in detail. Consequently, the less 'severe' or the so-called 'non-critical' contingencies are filtered out. A general filtering process can be summarized as follows, i.e.,

- (1) Estimate the expected severity of each contingency.
- (2) Rank contingencies according to their expected severity.
- (3) Select the higher ranked events for the contingency list.

2.2.1.1 Filtering Criteria

In order to justify whether one contingency is more severe than the others, a criterion for comparison is necessary. In general, two distinct criteria are used, namely the Scalar Performance Index (SPI) and the Vector Performance Index (VPI).

A SPI is a scalar quantity used to estimate the severity of a contingency. This scalar quantity is a positive definite function, a function which is always positive, of the system variables deviations

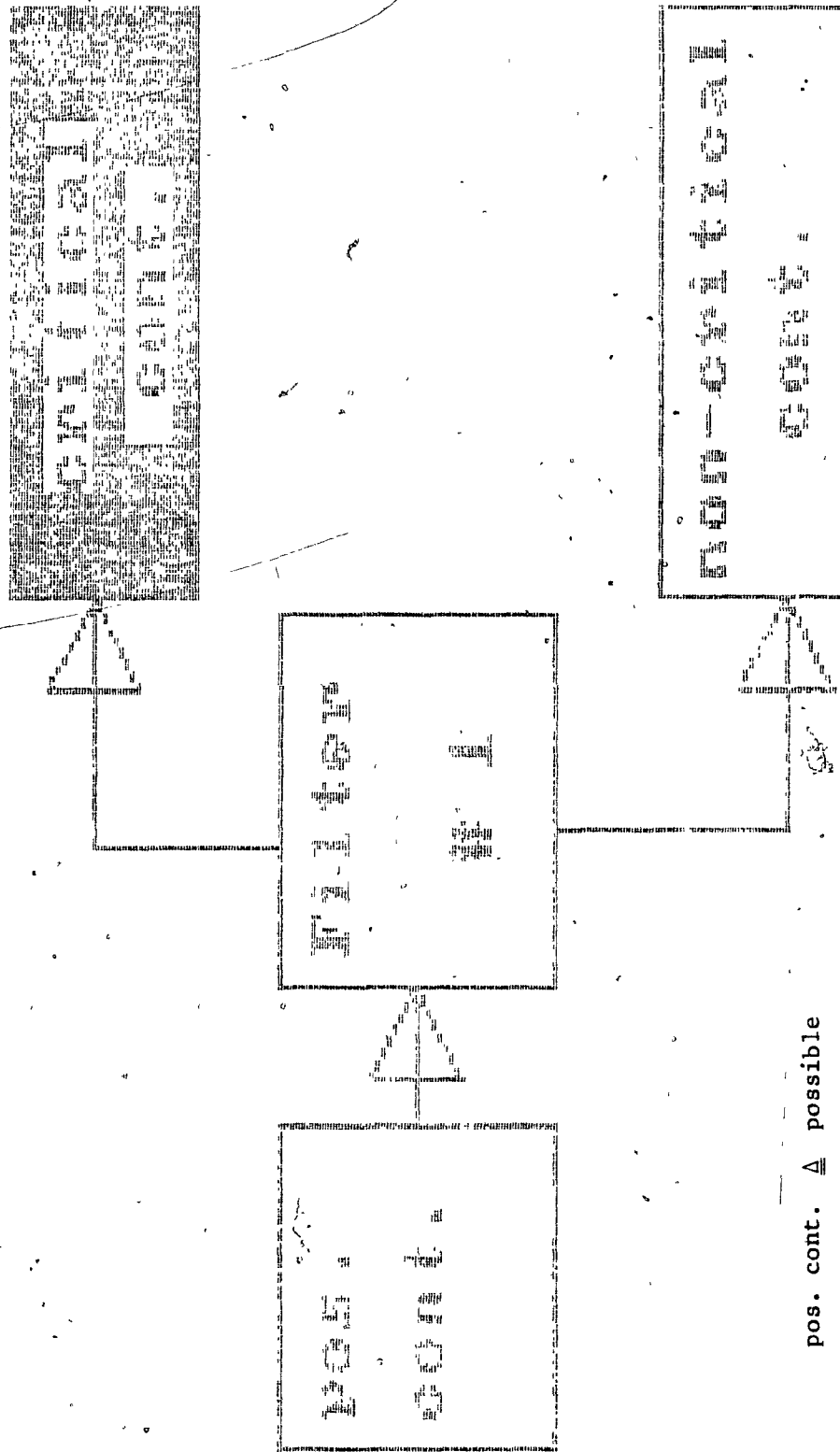
from their limits or rated values. The decisions of ranking and selection for each contingency are thus based on the value of a single scalar quantity.

However, a VPI is a vector quantity where each member in the vector contributes to the determination of the severity of a contingency. For example, each member can be a system variable deviation measurement, or a function of the system variable(s). The decision of selection for each contingency therefore relies on a vector quantity rather than a scalar value. Thus, a load flow simulation is an example of one of the VPI based methods. Note that VPI based methods identify contingencies as either 'critical' or 'non-critical' directly without passing through the step of 'ranking'.

In the following review, ACS methods proposed by different authors are classified and presented according to the above mentioned filtering criteria.

2.2.1.2 Filtering Strategies

Contingency filtering can be executed in a one-stage or a multi-stage strategy. In one-stage filtering, all postulated contingencies are classified into either 'critical' or 'non-critical' after passing through one filter. On the other hand, multi-stage filtering has a series of filters. After passing through each one of



pos. cont. Δ possible
contingencies

Fig. 2.5 One-stage Filtering Strategy

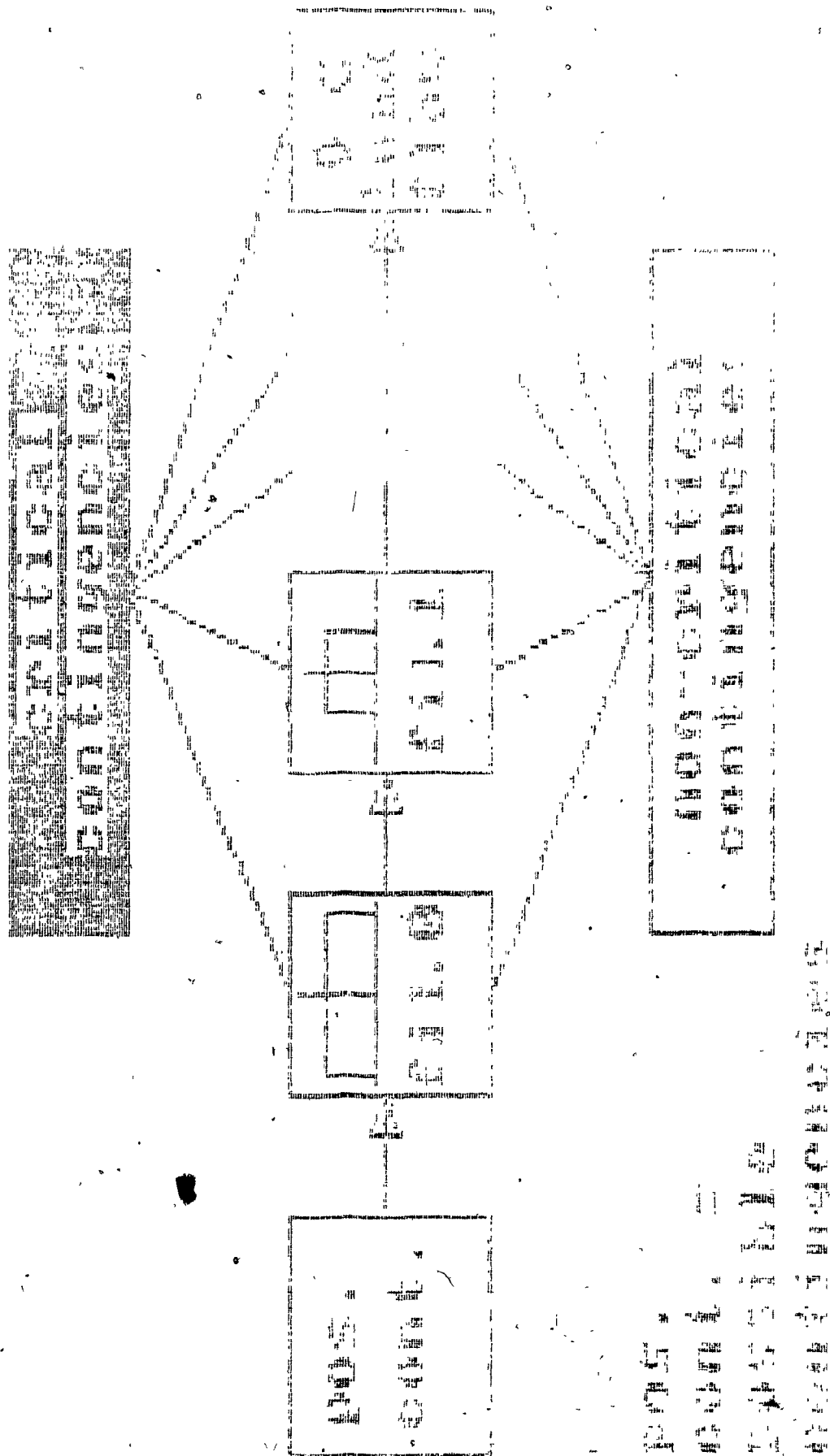


Fig. 2.6 Multi-stage Filtering Strategy

these filters, the incoming contingencies are classified into either 'critical', 'non-critical' or 'uncertain'. An 'uncertain' contingency is defined as a contingency where the results from the filtering process is not adequate to decide whether it is 'critical' or 'non-critical'. These uncertain contingencies are thus passed on to the subsequent filter for more detailed investigations. The final filter is usually a load flow study which assures to identify any remaining 'uncertain' contingencies. Figures 2.5 and 2.6 illustrate the basic ideas of these two different strategies in a schematic manner.

2.2.2 ACS Methods Based on a Scalar Performance Index

2.2.2.1 General Concept

This methodology uses a scalar quantity, commonly known as the 'Performance Index', to indicate the severity of a contingency upon the system. In this thesis, this scalar quantity is referred as the Scalar Performance Index (SPI) in order to be distinguished from the Vector Performance Index (VPI).

Using the magnitudes of these indices, where each index represents a contingent event, the relative severity between contingencies can be compared numerically, i.e. a contingency with a larger SPI value will likely be more 'severe' than a contingency with a smaller SPI value. Thus all postulated outages can be ranked in a descending order according to their relative severity using the corresponding SPI values. The contingency list is thus assembled by including only the higher ranked events.

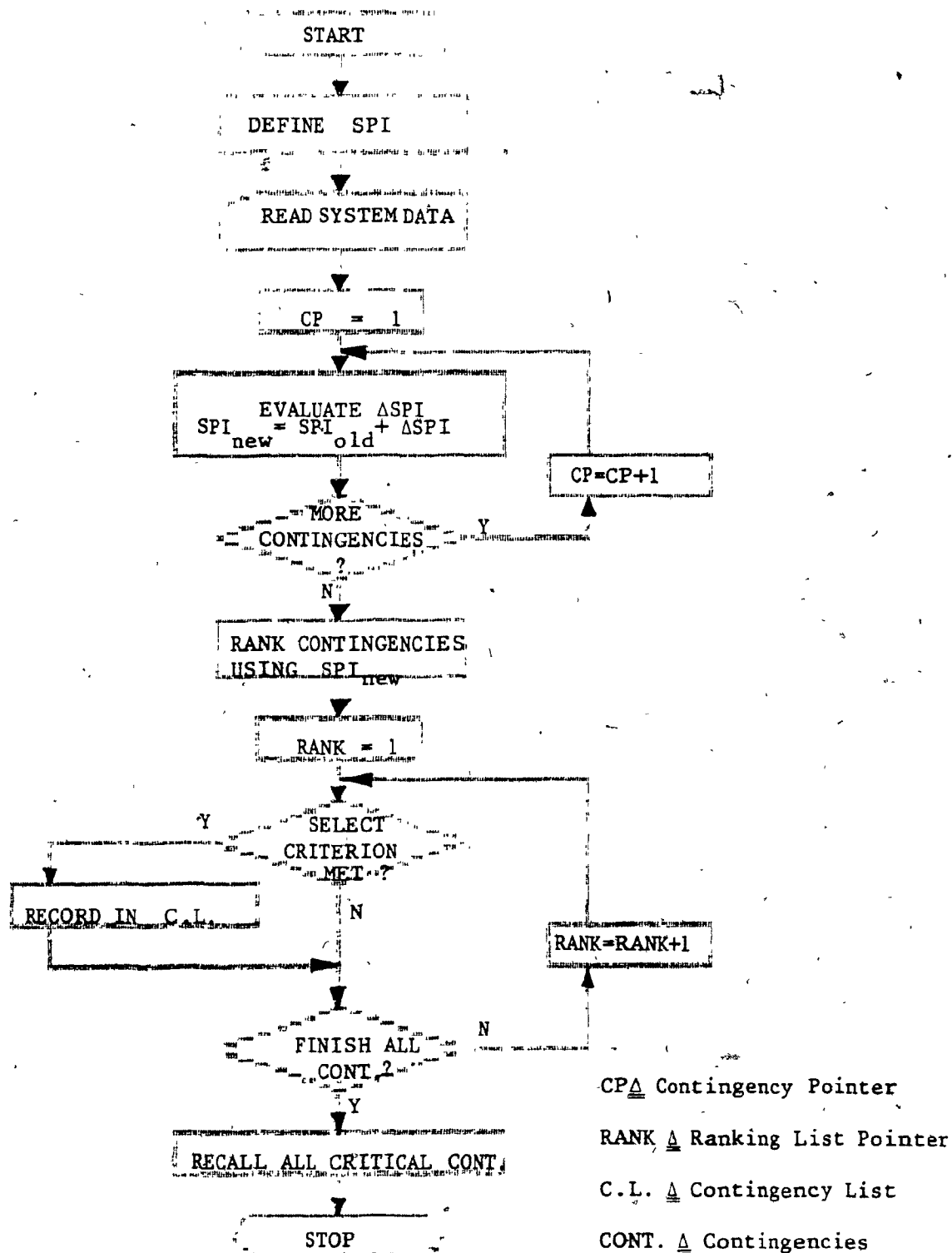


Fig. 2.7 General Algorithm of ACS Methods Based
 on a SPI

Figure 2.7 depicts a general algorithm of the ACS methods based on a SPI. The SPI has to be first defined because different problems require different SPIs (i.e. overload problem and voltage degradation problem caused by a contingency require different SPI definitions). A SPI will then be calculated for each contingency. The numerical values of these scalar quantities are compared and ranked in a descending order. The contingencies are thus selected according to a criterion based on the SPI values. Usually, that is a number specifying the maximum number of contingencies to be studied from the highest ranked events (e.g. the top 20). Alternatively, it can also be a threshold value in terms of the SPI. Thus for any contingency which has a SPI value higher than this threshold will be selected [Halpin 1982].

2.2.2.2 Defining a General Form of Scalar Performance Index

Various SPI have been defined by different authors for different application purposes, however a general form of the SPI can be written as follows [Halpin 1982], i.e.,

$$J = \sum_{i=1}^{N_J} w_i [f_i(\underline{z})]^p \quad (2.1)$$

where J is the scalar SPI; (\underline{z}) is a vector of system variables normalized by their corresponding limits or rated values (e.g. line

flows normalized by their thermal ratings); $f_i(.)$ is a real value linear function which in general is an identity function [Haplin 1982]; p is the exponent which is usually chosen to be 2; w_i is the weighting factor which can be used to emphasize or suppress special terms in the summation (e.g. putting heavy weights on the system tie-lines or neglecting a line completely); finally the number N_j denotes the total number of terms considered by the summation (e.g. total number of lines for overload evaluations, or total number of buses for voltage violation evaluations).

With such a formulation as shown in (2.1), should any violation occur in the system, i.e. some z_i exceed unity, the resulting SPI will yield a large value due to the penalty effect induced by the exponent p . If the contingency causes no violations, i.e. all z_i are less than unity, the resulting SPI will yield a small value. The relative magnitudes of the SPIs, where each SPI represents a contingency case, can therefore be interpreted as a measure of the relative severity measurements between contingencies. Contingencies can thus be ranked, with such measurements, in a decreasing order according to their relative severity, i.e. from the largest SPI to the smallest SPI.

It is pertinent to note that the actual SPI for each contingent case is not required because that will require a load flow study for each case. Rather, the change of SPI, denoted by ΔSPI , due to a change in the system (e.g. a contingency) is estimated.

The change of SPI (Δ SPI) is then used to approximate the actual corresponding new SPI (i.e. the contingency SPI). Subsequently, this approximation is used for ranking.

2.2.2.3 Summary of ACS Methods Based on a SPI

Since the main concern of this thesis is to select contingencies which can cause branch overloads, the following review will only focus on the ACS methods used for branch overload evaluation based on a SPI. ACS methods for the selection of contingencies which can cause violations of voltage and/or reactive power will only be briefly mentioned, however, the reader is referred to a more detailed review conducted by Halpin [Halpin 1982].

Table 2.1 Summary of ACS Methods Based on a SPI

AUTHORS	z_i	$f_i(z)$	w_i	p	N_j	SPI CALCULATION METHODS	REMARKS
(1) Ejebe & Mollenberg (Ejebe et al., 1979)	P_1/P_1^{lim}	z_i	w_{os}	2	NL	- dSPI is approximated by the 1st order sensitivity term calculated by using the Tellegen's Theorem.	- Capture Rate (CR) : 0.6-0.8 compared to AC load flow results. - w_{os} = weighting factor selected by operator, usually $w_{os} = 1/2$.
(2) Irisarri, Lerner & Sasson (Irisarri et al., 1979)	P_1/P_1^{lim} Q_1/K_1^{lim}	z_i	w_{os}	2	NL	- 1st & 2nd order sensitivity terms are used to approximate the dSPI based on flows & the dSPI based on angle differences. - SPI based on flows are also calculated using the results from DC load flow.	- technique proposed in (1) is shown to be unreliable even if the 2nd order terms are included. - ranking according to the SPI based on angle differences is shown to give erratic results. - the SPI based on flows using the DC load flow results shows good ranking performance.
(3) Albuyeh (Albuyeh, 1980)	Q_1/K_1^{lim}	z_i	$(w_{os} r_i)/N_L$	2	NL	- elements from the sensitivity matrix of the DC model w.r.t. outages are used as weighting factors (w_i). - SPI is based on angle differences.	- w_i = element corresponding to line i in the sensitivity matrix (ibid). - r_i = unit of capacity to be removed from line i .
(4) Irisarri & Sasson (Irisarri et al., 1981)	P_1/P_1^{lim}	z_i	w_{os}	2	NL	- two methods tested : 1. calculate SPI using DC load flow. 2. dSPI is approximated by including up to the 50th terms in a Taylor series expansion of SPI.	- the DC load flow approach is similar to the one introduced previously by the authors (2) but speed is increased by pre-calculating two vectors (ibid). - results of the two methods are similar but the DC approach is more direct and easier to compute.
(5) Nikolinas & Mollenberg (Nikolinas et al., 1981)	P_1/P_1^{lim}	z_i	w_{os}	2	NL	- dSPI is derived in closed form such that all terms in the Taylor series expansion are included.	- accuracy approaches DC load flow results. - CR : 0.9-1.0 compared to DC load flow.
(6) Albuyeh, Bose & Heath (Albuyeh et al., 1982)	P_1/P_1^{lim}	z_i	w_{os}	2	NV	- SPI based on flows are evaluated using the first iteration results from the fast decoupled load flow.	- only the overloaded lines are included in summation. - CR : 0.85-1.0 compared to AC load flow results.
(7) Halpin, Fischl & Fink (Halpin et al., 1984)	P_1/P_1^{lim}	z_i	w_s	2	NL	- an optimum set of weighting factors are calculated for the SPIs.	- w_s = optimum weighting factor. - the weighting factor is optimized so that the FR is minimized & CR is maximized.

where :

- P_1 is the real power flow of line 1.
- P_1^{lim} is the limit of real power flow of line 1.
- NL is the total number of branches.
- θ_1 is the angle difference between two connecting nodes of line 1.
- K_1^{lim} is the constant limiting the maximum angle difference between the connecting nodes of line 1.
- NV is the total number of violated lines.
- dSPI is the same as ΔSPI .
- CR is the Capture Rate, defined as the fraction of the worst N contingencies (known from either a full AC or DC load flow simulation) that appear in the first N entries of the ranking list [Mikolinnas et al. 1981].
- FR is the False-alarm Rate, defined as the ratio of the number of secure contingencies in the first N entries of critical contingencies. These two numbers (CR and FR) allow us to compare the efficiencies of different SPI methods [Halpin 1982].

2.2.3.4

Discussion

The biggest attraction of this approach is its speed to evaluate the approximate SPI for each contingency and subsequently to use the approximations for ranking. However, such an approach also renders itself to some disadvantages as follows, i.e.,

- (1) Masking effect : In some instances, the SPI cannot truly represents the severity of some contingencies. For example, a case with one heavily overloaded line but causing some other lines to decrease their loadings may give a decreased SPI and hence the contingency will be ranked rather low. Consequently, the selection may possibly miss such a critical case. This kind of phenomenon is called 'masking' [Irisarri et al. 1981]. In addition to misranking the critical contingencies, the masking effect also gives rise to the 'false-alarm' cases, where non-critical cases are classified as critical [Halpin 1982]. This will cause the detailed analysis spending unnecessary time in evaluating secure events.

Some possible remedies for the masking effect have been proposed by different authors. For instance, the exponent p in (2.1) can be raised to a higher value in order to amplify the penalty effect and eventually reduce the masking [Irisarri et al. 1981; Mikolinnas et al. 1981]. However, this increases the complexity of the SPI function

and an efficient evaluation method of Δ SPI with p larger than 2 still remains to be resolved.

Albuyeh and others proposed to sum only the overloaded lines in order to reduce 'noise' from the non-overloaded lines [Albuyeh et al. 1982]. However, this method has to either neglect the potentially dangerous events (e.g. heavily loaded lines) or has to set up a separate ranking list for the non-overloaded cases.

Halpin and others calculated an optimum threshold value for the SPI and a set of optimum weighting factors (w_i) such that the CR^1 is maximized and meanwhile the FR^2 is minimized [Halpin et al. 1984]. Such an approach seems to be promising but it requires a set of pre-calculated weighting factors which are very sensitive to the system structure and limits [Ibid].

- (2) Non-linear characteristic of the SPI function : The SPI function defined in (2.1) is a highly non-linear function which depends largely on system loading and structure. Using a first order [Ejebe et al. 1979] or even a second order [Irisarri et al. 1979] sensitivity term to approximate the Δ SPI due to an outage has been shown to be unreliable [Ibid].

1. CR is the Capture Rate defined in 2.2.2.3
 2. FR is the False-alarm Rate defined in 2.2.2.3

If higher terms are included, the computational burdens will also increase drastically [Irisarri et al. 1979, 1981].

- (3) Tuning of the SPI : In order to achieve good ranking results, the indices have to be 'tuned', using the weighting factors, accordingly to suit each system. This procedure requires the operator's experience with the system and that is not desirable in terms of a true ACS [Ejebe et al. 1979].
- (4) Limitations of a scalar value in representing the system security : Power systems are very complex in nature, and the performance of the system is multi-faceted. Using only a simple scalar quantity to represent and evaluate the system as a whole is bound to suffer a great deal of loss of information .

For the evaluation of contingencies which will cause voltage and/or reactive power violations, a separate but similarly defined SPI as shown in (2.1) can be used [Halpin 1982, 1984]. However, the system variables (z) become the normalized voltages or reactive power injections.

Ejebe and Wollenberg had employed the sensitivity approach to approximate the changes of such voltage indices due to contingencies but the resulting ranking was not very reliable [Ejebe et al. 1979].

Another proposal from Medicherla and Rastogi employed the total load curtailment necessary to restore the original system voltage level as the SPI, which has been shown to be quite reliable [Medicherla et al. 1982], however the required computational efforts still remained to be improved.

In terms of filtering strategy, all methods based on SPI use the one-stage filtering strategy. That means the SPI for every contingency is only evaluated once for each selection. The results of SPI are then used to rank the contingencies in descending order in terms of severity. The higher ranked contingencies are treated as 'critical' contingencies and the lower ranked ones are treated as 'non-critical'. The threshold used to distinguish these two types can be determined by the algorithm itself (e.g. always selecting the top 20 ranked lines) or by the operator's choice or both.

Finally, it has to be mentioned that some methods based on a SPI do carry a load flow study for each contingency, namely the method proposed by Irisarri and others [Irisarri et al. 1979] where a DC load flow was used, or in Albuyeh's method [Albuyeh et al. 1982] where a decoupled load flow was used. The contingent conditions obtained from these approximate load flow studies are then used to compute the SPI and eventually using the SPI for ranking. Such practices are indeed a combination of the SPI based methods and the VPI based methods, which will be described in the following section.

2.2.3 ACS Methods Based on a Vector Performance Index

2.2.3.1 General Concept

The severity of a contingency is evaluated using a Vector Performance Index (VPI) rather than a scalar value as in the preceding approach. This vector, denoted as the VPI, contains a number of variables which can reflect the system contingency conditions. The variables can be the system operation variables (e.g. line flows or bus voltages) or functions of the system operation variables (e.g. deviation measurements or bounds of the load flow solution). These variables are required to be evaluated for each contingency before selection. During selection, each one of these variables are examined for each VPI. A decision is then granted to determine the status of the contingency, namely being 'critical' or 'non-critical', according to the status of the vector. For example, if for one or more of these variables (e.g. contingency line flows) are found that violations have occurred, the contingency is labeled as 'critical'.

Figure 2.8 depicts a general algorithm for the ACS methods based upon a VPI approach. The elements of each VPI have to be defined at the beginning. The elements can be all the contingency line flows or all the contingency bus voltages, depending on the particular problem. For each contingency represented by a VPI, the elements are evaluated (e.g. by a load flow study). Each element of a vector is thus checked for any violation. Should violation occur, the VPI is critical. After all contingency events are studied, those whose VPI have been labeled as 'critical' are selected for further studies.

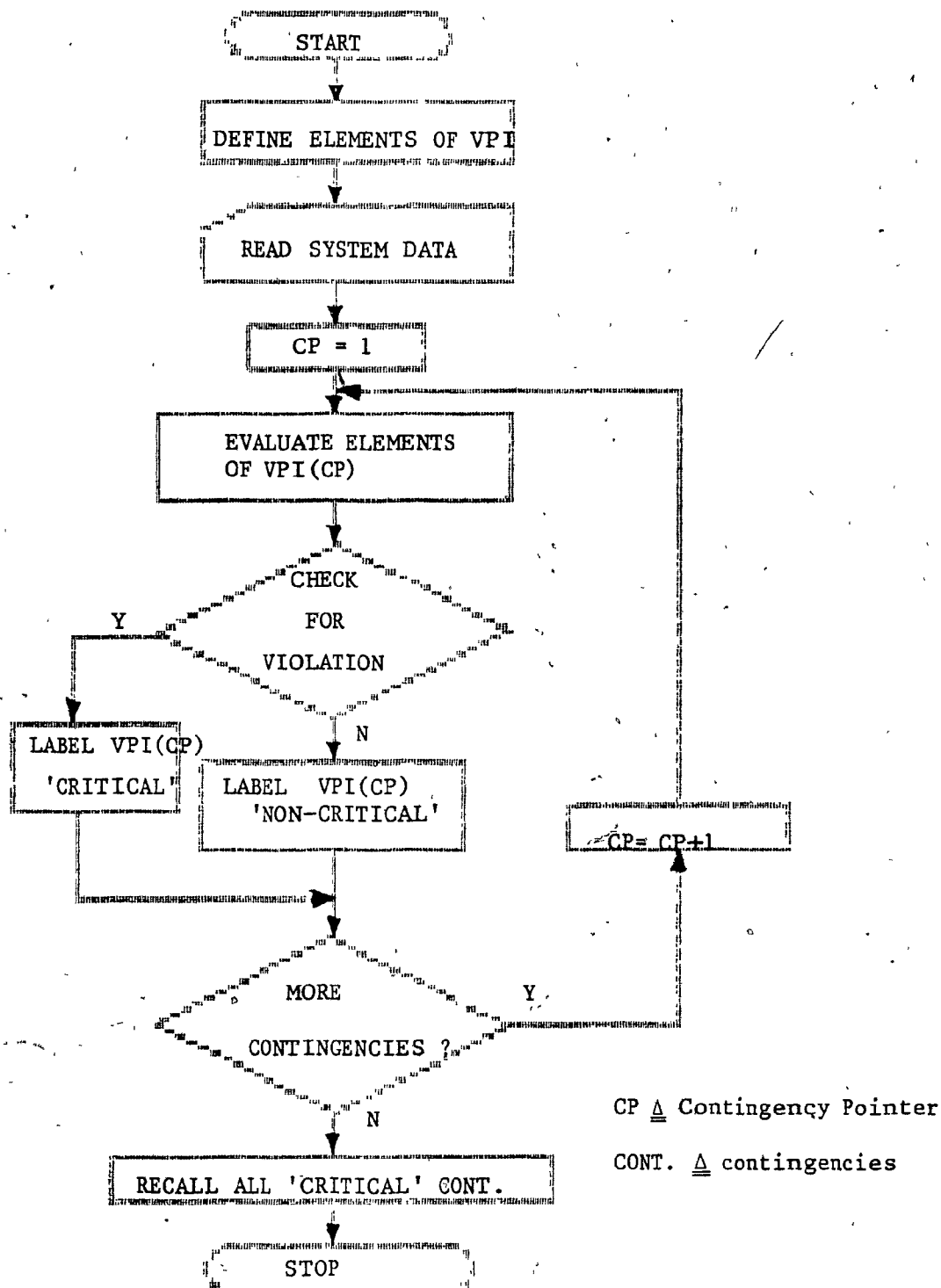


Fig. 2.8 General Algorithm of ACS Methods Based
 on a VPI

2.2.4.2 Summary of ACS Methods Based on a VPI

Two distinct methodologies have been used to calculate the elements of a VPI, namely approximate load flow methods and bound estimation methods.

Approximate load flow methods use the results from an approximate load flow study, e.g. results from the first iteration of a fast decoupled load flow [Albuyeh et al. 1982; Lauby et al. 1983], to form a VPI for each contingency. Each element of a VPI therefore represents a system operation variable (e.g. a contingency line flow or a contingency bus voltage). Should any violation occur after comparing these variables to their security limits (e.g. line thermal limits), the corresponding VPI will be labeled as 'critical'. Otherwise, the VPI is labeled as 'non-critical'. Eventually all 'critical' contingencies are selected for detailed analysis. Besides the fast decoupled load flow [Stott et al. 1974], the DC load flow [Irisarri et al. 1979] was also used. The 'concentric relaxation' method and the 'local solution' method [Zaborsky et al. 1980; Lauby et al. 1983] can also be put in this category. These methods are also commonly known as 'screening' methods.

Bound estimation methods evaluate a set of bounds on the system operation variables (e.g. bounds on contingency flows [Galiana 1984]). Each VPI is therefore composed of two sets of bounds, namely a set of upper bounds and a set of lower bounds, for all considered

system operation variables. These bounds are checked with the upper and lower security limits of the corresponding variables. Should all the bounds of a VPI lie within their security limits, the contingency is labeled as 'non-critical'. If one or more bounds lie totally outside their corresponding security limits, the contingency is labeled as 'critical'. For any other conditions, the contingency is labeled as 'uncertain' and further analysis for that particular contingency is required. The further analysis can be another filter which gives a tighter bound or eventually an exact load flow study. This methodology can be represented by the work from Kaye and Wu [Kaye et al. 1982], Galiana [Galiana 1984], Cheng and Galiana [Cheng et al. 1984].

2.2.3.3 Discussion

The advantages of these VPI based methods are multi-faceted and they can be summarized as follows, i.e.,

- (1) 'Masking' effects are eliminated. Methods based on VPI will not encounter the 'masking' effect common to most SPI methods because the summation used in SPI methods can be eliminated here, i.e. summation shown in (2.1).
- (2) Broader view of the system performance : Since a vector is used as a performance index, the information contained in the vector is definitely more in terms of quantity and reliability than a single scalar value. Therefore, the resulting selection will be more reliable.

- (3) Low misclassification risk : The worst misclassifications in this approach (VPI), if they exist, are generally associated with the contingencies causing only marginal violations. However, the most severe contingencies are usually captured, i.e. identified as 'critical'.
- (4) The VPI based methods can combine different techniques used in contingency analysis, e.g. point-wise or region-wise approaches described previously, to form a unifying filtering scheme which can utilize the different advantages from each different technique. For instance, characteristics of the non-linear load flow equations can be exploited such that bound estimates or the region of the solutions can be used in such a unifying filtering scheme [Kaye et al. 1982; Ilic-Spong 1984].
- (5) Scalar Performance Index (SPI) can be applied with better accuracy in conjunction with the VPI based methods. Since the conventional SPI is normally evaluated without any VPI type pre-filtering, the accumulated sum (i.e. the SPI value) contains a lot of 'noise' and hence the 'masking' problem arises. However, with the VPI pre-filtering, these problems are reduced and the filtering efficiency can be enhanced.

Perhaps the biggest concern about such methodologies regarding its disadvantage is the speed of processing while using the approximate load flow methods mentioned above. It is due to the fact that approximate load flow studies must be run exhaustively for all contingent events before selection can be done. This may become very time-consuming and undesirable for on-line usages. However, this drawback can be overcome by using a multi-stage filtering strategy. Fast and efficient approximation algorithms, which are comparatively less demanding than the load flow study and progressively more discriminatory, can be employed as the front filters [Galiana 1974,1984]. Since many contingencies have already been identified by these earlier filters, the more time-consuming evaluations are limited to a few cases only. Consequently the overall time can be significantly reduced [Cheng et al. 1984]. In this thesis, a multi-stage filtering strategy using a bound estimation VPI method was investigated. Later on, such a VPI based method is mixed with some SPI based selection algorithms to demonstrate the possibility and merits of applying both methods together.

CHAPTER III

CONTINGENCY FILTERING BASED ON LINEARIZED

FLOW BOUND ESTIMATES ; THEORY AND

COMPUTATIONAL CONSIDERATIONS

3.0 Introductory Remarks

In this thesis, contingency severity analysis is accomplished by employing a series of 'contingency filters' [Galiana 1984]. Through these filters, all postulated contingencies, all primary branch outages in this study, are categorized into either critical, non-critical or uncertain contingencies except after the final filter where all remaining uncertain contingencies are identified as critical or non-critical with no more uncertainty. Such filters are established based on bounding the contingency real power flows. Each filter calculates a set of bounds which are progressively tighter than the preceding filter. The final filter is a DC load flow simulation which calculates the exact values of the remaining uncertain contingency line flows.

This chapter presents the theory of this contingency filtering technique [Ibid]. The bound estimates of contingency real power flows are derived from a new interpretation of the well-known Line Outage Distribution Factors (LODF) [Wood et al. 1984] by exploiting some simple network topological characteristics. A series of filters are therefore constructed using different types of bound estimates.

Some contingency ranking and selection algorithms using the results from the filtering process are also presented. Finally, the computational aspects in terms of programming are explained and discussed.

3.1 Basic Concept

3.1.1 Contingency Flows Calculated from Base Case Flows

It is commonly known that the DC model¹ gives a good approximate solution and fast solution speed for the real power flow evaluation in power systems [Ejebe et al. 1979; Irisarri et al. 1979]. With such a model, the contingency real power flows can be calculated using the base case flows. In terms of mathematical expression, it can be written as follows, i.e.,

$$P_{lm/jk} = P_{lm} + \rho_{lm/jk} P_{jk} \quad (3.1)$$

where $P_{lm/jk}$ is the contingency real power flow of the line connecting nodes l and m while the line connecting nodes j and k is out of service; P_{lm} and P_{jk} are the base case real power flows through the line connecting nodes l and m , and nodes j and k respectively; $\rho_{lm/jk}$ is the so-called Line Outage Distribution Factor (LODF). Hence, for NTC single line outage contingencies to be analyzed in a NL branches system, a total of $NTC \times (NL-1)$ LODF are required.

1. A derivation of the DC model is shown in Appendix A.

3.1.2 Bounding Contingency Flows by Bounding the LODF

Since each of these Line Outage Distribution Factors (LODF) is invariant to the system loading but only depends on the network structure and parameters, some network topological characteristics can be applied to obtain an upper and lower bounds of the LODF. The true LODF value is therefore expected to lie within the range enclosed by these bounds, e.g.,

$$\tilde{\rho}_{lm/jk} \leq \rho_{lm/jk} \leq \hat{\rho}_{lm/jk} \quad (3.2)$$

where $\tilde{\rho}_{lm/jk}$ and $\hat{\rho}_{lm/jk}$ denote the lower and upper bounds of the LODF respectively. If the LODF is bounded, the corresponding contingency real power flow is also bounded, i.e.,

$$\tilde{P}_{lm/jk} \leq P_{lm/jk} \leq \hat{P}_{lm/jk} \quad (3.3)$$

where :

$$\begin{aligned} \hat{P}_{lm/jk} &\triangleq P_{lm} + \max. \{ \tilde{\rho}_{lm/jk} P_{jk}, \hat{\rho}_{lm/jk} P_{jk} \} \\ &\triangleq \text{maximum contingency flow} \end{aligned} \quad (3.4)$$

$$\begin{aligned} \tilde{P}_{lm/jk} &\triangleq P_{lm} + \min. \{ \tilde{\rho}_{lm/jk} P_{jk}, \hat{\rho}_{lm/jk} P_{jk} \} \\ &\triangleq \text{minimum contingency flow} \end{aligned} \quad (3.5)$$

3.1.3 Safe, Unsafe and Uncertain Contingency Flows

After comparing the results obtained from (3.4) and (3.5) with the branch security limits (e.g. long or short term thermal ratings or the stability limits), each contingency flow can be classified as one of the following, i.e.,

- (1) 'Safe' contingency flow, where its upper and lower bounds both lie within the range covered by the line upper and lower ratings (or limits). This implies that the true flow value, according to a DC model, will definitely be 'secure'.
- (2) 'Unsafe' contingency flow, where its upper and lower bounds both lie outside the range covered by the line upper and lower ratings (or limits). This implies that the true flow value will definitely exceed the security limit.
- (3) 'Uncertain' contingency flow, where its bound locations are neither (1) nor (2). This implies that the bounds cannot conclude any decision whether the flow is secure or not.

In Figure 3.1, some examples for different contingency flows are shown. Note that the heights are meaningless but only used to differentiate the bounds and the limits.

$P_{lim}, -P_{lim}$ Δ limits of line flow

\hat{P}_b Δ max. bound

\tilde{P}_b Δ min. bound

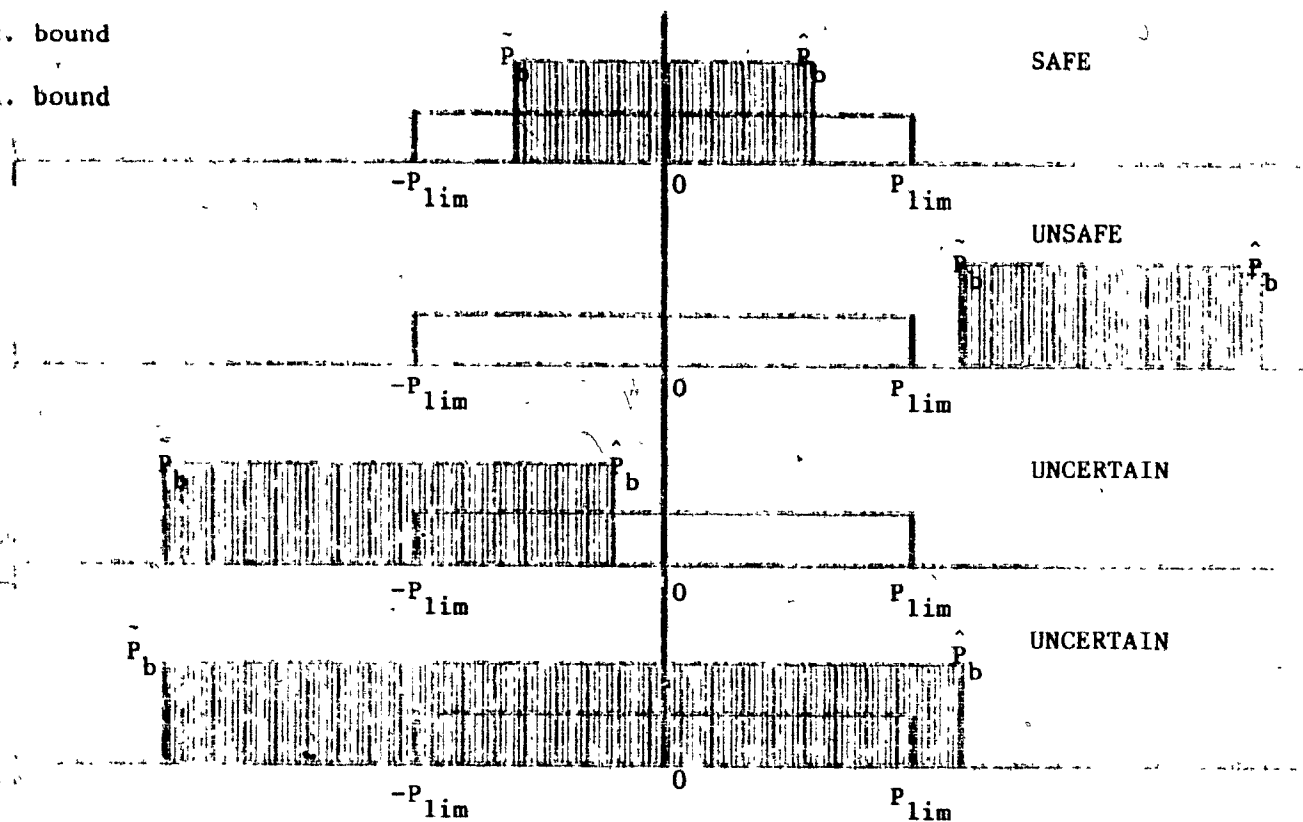


Fig. 3.1 Examples of Safe, Unsafe and Uncertain Contingency Flows

3.1.4 Critical, Non-critical and Uncertain Contingencies

Knowing how many safe, unsafe and uncertain contingency flows can be caused by a contingency, a decision on whether such a contingency is critical or not can be made, i.e.,

- (1) A contingency is said to be 'critical' if it has one or more unsafe contingency flows. Since the unsafe contingency flow(s) indicates definite violation(s), such a contingency is considered as a severe case.
- (2) A contingency is said to be 'non-critical' if all of its contingency flows are identified as safe.
- (3) A contingency is said to be 'uncertain' if it has one or more uncertain contingency flows. Since the uncertain contingency flows may result in violations, it is not possible to justify that the contingency is critical or non-critical. Further analysis will therefore be required.

3.1.5 Contingency Filters

A 'Contingency Filter (CF)' is defined as a filter which can eliminate the critical and non-critical contingencies from the incoming list of contingent events so that only the uncertain contingencies and their uncertain flows are sent to the output for further analysis.

These uncertain contingencies, along with their uncertain flows, are then submitted to the next CF where tighter bound estimates

are calculated, i.e.,

$$| \hat{P}_{lm/jk}^b - \tilde{P}_{lm/jk}^b | \geq | \hat{P}_{lm/jk}^{b+1} - \tilde{P}_{lm/jk}^{b+1} | \quad (3.6)$$

where b is a number used in this thesis to label different filters (e.g. $b=0$ for the first filter, $b=1$ for the second filter etc.). It has to be noted that only the uncertain flows in each uncertain contingency are required to be investigated in the subsequent filter because all other line flows belonging to the same uncertain contingency case have already been identified as safe flows.

A series of CFs (e.g. CF^b , CF^{b+1} , ... where $b=0,1,2, \dots$) can therefore be assembled in an ascending order according to the tightness of their bound estimates (as shown in Figure 2.6). Each subsequent filter is capable of calculating a set of tighter bounds for the uncertain contingency flows inherited from the previous filters. The final filter is a DC load flow simulation which calculates the exact values for the remaining uncertain flows.

Consequently, all postulated contingencies are separated into the 'critical' and the 'non-critical' groups. The critical group is then selected for more detailed examinations (e.g. full AC load flow simulations) and the non-critical group is excluded from the contingency list. Due to the filtering process, each filter has less contingencies required to be studied compared to the preceeding filter.

Furthermore, since only the uncertain contingency flows are required to be re-examined, the number of flow studies per contingency are also reduced. These merits are unique and desirable for such an analysis. In the sequel, the derivation of the above mentioned bound estimates is presented.

3.2 Derivation of Bound Estimates on the LODF

3.2.1 Derivation of the LODF

The following assumptions are made in order to derive the Line Outage Distribution Factor (LODF), i.e.,

- (A 3.1) The power system is represented by a DC model.
- (A 3.2) The net real power injections are unchanged.
- (A 3.3) The 'contingency' here means a single line outage case.

From (A 3.1), the relationships between the bus phase angles ($\underline{\delta}$) and the net real power injections (\underline{P}) can be written as follows, i.e.,

$$\underline{B} \underline{\delta}_{\text{base}} = \underline{P} \quad (3.8)$$

or

$$\underline{\delta}_{\text{base}} = \underline{B}^{-1} \underline{P} \quad (3.9)$$

where \underline{B} is the DC load flow Jacobian matrix of a $(n+1)$ bus power system (note : $\delta_i = 0$ at the reference bus and \underline{P} is the injections of all net P_i except the power injection at the reference bus). The subscript 'base' denotes that it is the 'base case' values. If the system is now subjected to a contingency (A 3.3), where (A 3.2) is also being applied, the new phase angle vector ($\underline{\delta}$) will become :

$$\underline{\delta}_{\text{cont}} = [\underline{B} - \underline{e}_{jk} \Delta y_{jk} \underline{e}_{jk}^T]^{-1} \underline{P} \quad (3.10)$$

where :

$\underline{\delta}_{\text{cont}} \triangleq$ contingency bus phase angles $(n \times 1)$.

$\Delta y_{jk} \triangleq$ the admittance value to be removed from the outage line connecting nodes j and k .

$$\underline{e}_{jk} \triangleq [0, \dots, \underset{\uparrow}{1}, \dots, \underset{\uparrow}{-1}, \dots, 0]^T_{(1 \times n)} \quad (3.11)$$

or

$$\underline{e}_{jk} \triangleq [0, \dots, \underset{\uparrow}{1}, \dots, \dots, 0]^T_{(1 \times n)} \quad (3.12)$$

(if k is the reference node)

or

$$\underline{e}_{jk} \triangleq [0, \dots, \dots, \underset{\uparrow}{-1}, \dots, 0]^T_{(1 \times n)} \quad (3.13)$$

(if j is the reference node)

Applying the matrix inversion lemma to expand the terms in (3.10), the following can be obtained, i.e.,

$$\underline{\delta}_{\text{cont}} = \left[\underline{B}^{-1} + \frac{\underline{B}^{-1} \underline{e}_{jk} \underline{e}_{jk}^T \underline{B}^{-1}}{\Delta y_{jk}^{-1} - \underline{e}_{jk}^T \underline{B}^{-1} \underline{e}_{jk}} \right] \underline{P} \quad (3.14)$$

$$= \underline{\delta}_{\text{base}} + \left[\frac{\underline{B}^{-1} \underline{e}_{jk} \underline{e}_{jk}^T}{\Delta y_{jk}^{-1} - \underline{e}_{jk}^T \underline{B}^{-1} \underline{e}_{jk}} \right] \underline{\delta}_{\text{base}} \quad (3.15)$$

Again from (A 3.1), the real power flows can be expressed in a linear form as follows, i.e.,

$$P_{lm} = y_{lm} \underline{e}_{lm}^T \underline{\delta} \quad (3.16)$$

where :

P_{lm} $\underline{\Delta}$ real power flow of the line connecting nodes 1 and m.

y_{lm} $\underline{\Delta}$ line admittance of the line connecting nodes 1 and m.

\underline{e}_{lm} $\underline{\Delta}$ same as (3.11-3.13) except nodes j and k are replaced by nodes 1 and m.

Substituting (3.15) in (3.16), the following is obtained, i.e.,

$$P_{lm/jk} = y_{lm} \underline{e}_{lm}^T \left[\underline{\delta}_{\text{base}} + \left(\frac{\underline{B}^{-1} \underline{e}_{jk} \underline{e}_{jk}^T}{\Delta y_{jk}^{-1} - \underline{e}_{jk}^T \underline{B}^{-1} \underline{e}_{jk}} \right) \underline{\delta}_{\text{base}} \right] \quad (3.17)$$

$$P_{lm/jk} = P_{lm} + \frac{y_{lm} \left(\underline{e}_{lm}^T \underline{B}^{-1} \underline{e}_{jk} \right)}{y_{jk} \left(\Delta y_{jk}^{-1} - \underline{e}_{jk}^T \underline{B}^{-1} \underline{e}_{jk} \right)} P_{jk} \quad (3.18)$$

where :

$P_{lm/jk}$, P_{lm} , P_{jk} have the same definitions as shown in (3.1).

$y_{jk} \triangleq$ admittance of the outage line.

(3.18) is obtained from multiplying the second term in (3.17) by y_{jk}/y_{jk} and combining $y_{jk} \underline{e}_{jk}^T \underline{\delta}_{base}$ to obtain P_{jk} .

Now defining :

$$P_{lm/jk} \triangleq \frac{y_{lm}}{y_{jk}} \frac{x_{lm/jk}}{(\Delta y_{jk}^{-1} - x_{jk})} \quad (3.19)$$

\triangleq Line Outage Distribution Factor (LODF)

where :

$$x_{lm/jk} \triangleq \underline{e}_{lm}^T \underline{B}^{-1} \underline{e}_{jk} \quad (3.20)$$

$$x_{jk} \triangleq \underline{e}_{jk}^T \underline{B}^{-1} \underline{e}_{jk} \quad (3.21)$$

(3.18) can thus be re-written as follows, i.e.,

$$P_{lm/jk} = P_{lm} + \rho_{lm/jk} P_{jk} \quad (3.22)$$

which is the same as (3.1) and hence the LODF is derived. It is easy to notice that the LODF is independent of the pre-contingency flows but only depends on the system structure and parameters (e.g. y_{lm} and y_{jk}) and two distinct values, defined as ' x_{jk} ' and ' $x_{lm/jk}$ '.

The approach taken to derive the bounds for the LODF is therefore to establish bounds on ' x_{jk} ' and ' $x_{lm/jk}$ '.

3.2.2 Bounding the LODF in Terms of x_{jk} and $x_{lm/jk}$

Intuitively, the extreme bounds of the LODF defined in the previous section can be conjectured as follows, i.e.,

$$-1 \leq \rho_{lm/jk} \leq 1 \quad (3.23)$$

The reason is that it is not possible to have more power distributed into the system than the total original power being transferred through the outaged line.

However, these bounds are somewhat too conservative. In order to tighten the bounds on $\rho_{lm/jk}$, the values of $x_{lm/jk}$ and

x_{jk} defined in (3.20) to (3.21) are bounded. In the following sections, different bounds on $x_{lm/jk}$ and x_{jk} will be derived and explained. At the moment, it is assumed that the upper and lower bounds on $x_{lm/jk}$ and x_{jk} are already known as follows, i.e.,

$$\tilde{x}_{lm/jk}^{bn} \leq x_{lm/jk} \leq \hat{x}_{lm/jk}^{bn} \quad (3.24)$$

$$\tilde{x}_{jk}^{bn} \leq x_{jk} \leq \hat{x}_{jk}^{bn} \quad (3.25)$$

where bn is a number used in this thesis to denote the type of bound.

For example, it is shown later that the extreme bounds of x_{jk} are as follows, i.e.,

$$\tilde{x}_{jk}^0 \triangleq 0 \leq x_{jk} \leq \frac{1}{y_{jk}} \triangleq \hat{x}_{jk}^0 \quad (3.26)$$

Hence, the bounds on the LODF in terms of the bounds of $x_{lm/jk}$ and x_{jk} can be expressed as follows, i.e.,

(1) Maximum LODF, $\hat{\rho}_{lm/jk}^{bn}$

Case 1 : $\hat{x}_{lm/jk}^{bn} > 0$

$$\hat{\rho}_{lm/jk}^{bn} = \frac{y_{lm}}{y_{jk}} \cdot \frac{\hat{x}_{lm/jk}^{bn}}{(\Delta y_{jk}^{-1} - \hat{x}_{jk}^{bn})} \quad (3.27)$$

Case 2 : $\hat{x}_{lm/jk}^{bn} < 0$

$$\hat{\rho}_{lm/jk}^{bn} = \frac{y_{lm}}{y_{jk}} \cdot \frac{\hat{x}_{lm/jk}^{bn}}{(y_{jk}^{-1} - \tilde{x}_{jk}^{bn})} \quad (3.28)$$

(2) Minimum LODF, $\tilde{x}_{lm/jk}^{bn}$

Case 3 : $\tilde{x}_{lm/jk} > 0$

$$\tilde{x}_{lm/jk}^{bn} = \frac{y_{lm}}{y_{jk}} \cdot \frac{\tilde{x}_{lm/jk}^{bn}}{(\Delta y_{jk}^{-1} - \tilde{x}_{jk}^{bn})} \quad (3.29)$$

Case 4 : $\tilde{x}_{lm/jk} < 0$

$$\tilde{x}_{lm/jk}^{bn} = \frac{y_{lm}}{y_{jk}} \cdot \frac{\tilde{x}_{lm/jk}^{bn}}{(\Delta y_{jk}^{-1} - \tilde{x}_{jk}^{bn})} \quad (3.30)$$

It is possible that the bounds obtained from any one of the equations shown above, i.e. (3.27) to (3.30) will give values larger than 1 or smaller than -1. This is because of the bounds used for $\tilde{x}_{lm/jk}$ and \tilde{x}_{jk} may be too conservative. In cases like this, the calculated bounds should be adjusted to the closest LODF extreme bounds (i.e. either 1 or -1).

3.2.3 Resistive Network Interpretation of $\tilde{x}_{lm/jk}$ and \tilde{x}_{jk}

A resistive network, which has exactly the same structure as the DC model and where its conductances also assume the same values as the corresponding susceptances, can be used to derive a circuit interpretation of $\tilde{x}_{lm/jk}$ and \tilde{x}_{jk} .

From basic circuit theory, the voltage-current relationships of a resistive network can be expressed as follows, i.e.,

$$\underline{V} = \underline{Y}^{-1} \underline{I} \quad (3.31)$$

where :

$\underline{V} \triangleq$ nodal voltages with respect to the reference node.

$\underline{I} \triangleq$ nodal current injections.

$\underline{Y} \triangleq$ conductance matrix.

The following analogies are then made, i.e.,

$$\underline{Y} \longleftrightarrow \underline{B} \quad (3.32)$$

$$\underline{I} \longleftrightarrow \underline{e}_{jk} \quad (3.33)$$

Recalling the definitions of $x_{lm/jk}$ and x_{jk} from (3.20) and (3.21), i.e.,

$$x_{lm/jk} \triangleq \underline{e}_{lm}^T \underline{B}^{-1} \underline{e}_{jk} \quad (3.34)$$

$$x_{jk} \triangleq \underline{e}_{jk}^T \underline{B}^{-1} \underline{e}_{jk} \quad (3.35)$$

The term $(\underline{B}^{-1} \underline{e}_{jk})$ in both definitions can thus be represented by a nodal voltage vector (\underline{V}) using the analogies proposed in (3.32) and (3.33). Such a voltage vector (\underline{V}) is obtained from (3.31) by injecting a unit current at node j and removing it completely from node k .

of the resistive network. Therefore, according to (3.34) and (3.35) $x_{lm/jk}$ and x_{jk} can be viewed as the voltage difference between nodes 1 and m, and the voltage difference between nodes j and k respectively, i.e.,

$$x_{lm/jk} = (V_1 - V_m) \Big|_{I_j=1, I_k=-1} \quad (3.36)$$

$$x_{jk} = (V_j - V_k) \Big|_{I_j=1, I_k=-1} \quad (3.37)$$

where :

$V_1, V_m, V_j, V_k \triangleq$ the 1, m, j, k terms in \underline{V} defined in (3.31).

$I_j, I_k \triangleq$ the j, k terms in \underline{I} defined in (3.31) and (3.33).

Next, if nodes j,k and nodes 1,m are thought of as forming two-ports of the resistive network as shown in Figure 3.2, the two-port voltage-current transfer functions can be written as follows, i.e.,

$$\begin{bmatrix} V_{jk} \\ V_{lm} \end{bmatrix} = \begin{bmatrix} z_{jk} & z_{jk/lm} \\ z_{lm/jk} & z_{lm} \end{bmatrix} \begin{bmatrix} I_{jk} \\ I_{lm} \end{bmatrix} \quad (3.38)$$

where :

$V_{jk}, V_{lm} \triangleq$ voltages across port(j,k) and port(1,m) respectively.

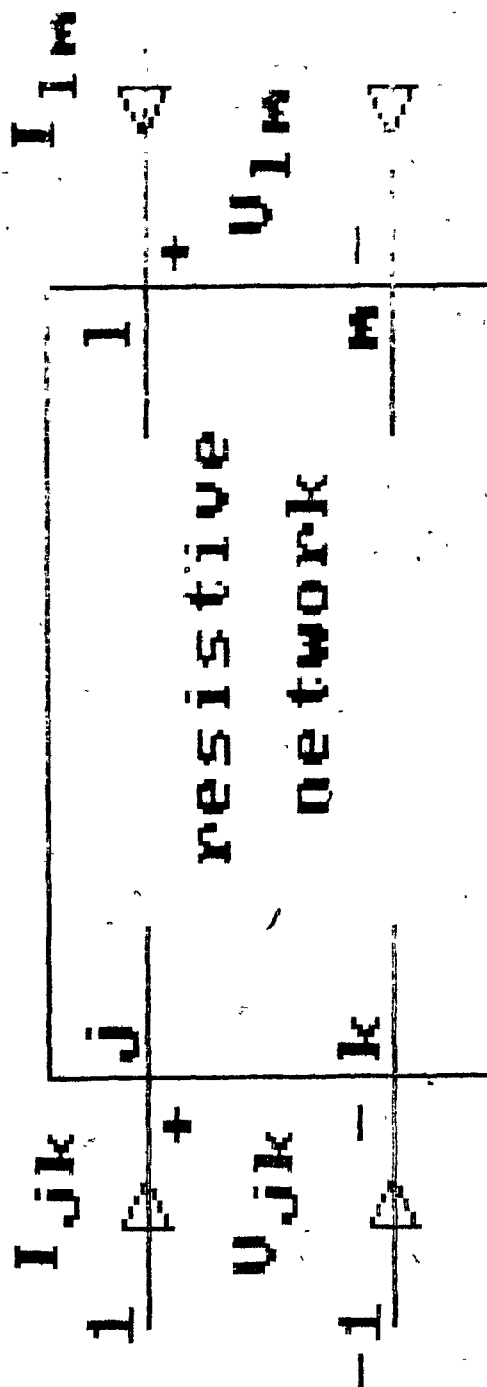


Fig. 3.2 Two-port Resistive Network

$I_{jk}, I_{lm} \triangleq$ current injected at port(j,k) and port(l,m), in the directions as shown, respectively.

$z_{jk}, z_{lm} \triangleq$ input resistance looking in from port (j,k) and port(l,m) respectively.

$z_{jk/lm}, z_{lm/jk} \triangleq$ transfer resistances from port(j,k) to port(l,m) and vice versa.

Since I_{lm} is always zero in this case (i.e. unit current is only injected at node j and removed at node k), the transfer and input resistances defined above for this two-port resistive network can be written as follows, i.e.,

$$z_{lm/jk} = z_{jk/lm} = \left. \frac{V_{lm}}{I_{jk}} \right|_{I_{lm} = 0} \quad (3.39)$$

$$z_{jk} = \left. \frac{V_{jk}}{I_{jk}} \right|_{I_{lm} = 0} \quad (3.40)$$

Finally, since I_{jk} is always unity, (3.39) and (3.40) are indeed the same as (3.36) and (3.37). Therefore $x_{lm/jk}$ and x_{jk} can be interpreted as the 'transfer resistance' and 'input resistance' of this equivalent resistive network looking in from port (j,k).

3.2.4 Extreme Bounds on $x_{lm/jk}$ and x_{jk}

After recognizing such a resistive network interpretation, some network topological characteristics can be applied to evaluate the bounds of $x_{lm/jk}$ and x_{jk} . The most primitive bounds on $x_{lm/jk}$ and x_{jk} can thus be easily derived as shown in the following.

The extreme cases of the 'transfer resistance' ($x_{lm/jk}$) are to be considered first. From a circuit point of view, $x_{lm/jk}$ from (3.36) can also be thought of as follows, i.e.,

$$x_{lm/jk} = \frac{i_{lm}}{y_{lm}} \quad (3.41)$$

where :

$i_{lm} \triangleq$ current through branch(1,m).

$y_{lm} \triangleq$ conductance of branch(1,m).

Hence, $x_{lm/jk}$ will be extremized if the current through branch(1,m) is extremized, i.e. maximizing i_{lm} will give $\hat{x}_{lm/jk}$ and minimizing i_{lm} will give $\tilde{x}_{lm/jk}$.

Figure 3.3 depicts an extreme connection pattern which will give the highest possible current, denoted by \hat{i}_{lm} , through

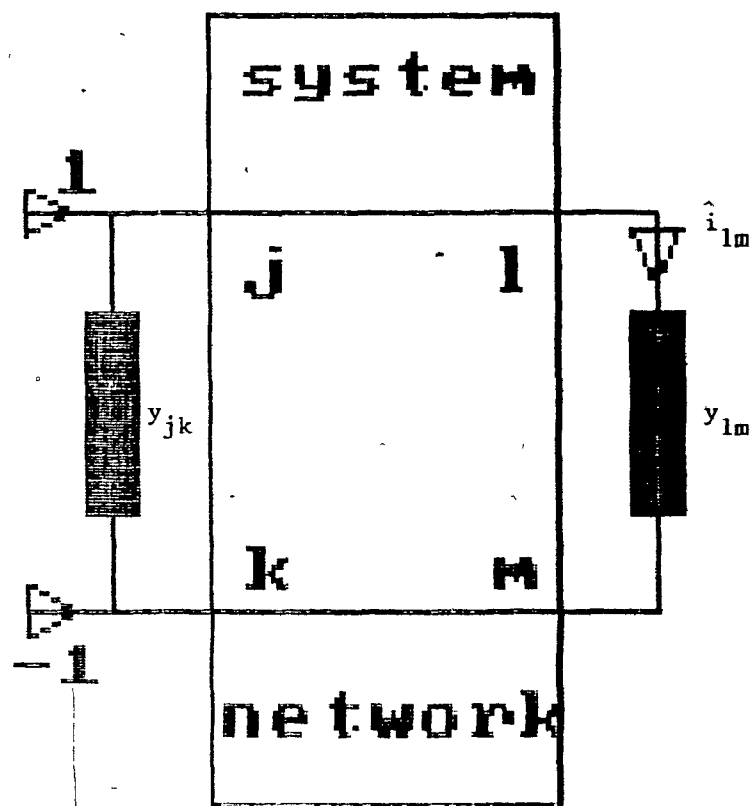


Fig. 3.3 Extreme Connection for $\hat{x}_{lm/jk}^0$

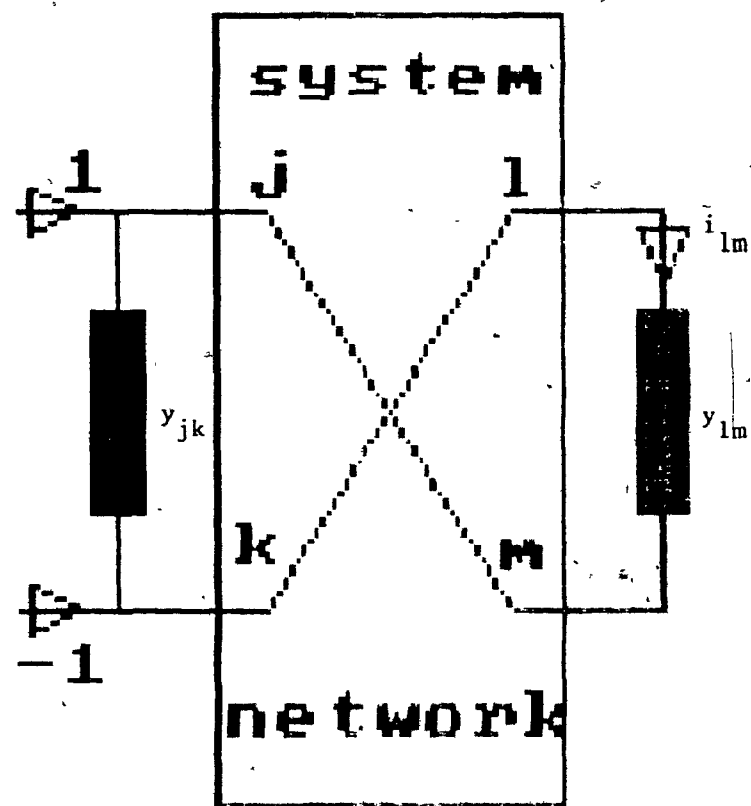


Fig. 3.4 Extreme Connection for $\hat{x}_{lm/jk}^0$

branch(1,m), i.e.,

$$\hat{i}_{lm} = \frac{y_{lm}}{y_{jk} + y_{lm}} \quad (3.42)$$

For the other extreme case, Figure 3.4 shows the reverse connection which will yield the smallest possible current, denoted by \tilde{i}_{lm} , through branch(1,m), i.e.,

$$\tilde{i}_{lm} = \frac{-y_{lm}}{y_{jk} + y_{lm}} = -\hat{i}_{lm} \quad (3.43)$$

Substituting (3.42) and (3.43) into (3.41), the first set of bounds on $x_{lm/jk}$ can be written as follows, i.e.,

$$\frac{-1}{y_{jk} + y_{lm}} \triangleq \tilde{x}_{lm/jk}^0 \leq x_{lm/jk} \leq \hat{x}_{lm/jk}^0 \triangleq \frac{1}{y_{jk} + y_{lm}} \quad (3.44)$$

Note that the bound type (bn) is denoted by a zero, meaning that it is the extreme bound type.

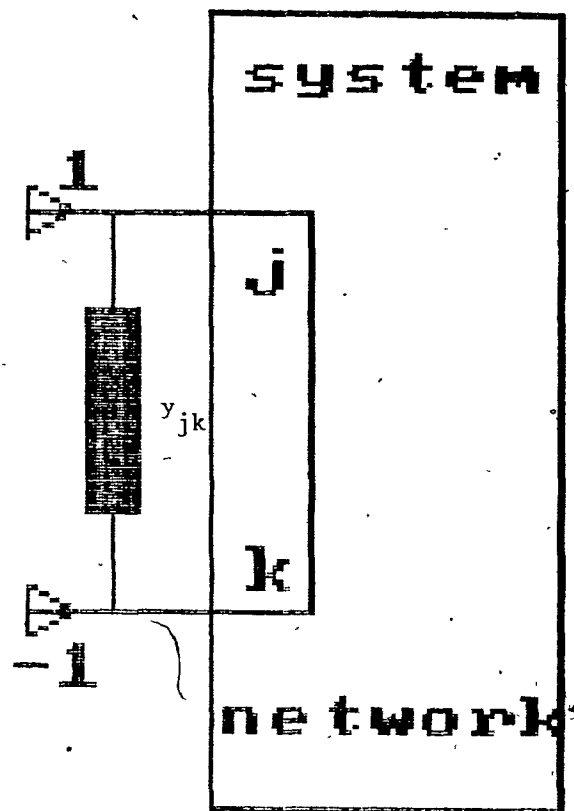


Fig. 3.5 Extreme Connection for \hat{x}_{jk}^0

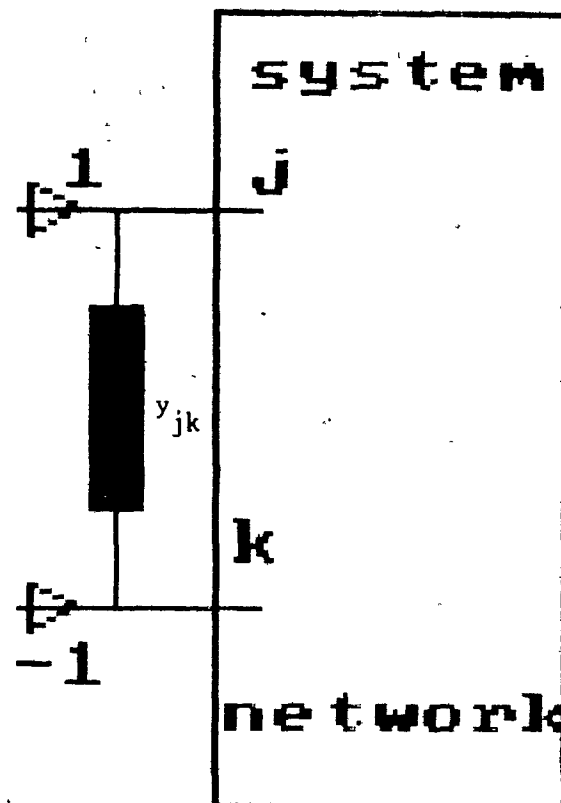


Fig. 3.6 Extreme Connection for \hat{x}_{jk}^0

Next, the extreme bounds on the 'input resistance' (x_{jk}) are considered. In Figures 3.5 and 3.6, two extreme connection patterns are shown. Figure 3.5 shows that nodes j and k are shorted inside the system, hence it will give a zero input resistance value, i.e. $\tilde{x}_{jk} = 0$. Figure 3.6 shows that nodes j and k are opened inside the network such that the input resistance is the resistance of branch(j,k) itself only, i.e. $\hat{x}_{jk} = 1/y_{jk}$. As a result, the first set of bounds on x_{jk} can be written as follows, i.e.,

$$0 \triangleq \tilde{x}_{jk}^0 \leq x_{jk} \leq \hat{x}_{jk}^0 \triangleq \frac{1}{y_{jk}} \quad (3.45)$$

hence, (3.45) verifies (3.26) stated in previous section.

3.2.5 Tighter Bounds on the Input Resistance (x_{jk})

To establish bounds on the 'input resistance' (x_{jk}) in general, with the resistive network interpretation described above, the original network is first split into two sub-networks. These two sub-networks are denoted as N_1 and N_2 as shown in Figure 3.7.

N_1 is called the 'retained' network [Galiana 1984] which is composed of at least nodes j and k (the ending nodes of the outaged branch) and possibly a few more other nodes adjacent to nodes j and k . N_2 is the remainder of the original network excluding N_1 . N_1 and N_2

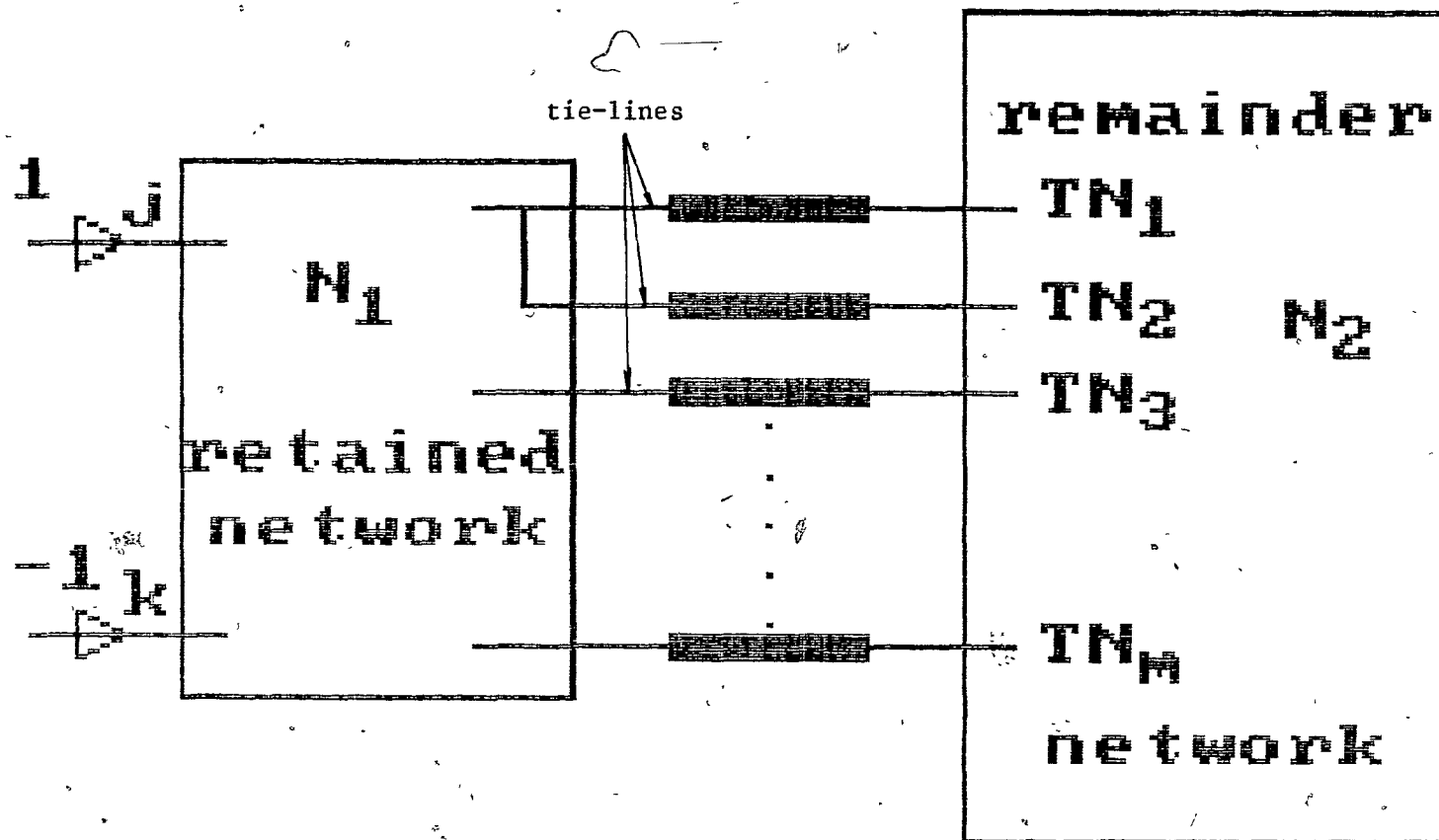


Fig. 3.7 Network Subdivision

are connected to each other by a number of so-called 'tie-lines'. The ending nodes of these 'tie-lines' in N_2 are labeled as follows, i.e.,

$$\Phi = \{ TN_i \mid i=1,2,3,\dots,m \} \quad (3.46)$$

where :

Φ Δ the set of all the ending nodes of the 'tie-line' in N_2 .

TN_i Δ tie-line node i in N_2 .

m Δ total number of tie-line nodes in N_2 .

After separating the original network into N_1 and N_2 , the upper and lower bounds on the input resistance (x_{jk}) looking in from the port defined by the nodes j and k can be established by considering the following two equivalent networks shown in Figures 3.8 and 3.9 .

In both figures, the connections between the tie-lines and the nodes j and k in N_1 are intentionally left out to allow different number of nodes to be retained for the network N_1 according to different bound types. They are not opened inside N_1 but rather all connected with the nodes in N_1 .

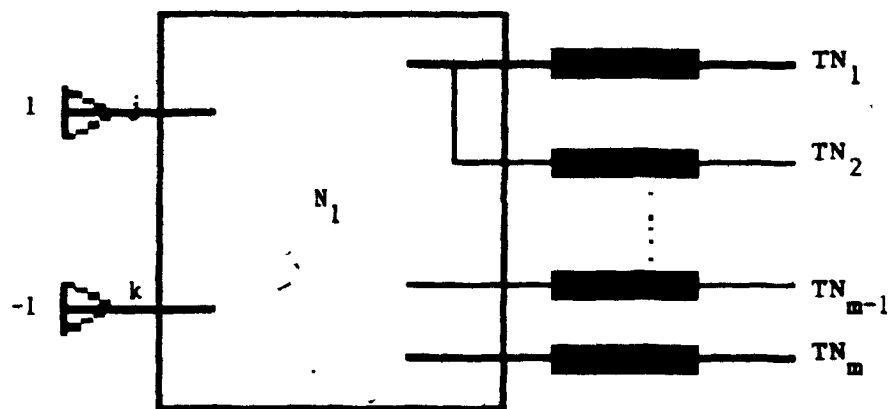


Fig. 3.8 N_1 with Tie-lines Opened

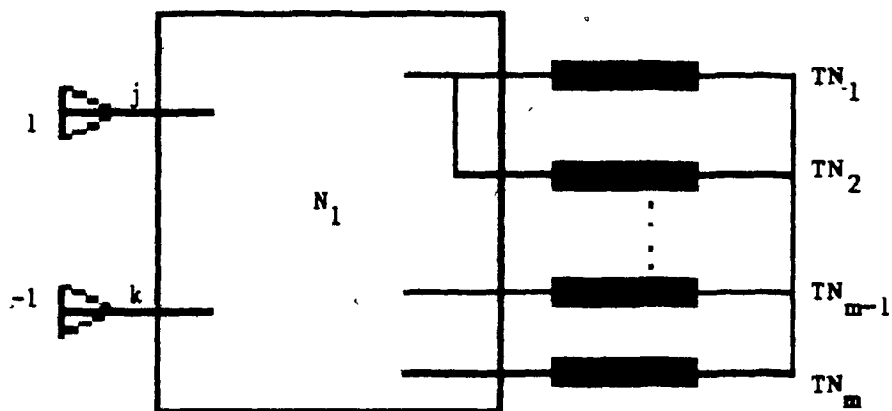


Fig. 3.9 N_1 with Tie-lines Shorted

In Figure 3.8, all tie-lines are opened at their tie-line nodes (i.e. TN_i , for all i) and hence separating N_1 and N_2 . The resulting input resistance looking in from the port defined by the nodes j and k will therefore give the maximum input resistance (\hat{x}_{jk}) of the complete network, i.e. $N_1 + N_2$, looking in at port(j,k). This is due to the fact that any connections beyond the tie-line nodes will only reduce the value of this x_{jk} .

To evaluate \hat{x}_{jk} , the following modifications are made to (3.21), i.e.,

$$\hat{x}_{jk}^{bn} = \underline{e}_{rjk}^T (\hat{\underline{B}}_r^{bn})^{-1} \underline{e}_{rjk} \quad (3.47)$$

where :

$bn \triangleq$ a number used to denote the type of bound.

$\underline{e}_{rjk} \triangleq [0, \dots, \underset{j'}{\uparrow} 1, \dots, \underset{k'}{\uparrow} -1, \dots, 0]^T_{(nrn \times 1)}$

$j', k' \triangleq$ the nodes in the retained network corresponding to the nodes j and k .

$nrn \triangleq$ total number of nodes in the retained network N_1 .

$\hat{\underline{B}}_r^{bn} \triangleq$ conductance matrix of N_1 , where all tie-line conductances are neglected.

Since $\hat{\underline{B}}_r^{bn}$ in (3.47) is a singular matrix, a reference node has to be specified here in order that (3.47) can be evaluated. In this thesis,

the node k' (corresponding to node k in the complete network) is chosen as the reference node.

For the lower bound of the input resistance (\tilde{x}_{jk}), Figure 3.9 shows the other extreme connection pattern. All the tie-lines are now shorted at their tie-line nodes (i.e. TN_i , for all i). In this case, the input resistance will yield a minimum value of the input resistance (\tilde{x}_{jk}) of the complete network. This is because any non-zero conductances connecting the tie-lines beyond their tie-line nodes will only increase the value of the input resistance obtained from this connection pattern.

To evaluate \tilde{x}_{jk} , the following is used, i.e.,

$$\tilde{x}_{jk}^{bn} = \underline{e}_{rjk}^T (\underline{B}_r^{bn})^{-1} \underline{e}_{rjk} \quad (3.48)$$

where :

$$\begin{array}{ll} \underline{e}_{rjk} & \Delta \text{ same definition as in (3.47)} \\ \underline{B}_r^{bn} & \Delta \text{ conductance matrix of } N_1, \text{ where all tie-} \\ & \text{lines conductances are included.} \end{array}$$

Noted that in Figure 3.9, an additional node is created at the common point where all tie-lines are shorted. This point is then used as the reference point in order that (3.48) can be evaluated.

By inspection, the simplest and smallest retained network will be the one which only includes branch(j,k). This will eventually give the extreme cases of x_{jk} as described previously in (3.45), i.e.,

$$0 \leq \tilde{x}_{jk}^0 \leq x_{jk} \leq \hat{x}_{jk}^0 \leq \frac{1}{y_{jk}} \quad (3.49)$$

These bounds are very easy to obtain but also too conservative because the upper bound will cause (3.27) and (3.30) to go to infinity. Hence, less conservative bounds are required. This can be accomplished by including some adjacent nodes near the nodes j and k. However, in order to ensure that the upper bound will be less than the upper bound depicted in (3.49), the retained network (N_1) must contain at least one closed loop which includes the outaged branch(j,k). Therefore the next set of bounds on x_{jk} will be defined by a retained network composed of all the nodes which form such a loop. By using the bound type number (bn) to denote the number of closed loop, the next type of bound on x_{jk} can be written as :

$$\tilde{x}_{jk}^1 \leq x_{jk} \leq \hat{x}_{jk}^1 \quad (3.50)$$

where :

$$\tilde{x}_{jk}^1 \triangleq \underline{e}_{rjk}^T (\tilde{B}_r^1)^{-1} \underline{e}_{rjk} \quad (3.51)$$

$$\hat{x}_{jk}^1 \triangleq \underline{e}_{rjk}^T (\hat{B}_r^1)^{-1} \underline{e}_{rjk} \quad (3.52)$$

For an even tighter bound, the retained network will consist two closed loop and the type of bound on x_{jk} is denoted as follows, i.e.,

$$\tilde{x}_{jk}^2 \leq x_{jk} \leq \tilde{x}_{jk}^2 \quad (3.53)$$

where :

$$\tilde{x}_{jk}^2 \triangleq \underline{e}_{rjk}^T (\underline{B}_r^2)^{-1} \underline{e}_{rjk} \quad (3.54)$$

$$\hat{x}_{jk}^2 \triangleq \underline{e}_{rjk}^T (\hat{B}_r^2)^{-1} \underline{e}_{rjk} \quad (3.55)$$

Theoretically speaking, if more loops are used until all nodes in the system are included, N_1 will become the complete network and the bounds will be the same, i.e.,

$$\tilde{x}_{jk}^\infty \longrightarrow x_{jk} \longleftarrow \hat{x}_{jk}^\infty \quad (3.56)$$

where :

∞ \triangleq denoting the bound type where all nodes in the system are included N_1 .

However, in order to simplify the calculations, the more conservative bounds (i.e. bounds with only one or two closed loops) are used. Since the dimensionality of equation (3.47) and (3.48) are small, they can be efficiently and rapidly solved (e.g. by LU factorization

and backward-forward substitutions).

There are two cases which require special attentions here because no closed loop will be found in these kind of configurations.

Case 1 Islanding line : In Figure 3.10, branch(j,k) is the only connection between area A and area B. Should branch(j,k) is disconnected, the system is split into two sub-systems. For instance, a tie-line connecting two major systems is a typical example. In this kind of configuration, no closed loop can be established and hence the bounding of x_{jk} will fail. Usually a DC load flow simulation is required to detect such a configuration.

Case 2 Semi-independent line : In Figure 3.11, branch(j,k) is called a 'semi-independent' line in this thesis. This is actually a special case of the preceeding one. However, there is only one node (in this figure, it is node k) isolated from the main network after the outage. Because of the single node isolation, this case is relatively easiler to be detected.

Both cases are considered as critical contingencies as soon as they are detected. This is due to the fact that they both will generally create a large imbalance of the energy supply, e.g. isolating a small area from the main grid or disconnecting a remote hydro-station.

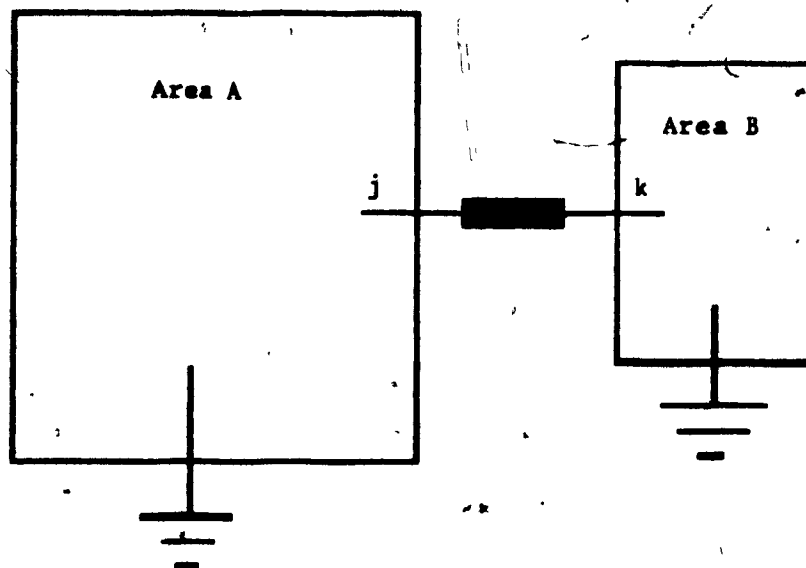


Fig. 3.10 Islanding Line

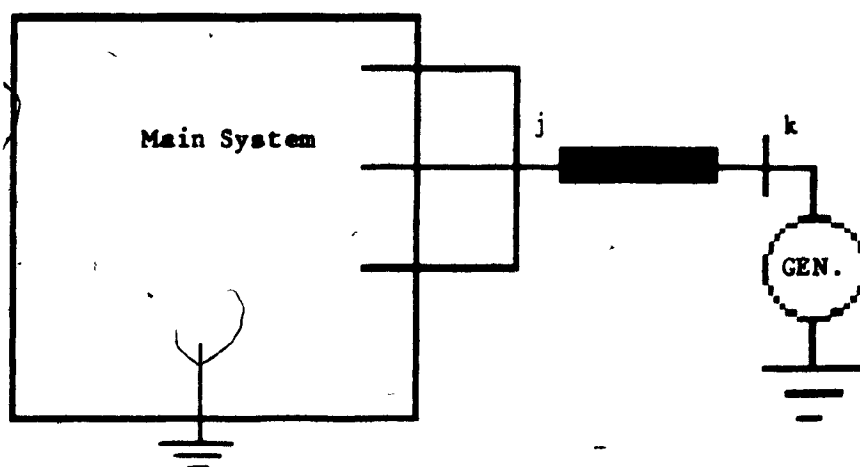


Fig. 3.11 Semi-independent Line

In the original proposal of this bounding method [Galiana 1984], the retained nodes of N_1 are selected by inspection. However, the present study has developed an algorithm, the so-called Automatic Loop Searcher (ALS), to systematically look for the necessary nodes (i.e. those will form a loop). Also, such an algorithm will be able to identify the 'semi-independent' lines in the system. Should an outaged line not be found with at least one closed loop, such a contingency will by-pass the other filters and will be directly submitted to the final filter, i.e. the DC load flow, for analysis. If this contingency is indeed an 'islanding' line, it will be detected by the DC load flow.

The bounds on x_{jk} can also be derived from other approaches, a more theoretical approach using the partitioned matrices of \underline{B} was also introduced by Galiana [Galiana 1984]. However, such a theoretical bound is more computationally demanding. The network interpretation approach is chosen in this study because it is relatively simple to derive and to evaluate.

3.2.6 Tighter Bounds on $x_{lm/jk}$, the Transfer Resistance'

3.2.6.1 Type 1 Bound on $x_{lm/jk}$

Occasionally, the extreme bounds developed are not sufficiently tight enough. Indeed, it is shown in a later chapter that the numerical values are too conservative. It is very often that a less

conservative set of bound estimates is required. In the following, a set of tighter bounds are developed by including more information on the structure of the network.

A generalized retained network, denoted by M_1 , is extracted from the original network as shown in Figure 3.12. The remaining network is denoted by M_2 . The retained network M_1 is characterized by consisting only four nodes, i.e. nodes j, k, l, m . Nodes j and k are the ending nodes of the outaged branch (j, k) , and l and m are the ending nodes of any arbitrary branch (l, m) . As shown in Figure 3.12, the retained nodes are assumed to be directly connected to each other by branch (j, l) , branch (j, m) , branch (k, l) and branch (k, m) . These 'direct links' are shown as shaded elements in Figure 3.12. The non-shaded elements represent the equivalent connections between the retained nodes and the remaining network M_2 . Their admittance values can be written as :

$$yy_j = \sum_{r=1}^{\alpha} y_{jr} \quad \text{where } j, k, l, m \notin \alpha \quad (3.57)$$

$$yy_k = \sum_{r=1}^{\beta} y_{kr} \quad \text{where } j, k, l, m \notin \beta \quad (3.58)$$

$$yy_l = \sum_{r=1}^{\mu} y_{lr} \quad \text{where } j, k, l, m \notin \mu \quad (3.59)$$

$$yy_m = \sum_{r=1}^{\nu} y_{mr} \quad \text{where } j, k, l, m \notin \nu \quad (3.60)$$

where α, β, μ, ν are the index sets of the nodes which nodes j, k, l, m are connected to in M_2 .

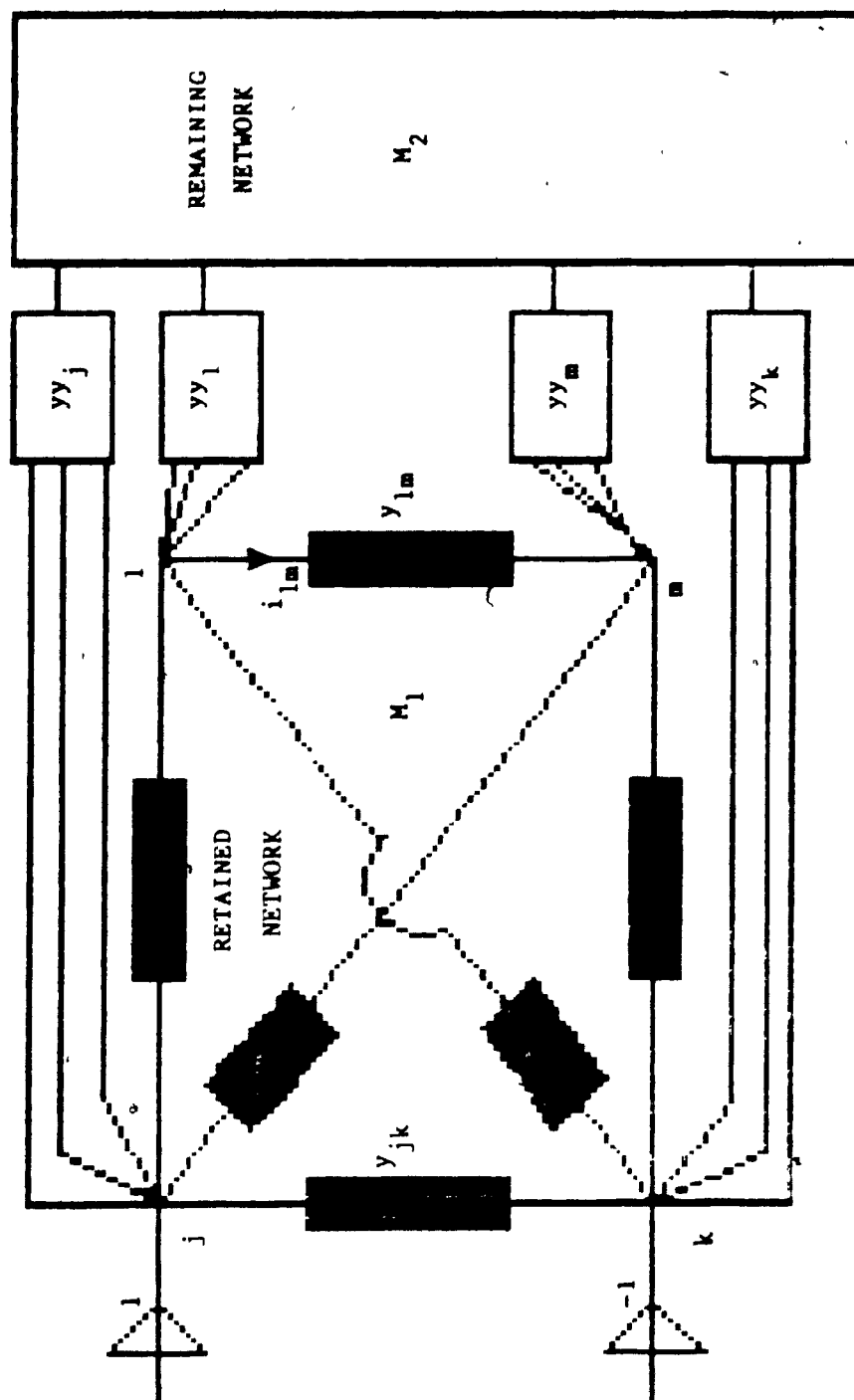


Fig. 3.12 Network Subdivision for $x_{lm/jk}$ Bound

Evaluations

After introducing such a retained network perspective and recalling the two-port resistive network interpretation of $x_{lm/jk}$ introduced earlier, a set of bound estimates can be developed by considering only M_1 and its equivalent connection elements only.

Depending on the values of the direct links (i.e. y_{jl} , y_{jm} , y_{kl} , y_{km}), three different cases are considered and they are explained in the following.

Case a : No direct connection between branch(j,k) and branch(l,m).

If there are no direct links, i.e. $y_{jl} = y_{jm} = y_{kl} = y_{km} = 0$, Figures 3.13 and 3.14 will show two extreme connection patterns where maximum and minimum currents will flow through branch(l,m) respectively (Recall the argument introduced in 3.2.3 that maximizing (or minimizing) the current through branch(l,m) gives the maximum (or minimum) value of $x_{lm/jk}$).

In Figure 3.13, where yy_j , yy_l , y_{lm} , yy_m , yy_k are connected in sequence, the current i_{lm} will have the maximum value because any non-zero element added between yy_j and yy_l , and yy_m and yy_k can only reduce the magnitude of this calculated i_{lm} . Hence the upper bound of $x_{lm/jk}$ for this case can be expressed as :

$$\hat{x}_{lm/jk}^{1a} = \frac{y_{eq}}{y_{jk} + y_{eq}} \cdot \frac{1}{y_{lm}} \quad (3.61)$$

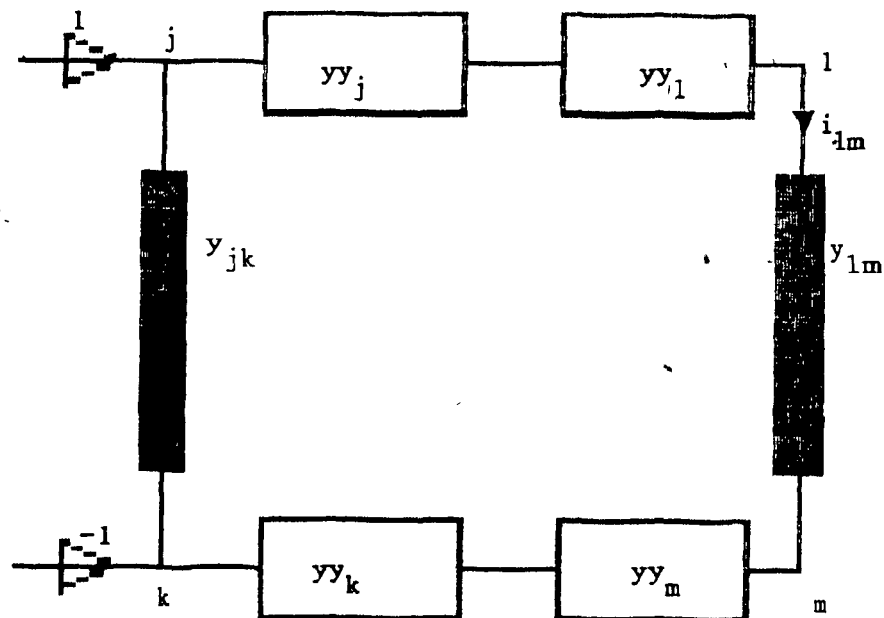


Fig. 3.13 Extreme Connection Pattern for $\hat{x}_{lm/jk}^{la}$

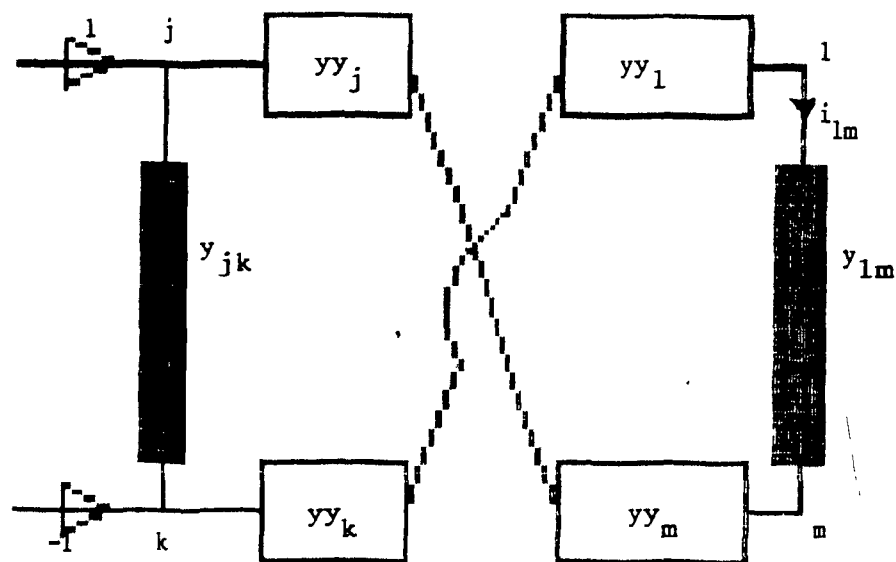


Fig. 3.14 Extreme Connection Pattern for $\tilde{x}_{lm/jk}^{la}$

where :

$$y_{eq} = \left(\frac{1}{yy_j} + \frac{1}{yy_l} + \frac{1}{y_{lm}} + \frac{1}{yy_m} + \frac{1}{yy_k} \right)^{-1} \quad (3.62)$$

The lower bound is obtained in a similar fashion but the connection sequence is now reversed, i.e. $yy_j, yy_m, y_{lm}, yy_l, yy_k$, as shown in Figure 3.14. Note that such a connection also gives the same magnitude of current as (3.61) but with the sign reversed, therefore :

$$\tilde{x}_{lm/jk}^{la} = - \hat{x}_{lm/jk}^{la} \quad (3.63)$$

Case b : Direct connections exist between branch(j,k) and branch(l,m).

Should any one of $y_{jl}, y_{jm}, y_{kl}, y_{km}$ be a non-zero term, the outaged branch(j,k) will be directly connected to the arbitrary branch(l,m). In this case, the evaluation method presented in the preceeding case does not apply because the current i_{lm} now depends on the nature of the connection and also the relative values of the direct links.

The minimum and maximum values on i_{lm} can be analyzed in the following manner. First, M_1 is separated from M_2 and to be considered as a 4-node network. Meanwhile, for the time being, the equivalent elements (e.g. yy_j, yy_k , etc.) are also neglected.

By injecting a unit current at node j and removing it at node k , the nodal equations of this 4-node network can be written as follows, i.e. (with node k chosen as the reference node),

$$\begin{bmatrix} y_1 & -y_{j1} & -y_{jm} \\ -y_{j1} & y_2 & -y_{lm} \\ -y_{jm} & -y_{lm} & y_3 \end{bmatrix} \begin{bmatrix} V_j \\ V_1 \\ V_m \end{bmatrix} = \begin{bmatrix} 1 \\ 0 \\ 0 \end{bmatrix} \quad (3.64)$$

where :

$$y_1 = y_{jk} + y_{jm} + y_{j1} \quad (3.64a)$$

$$y_2 = y_{j1} + y_{lk} + y_{lm} \quad (3.64b)$$

$$y_3 = y_{lm} + y_{jm} + y_{mk} \quad (3.64c)$$

Recall from 3.2.5, i.e. the resistive network interpretation of $x_{lm/jk}$, by solving (3.64), the transfer resistance ($x_{lm/jk}$) can be obtained as follows, i.e.,

$$x_{lm/jk}^{lb} = V_1 - V_m \quad (3.65)$$

Next, consider Figures 3.15 to 3.17. These figures depict three extreme and possible connection patterns of the equivalent connection elements in M_2 . It can be thought of as that these different connections are actually adding parallel branches to the direct links. To which direct links that it is going to affect depends on the connection pattern. Hence, the value of $x_{lm/jk}^{lb}$ in these three conditions can be evaluated as follows, i.e.,

- (i) For Figure 3.15, the following adjustments are made to the direct links, i.e.,

$$y_{jl}^{\text{new}} = y_{jl} + \left(\frac{1}{yy_j} + \frac{1}{yy_l} \right)^{-1} \quad (3.66)$$

$$y_{km}^{\text{new}} = y_{km} + \left(\frac{1}{yy_k} + \frac{1}{yy_m} \right)^{-1} \quad (3.67)$$

y_{jl}^{new} and y_{km}^{new} thus replace the original y_{jl} and y_{km} in (3.64), the result obtained from solving (3.64) and (3.65) is then denoted as $(x_{lm/jk}^{\text{lb}})_1$.

- (ii) For Figure 3.16, the following adjustments are made :

$$y_{jk}^{\text{new}} = y_{jk} + \left(\frac{1}{yy_j} + \frac{1}{yy_k} \right)^{-1} \quad (3.68)$$

$$y_{lm}^{\text{new}} = y_{lm} + \left(\frac{1}{yy_l} + \frac{1}{yy_m} \right)^{-1} \quad (3.69)$$

y_{jk}^{new} and y_{lm}^{new} thus replace their original values and the result obtained from (3.64) and (3.65) is denoted as $(x_{lm/jk}^{\text{lb}})_2$.

- (iii) For Figure 3.17, the following adjustments are made :

$$y_{jm}^{new} = y_{jm} + \left(\frac{1}{yy_j} + \frac{1}{yy_m} \right)^{-1} \quad (3.70)$$

$$y_{kl}^{new} = y_{kl} + \left(\frac{1}{yy_k} + \frac{1}{yy_l} \right)^{-1} \quad (3.71)$$

Again, similar to the two preceding cases, the transfer resistance $(x_{lm/jk})$ is calculated using (3.64) and (6.65) and is denoted as $(x_{lm/jk}^{lb})_3$.

All three cases are required to be evaluated because it is generally not known beforehand whether which one of these conditions will give the maximum or minimum. It has to be noted that after the evaluation of each case, the adjusted values, e.g. y_{jl}^{new} , y_{km}^{new} , etc., have to be restored to their original values for the next case evaluation. Otherwise, erroneous results will be obtained.

Finally, to determine the upper bound of $x_{lm/jk}$, the maximum value among the three obtained results is chosen, i.e.,

$$\hat{x}_{lm/jk}^{lb} = \max. \{ (x_{lm/jk}^{lb})_1, (x_{lm/jk}^{lb})_2, (x_{lm/jk}^{lb})_3 \} \quad (3.72)$$

and the lower bound will be obtained from :

$$\hat{x}_{lm/jk}^{lb} = \min. \{ (x_{lm/jk}^{lb})_1, (x_{lm/jk}^{lb})_2, (x_{lm/jk}^{lb})_3 \} \quad (3.73)$$

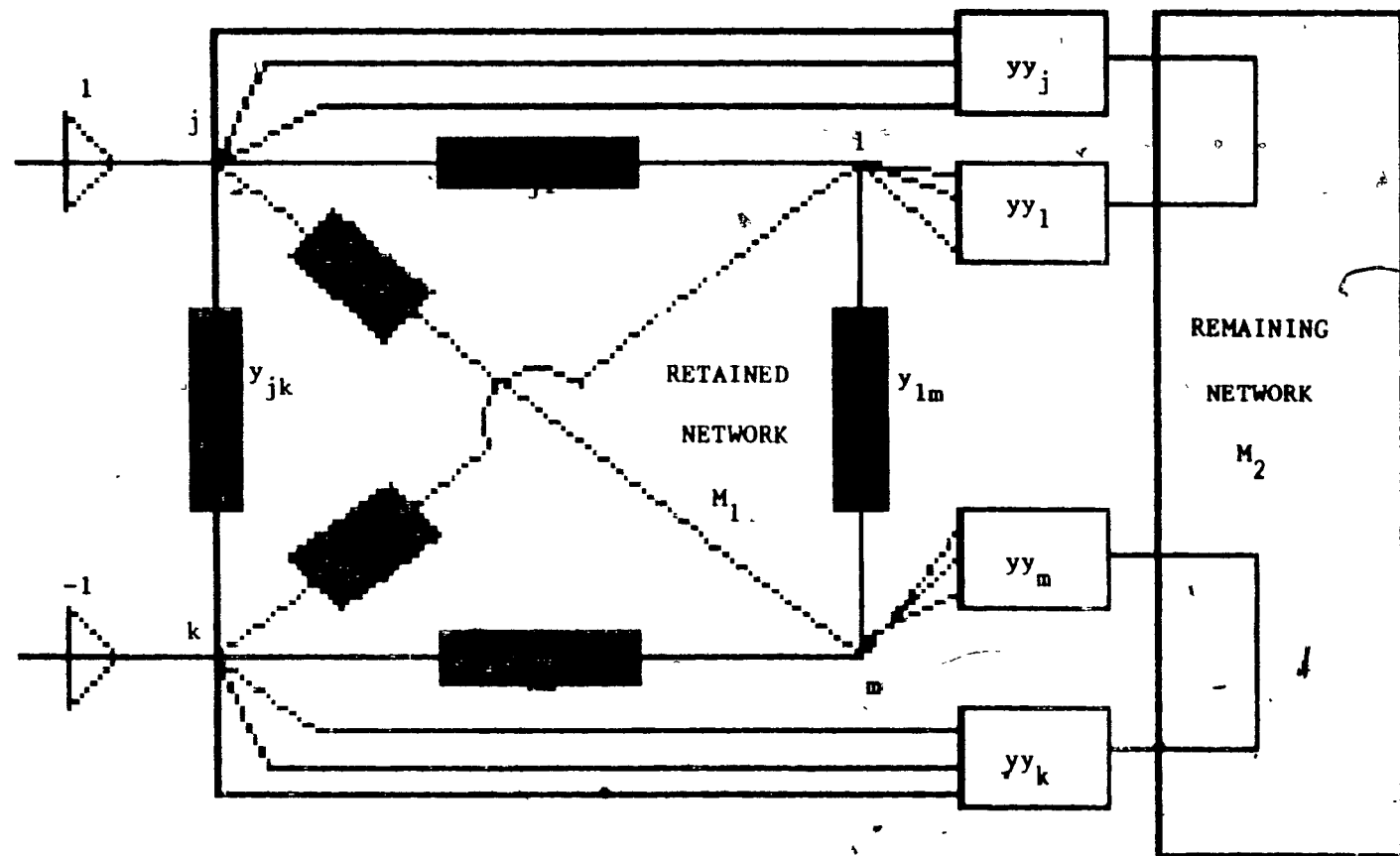


Fig. 3.15 Extreme Connection Pattern for $(x_{lm/jk}^{lb})_1$

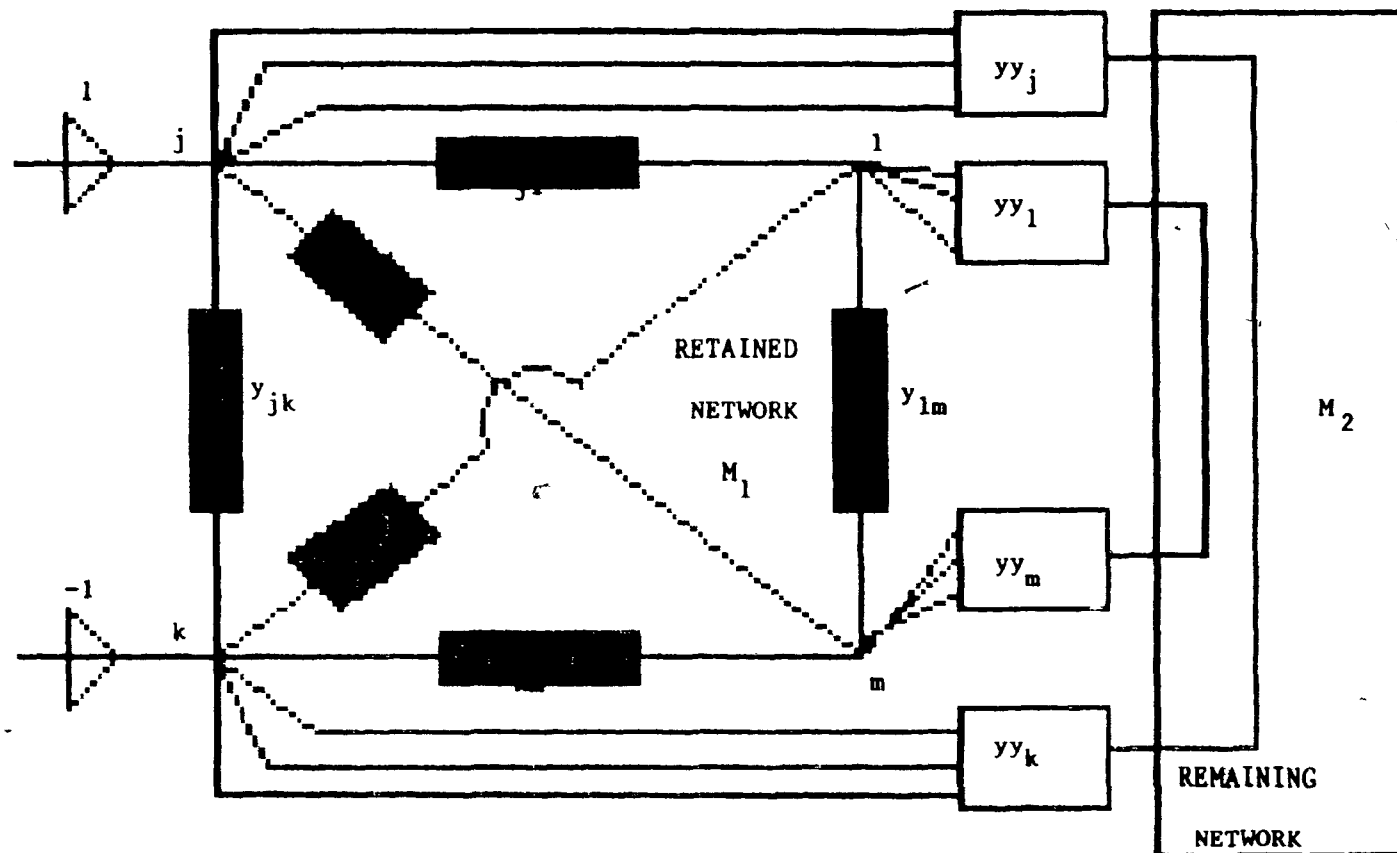


Fig. 3.16 Extreme Connection Pattern for $(x_{lm/jk}^{lb})_2$

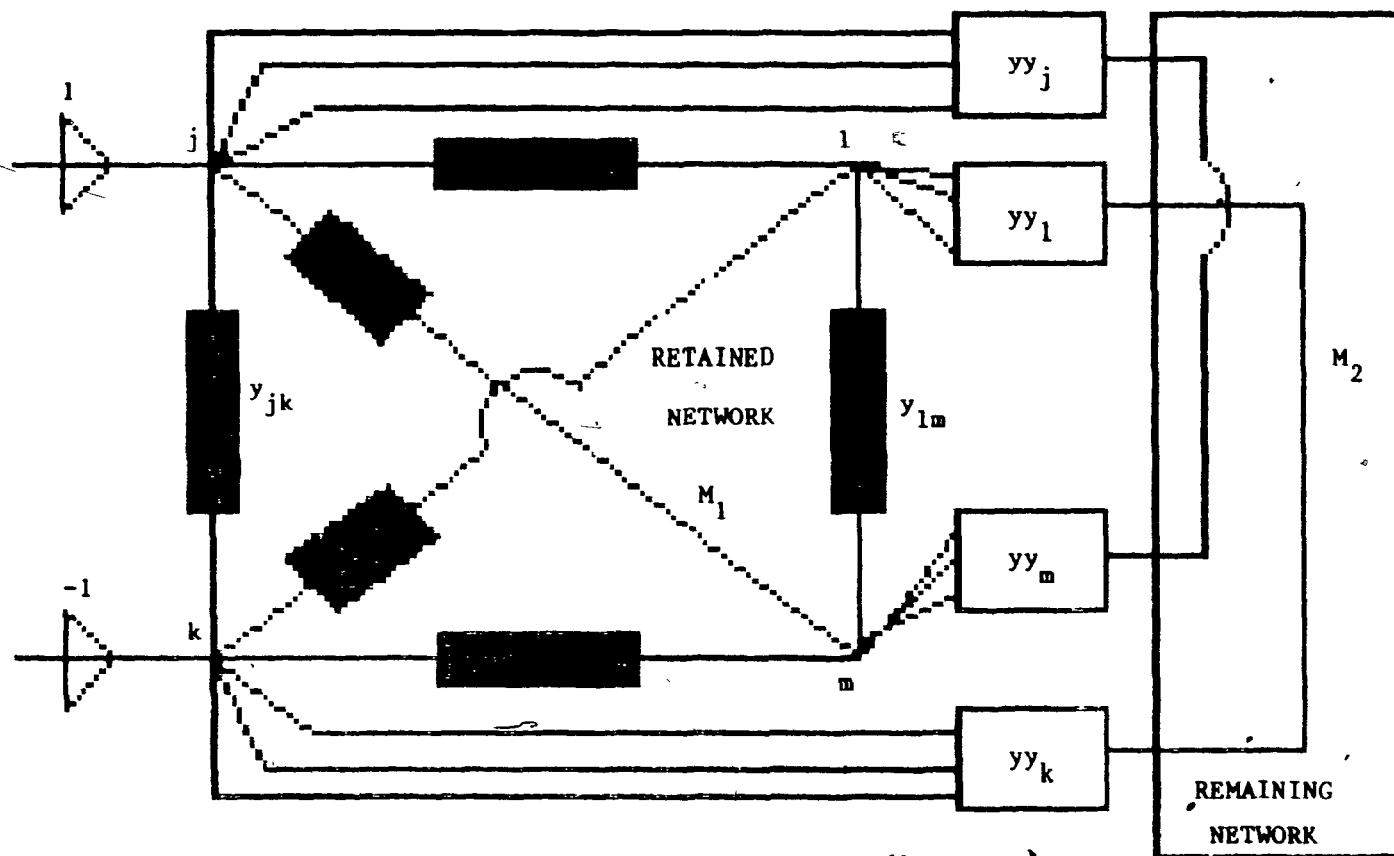


Fig. 3.17 Extreme Connection Pattern for $(x_{lm/jk}^{lb})_3$

Case c : Triangular case

If one of the direct links connecting nodes l,m,j,k is infinite, the retained network shown in Figure 3.12 will be reduced to only 3 nodes. This case is referred as a triangular case here.

Consider a general layout in Figure 3.18, where node c represents the node of the arbitrary branch(l,m) not common to either nodes j or k. The equivalent connection elements to the remaining network (M_2) are denoted as yy_j , yy_k and yy_c for nodes j,k, and c respectively. Taking a similar kind of approach as before, a 3-node network with all equivalent elements (e.g. yy_j , yy_k and yy_c) neglected, the nodal equations for the triangular case can be written as follows :

$$\begin{bmatrix} y_1 & -y_{jc} \\ -y_{jc} & y_2 \end{bmatrix} \begin{bmatrix} v_j \\ v_c \end{bmatrix} = \begin{bmatrix} 1 \\ 0 \end{bmatrix} \quad (3.74)$$

where :

$$y_1 = y_{jk} + y_{jc} \quad (3.74a)$$

$$y_2 = y_{jc} + y_{ck} \quad (3.74b)$$

(Note that node k is again chosen as the reference node and unit currents are injected at node j and removed from node k). Hence, depending on the common node shared by the outaged branch(j,k) and the arbitrary branch(l,m), $x_{lm/jk}$ can be evaluated according to the following table :

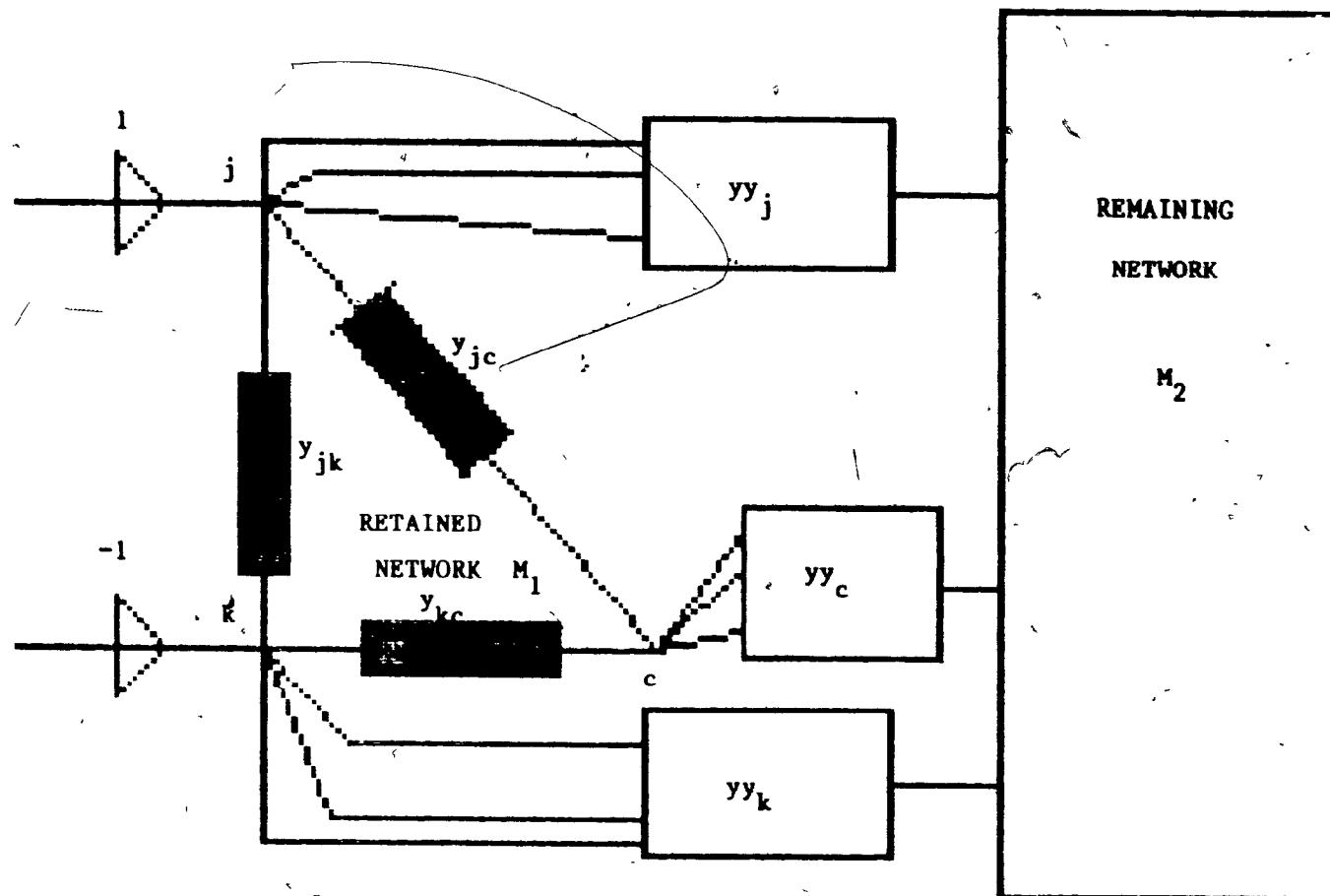
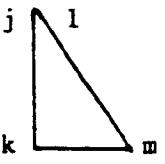
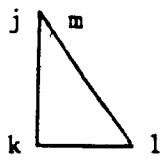
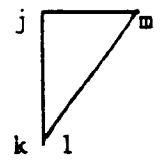
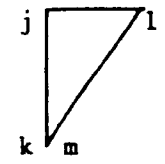


Fig. 3.18 Network Subdivision for the Triangular Case

Table 3.1 $x_{lm/jk}^{lc}$ as Functions of the Common Node

COMMON NODE	j=1	j=m	k=1	k=m
CONFIGU- RATION				
$x_{lm/jk}^{lc}$	$V_j - V_c$	$V_c - V_j$	$-V_c$	V_c

The next step will be to find the bounds on $x_{lm/jk}^{lc}$. For the lower bound of $x_{lm/jk}^{lc}$, Figure 3.19 depicts the connection which will give minimum current through branch(1,m). This connection can be interpreted as to put yy_j and yy_k first in series and then in parallel with branch(j,k). Hence the adjustment required is :

$$y_{jk}^{new} = y_{jk} + \left(\frac{1}{yy_j} + \frac{1}{yy_k} \right)^{-1} \quad (3.75)$$

By substituting (3.75) into (3.74) and solving the $x_{lm/jk}^{lc}$ according to Table 3.1, the lower bound will be obtained, denoted as $\tilde{x}_{lm/jk}^{lc}$.

For the upper bound of $x_{lm/jk}^{lc}$, it is less obvious because two connections are possible to yield a maximum current through branch(1,m) as shown in Figures 3.20 and 3.21.

For Figure 3.20, the following adjustment is required :

$$y_{kc}^{new} = y_{kc} + \left(\frac{1}{yy_k} + \frac{1}{yy_c} \right)^{-1} \quad (3.76)$$

By substituting (3.76) into (3.74) and solving for $x_{lm/jk}^{lc}$ using Table 3.1 again, an extreme value of $x_{lm/jk}^{lc}$ can be obtained and it is denoted as $(x_{lm/jk}^{lc})_1$.

Similarly, by making the following adjustment to y_{jc} according to the connection pattern shown in Figure 3.21, i.e.,

$$y_{jc}^{new} = y_{jc} + \left(\frac{1}{yy_j} + \frac{1}{yy_c} \right)^{-1} \quad (3.77)$$

another extreme value on $x_{lm/jk}^{lc}$ can be obtained and it denoted as $(x_{lm/jk}^{lc})_2$.

The upper bound of this case can thus be defined as the largest value of the two, i.e.,

$$\hat{x}_{lm/jk}^{lc} = \max. \{ (x_{lm/jk}^{lc})_1, (x_{lm/jk}^{lc})_2 \} \quad (3.78)$$

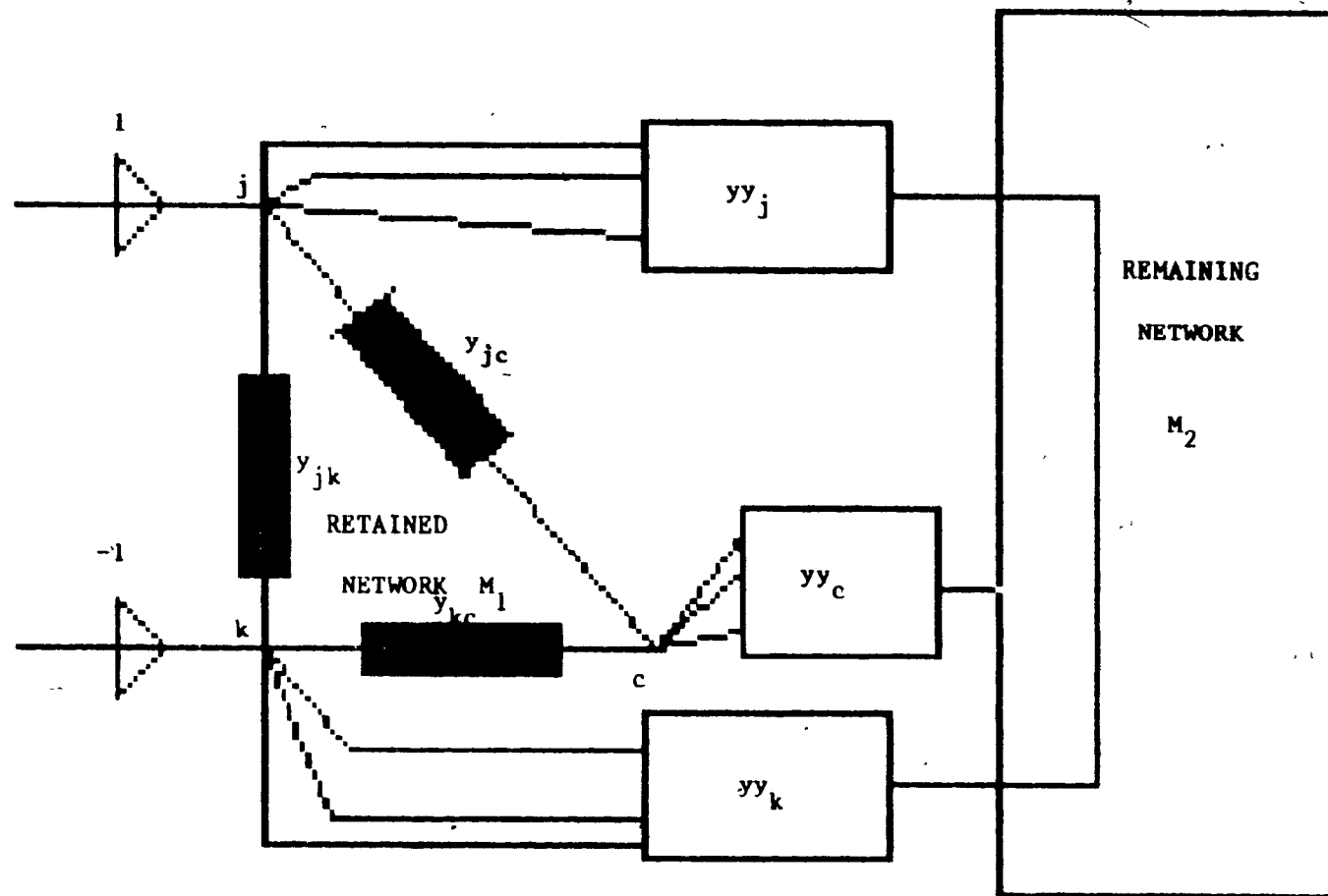


Fig. 3.19 Extreme Connection Pattern for $x_{lm/jk}^{lc}$

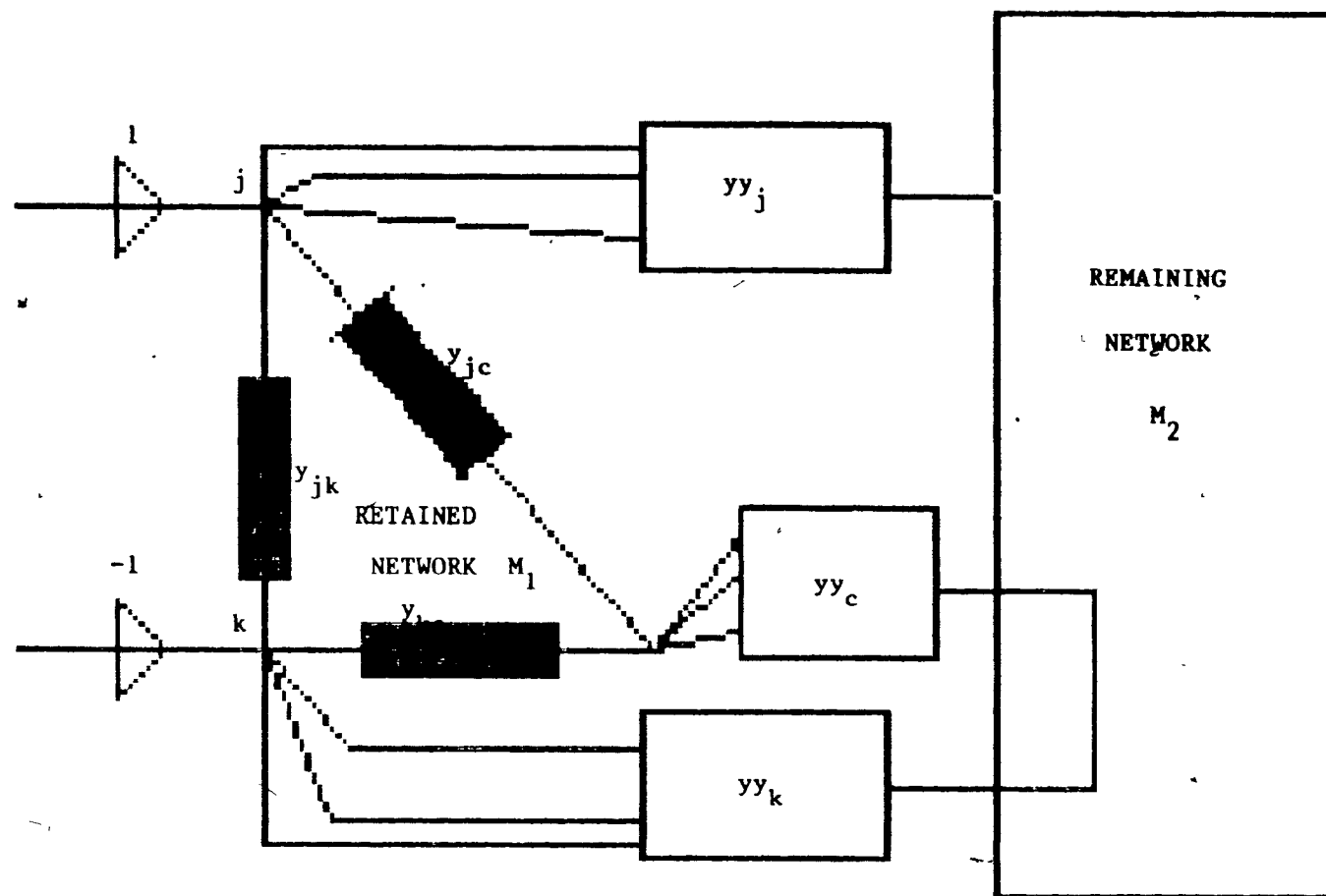


Fig. 3.20 Extreme Connection Pattern for $(x_{lm/jk}^{lc})_1$

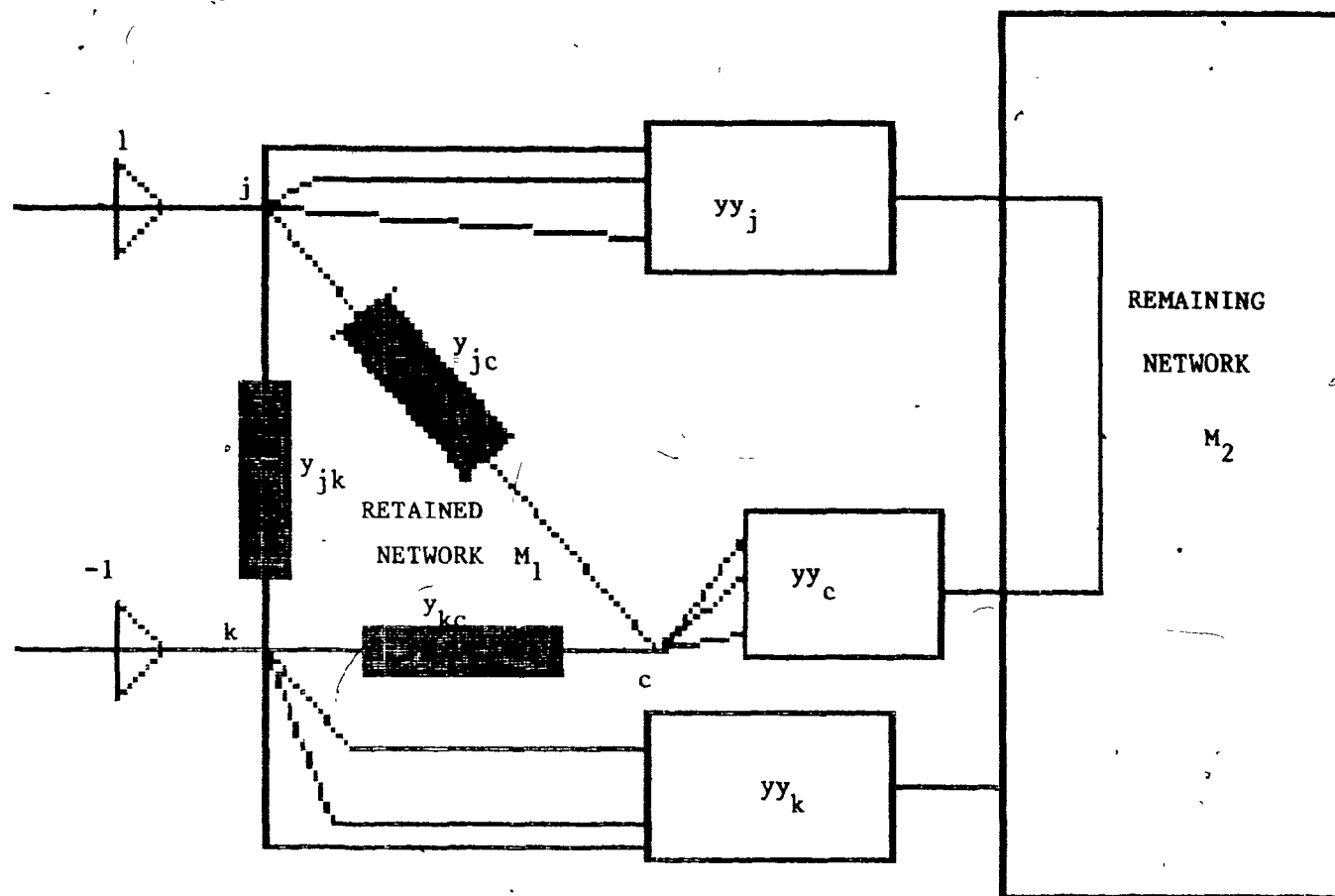


Fig. 3.21 Extreme Connection Pattern for $(x_{lm/jk}^{lc})_2$

3.2.6.2 Type 1 Bounds on $x_{lm/jk}$

In some occasions, due to the fact that the outraged branch (j,k) is far away from the arbitrary branch (l,m), an analytical bound type on $x_{lm/jk}$ can be derived in order to exploit such a characteristic. The idea is to consider the following quantity, i.e.,

$$x_{lmjk} = (\underline{e}_{lm} + \underline{e}_{jk})^T \underline{B}^{-1} (\underline{e}_{jk} + \underline{e}_{lm}) \quad (3.79)$$

$$= x_{jk} + x_{lm} + 2 x_{lm/jk} \quad (3.80)$$

the transfer resistance ($x_{lm/jk}$) can thus be expressed as :

$$x_{lm/jk} = \frac{x_{lmjk} - x_{jk} - x_{lm}}{2} \quad (3.81)$$

The quantity x_{lmjk} defined in (3.79) has the general properties of a resistance similar to x_{jk} and x_{lm} , however, the current injections are now applied to both nodes j and k, and also nodes l and m as shown in Figure 3.22. In order to derive bounds by using such a quantity, consider the case where the retained networks of x_{lm} and x_{jk} do not share any common lines (see Figure 3.22). Since there is no overlapping between the two retained networks, as in Figure 3.22 denoted as N_{jk} and N_{lm} , the mutual coupling term ($x_{lm/jk}$) vanishes. Hence the bounds of (3.80) can be expressed as follows, i.e.,

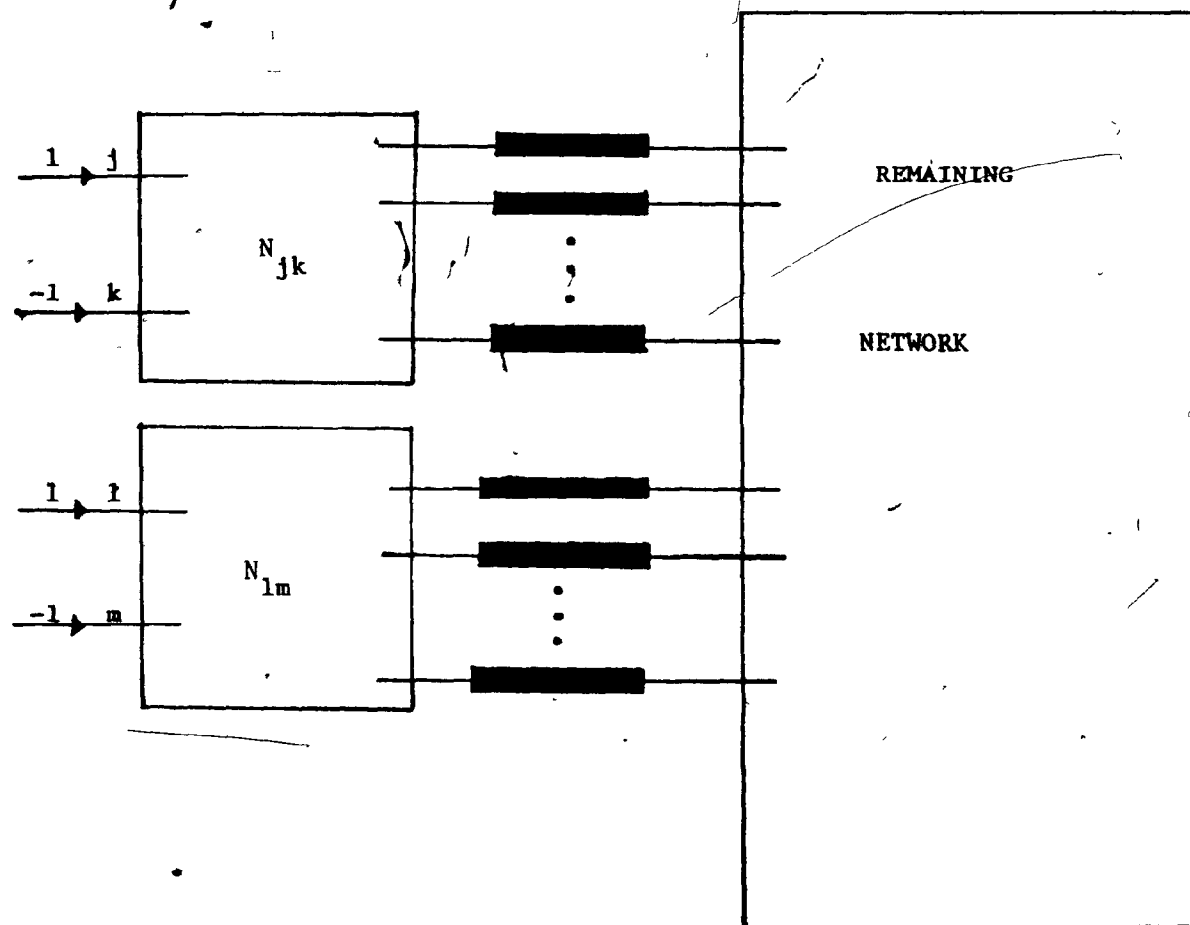


Fig. 3.22 Network subdivision for type 2 bounds of $x_{lm/jk}$

$$\hat{x}_{lmjk} = \hat{x}_{lm} + \hat{x}_{jk} \quad (3.82)$$

$$\tilde{x}_{lmjk} = \tilde{x}_{lm} + \tilde{x}_{jk} \quad (3.83)$$

Substituting (3.82) and (3.83) into (3.81), the type 2 bounds on

$x_{lm/jk}$ can be expressed as :

$$\hat{x}_{lm/jk}^2 = \frac{\hat{x}_{lmjk}^2 - \hat{x}_{lm}^2 - \hat{x}_{jk}^2}{2} \quad (3.84)$$

$$\tilde{x}_{lm/jk}^2 = \frac{\tilde{x}_{lmjk}^2 - \tilde{x}_{lm}^2 - \tilde{x}_{jk}^2}{2} \quad (3.85)$$

It is important to mention here that this type of bounds can only be applied to the case where both retained networks (N_{jk} and N_{lm}) do not have any common line. Therefore, for cases where branch (j,k) and branch (l,m) are far from each other, the possibility of overlapping is small and this bound type is more likely to be applicable. Note that such a type of bound does not require new information because all the bounds of x_{jk} and x_{lm} have already been obtained from previous evaluations (e.g., \hat{x}_{lm} , \tilde{x}_{lm} , \hat{x}_{jk} , \tilde{x}_{jk}).

3.3 Contingency Filter Arrangements

Using different combinations of the different bound types developed so far, a series of filters can be assembled. In

Table 3.2 Filtering Scheme #1

Contingency Filter Type	Bounds on $x_{lm/jk}$	Bounds on x_{jk}	Bounds on $\rho_{lm/jk}$
CF^0	-	-	$(-1, 1)$
CF^1	$(\tilde{x}_{lm/jk}^0, \hat{x}_{lm/jk}^0)$	$(\tilde{x}_{jk}^1, \hat{x}_{jk}^1)$	To be calculated according to (3.27) - (3.30)
CF^2	$(\tilde{x}_{lm/jk}^0, \hat{x}_{lm/jk}^0)$	$(\tilde{x}_{jk}^1, \hat{x}_{jk}^1)$	To be calculated according to (3.27) - (3.30)
CF^3	$(\tilde{x}_{lm/jk}^2, \hat{x}_{lm/jk}^2)$	$(\tilde{x}_{jk}^1, \hat{x}_{jk}^1)$	To be calculated according to (3.27) - (3.30)
CF^4	$x_{lm/jk}$	x_{jk}	$\rho_{lm/jk}$

Table 3.3 Filtering Scheme #2

Contingency Filter Type	Bounds on $x_{lm/jk}$	Bounds on x_{jk}	Bounds on $\rho_{lm/jk}$
CF^0	-	-	$(-1, 1)$
CF^1	$(\tilde{x}_{lm/jk}^0, \hat{x}_{lm/jk}^0)$	$(\tilde{x}_{jk}^2, \hat{x}_{jk}^2)$	To be calculated according to (3.27) - (3.30)
CF^2	$(\tilde{x}_{lm/jk}^1, \hat{x}_{lm/jk}^1)$	$(\tilde{x}_{jk}^2, \hat{x}_{jk}^2)$	To be calculated according to (3.27) - (3.30)
CF^3	$(\tilde{x}_{lm/jk}^2, \hat{x}_{lm/jk}^2)$	$(\tilde{x}_{jk}^2, \hat{x}_{jk}^2)$	To be calculated according to (3.27) - (3.30)
CF^4	$x_{lm/jk}$	x_{jk}	$\rho_{lm/jk}$

CF^4 is the DC load flow simulation which calculates the exact values of the LODF for the remaining uncertain flows. It is easy to notice that scheme #1 and scheme #2 only differ from each other in terms of their bounds on x_{jk} . This is intentionally used to test whether by including more closed loops will give a better accuracy and filtering performance.

3.4 Ranking and Selection Algorithms

In order to further reduce processing time, uncertain contingencies can be selected between filters such that only the most severe cases will be submitted to the subsequent filter for clarification. The common methodology is to assign each contingency with a scalar index (e.g., the SPI methods). Such an index reflects the severity of the contingency. Should this index exceed a threshold value, this contingency will be chosen and otherwise it will be assumed safe. In this thesis, two new selection indices are proposed as follows :-

Method A : Selection Based on the Total Number of Uncertain Flows

The index used here is the total number of uncertain flows of each uncertain contingency. Suppose the threshold is set at 30 lines, therefore any uncertain contingency whose total number of uncertain flows is more than 30 lines will be selected. For those which have less than 30 lines will be neglected and assumed to be safe. The threshold value currently is set by using a percentage of the total number of lines as a guideline. For example (20 - 40)% of the total number of lines is used here. The advantage of this method is that the required information is already available after each filtering.

Method B : Selection Based on the Relative Overload Expectation (ROE)

The Relative Overload Expectation (ROE) is defined as follows :-

$$ROE \triangleq \frac{1}{NU} \sum_{i=1}^{NU} \frac{\max\{|\tilde{P}_1|, |\hat{P}_1|\} - P_1^{lim}}{P_1^{lim}} \quad (3.86)$$

where :

$|\tilde{P}_1|$ $|\hat{P}_1|$ \triangleq absolute values of the lower and upper bounds of the contingency flows respectively.

P_1^{lim} \triangleq security limit of line 1 .

NU \triangleq number of uncertain lines.

ROE is a measure of the average overload range for all uncertain flows of an uncertain contingency. Relative means that it is normalized and compared to the line security limit. Hence, for any contingency whose ROE is greater than a threshold value (e.g., 5 - 10%) will be selected for the subsequent filter.

The testing results of these two methods are presented in the following chapter. Selection of contingencies between filters can be accomplished using two different algorithms.

The first one is to perform the selection for each contingency right after each filtering has been finished. For example, the n^{th} contingency gives m uncertain flows after CF^0 (see 3.3). If m is greater than a pre-set threshold value t , the n^{th} contingency,

with its m uncertain flows, will be submitted to CF^1 and so on until all uncertain flows in the same contingency are classified. Otherwise, if m is less than t , the contingency will be excluded from further analysis and assumed to be non-critical.

The second algorithm, performs the selection after all the postulated (or uncertain) contingencies have been analysed by a filter. For example, until all the number of uncertain flows for all postulated (or uncertain) contingencies are available, ranking is then performed based on the information (e.g., the indices derived above) from the filtering process and the highest ranked cases will be selected to go to the next filter.

Both methods are indeed viable, however, the latter one requires a large storage area and it is less straight forward to be applied. For example, the highest ranked contingency, denoted as the k^{th} contingency, has l uncertain flows after a filter. A storage vector of dimension l is therefore required. Theoretically speaking, l can be as large as the total number of lines. As a result, the storage requirement will increase significantly if such a selection algorithm is used (e.g., a matrix of $NL \times NL$ may be required). Also the extra time of retrieving the information will also be a handling burden to the process. Therefore, this thesis uses the first selection algorithm described above.

It was also speculated that these two selection methods (A and B) will give more reliable ranking results than the conventional methods because the filtering process has already eliminated a number of flows and contingencies which have been classified as either critical or non-critical. Hence, 'noise' in the conventional ranking indices described in the previous chapter is reduced.

3.5 Computational Considerations

3.5.1 Usage of the 'Link List' and 'SPARSPACK'

Due to the special nature of power systems, namely very large scale network and sparsely connected configuration, the DC Jacobian \underline{B} in (3.8) is generally very large and sparse. Storing the DC Jacobian \underline{B} in full not only requires a considerable amount of memory (e.g., $(n+1) \times (n+1)$, where $(n+1)$ is the total number of buses) but also reduces the computational efficiency. In this thesis, a 'Link List' data structure [Enns 1975] is used to store the system data in order to reduce the storage requirements and improve efficiency. The 'SPARSPACK' program developed at University of Waterloo [George et al. 1981] is also used here to solve all DC load flow simulation by exploiting the sparsity nature of \underline{B} .

It is not intended here to explain and describe in detail how the 'Link List' works. Rather, the merits of using such a data structure are discussed. Since the 'Link List' only stores the

non-zero elements of the sparse matrix, the storage requirement is drastically reduced. For example, it requires 13,689 (117 x 117) storage spaces of using a full storage mode to store all elements of the DC Jacobian of a 118 bus, 179 line system. However, the 'Link List' only needs 1131 storage spaces, which is 12 times less than the full storage mode. The other major benefit of using the 'Link List' is that it provides a systematic and efficient data structure of identifying connections between nodes. This merit is found to be a great advantage for the algorithm to be described later which will find the closed loops for the x_{jk} evaluation.

'SPARSPACK' is the Sparse Linear Equation Package developed at University of Waterloo [George et al. 1981]. The package solves a linear set of equations as follows :

$$\underline{A} \underline{x} = \underline{b} \quad (3.87)$$

where the coefficient matrix \underline{A} is sparse and positive definite in general.

The basic procedures of using this package is summarized as follows :

- (1) Invoke SPARSPACK.
- (2) Input the positions of the non-zero terms in \underline{A} .
- (3) Invoke re-ordering subroutine.
- (4) Input numerical values of the non-zero terms in \underline{A} .
- (5) Invoke the factorization subroutine.

- (6) Input the ~~right~~ hand side elements (b) .
- (7) Solve for the vector x by recalling the factorization subroutine.

In this study, the base case DC load flow and all the contingency DC load flows are solved using this package. 'SPARSPACK' provides a very efficient tool to evaluate the sparsely oriented system of equations considered in this work, e.g., (3.19) - (3.21), such that the processing time can be greatly reduced.

3.5.2 Automatic Loop Searcher

In the previous section where x_{jk} bounds are derived, it is stated that in order to obtain an upper bound less than the value $1/y_{jk}$ (see (3.26)), a closed loop including branch (j,k) must be present in the retained network. In this section, an algorithm is developed to find such a closed loop based on the following information :-

- (1) Given the ending nodes j and k of the outaged branch (j,k) .
- (2) Given the system Link List.

The algorithm is now explained with a small example.

Figure 3.23 shows a small 6-node network. Assume that node 1 (j) and node 2 (k) are the ending nodes of the outaged branch (j,k) , by inspection, a few closed loops can easily be determined, i.e., (1,3,2), (1,5,3,2), (1,3,4,2) and (1,5,3,4,2) .

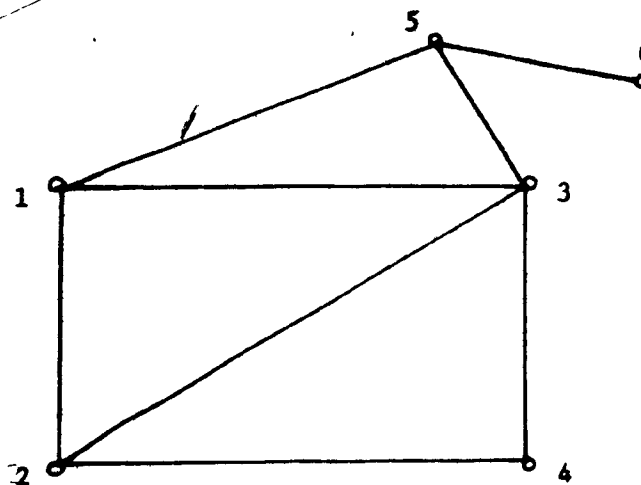


Fig. 3.23 A 6-node Example Network

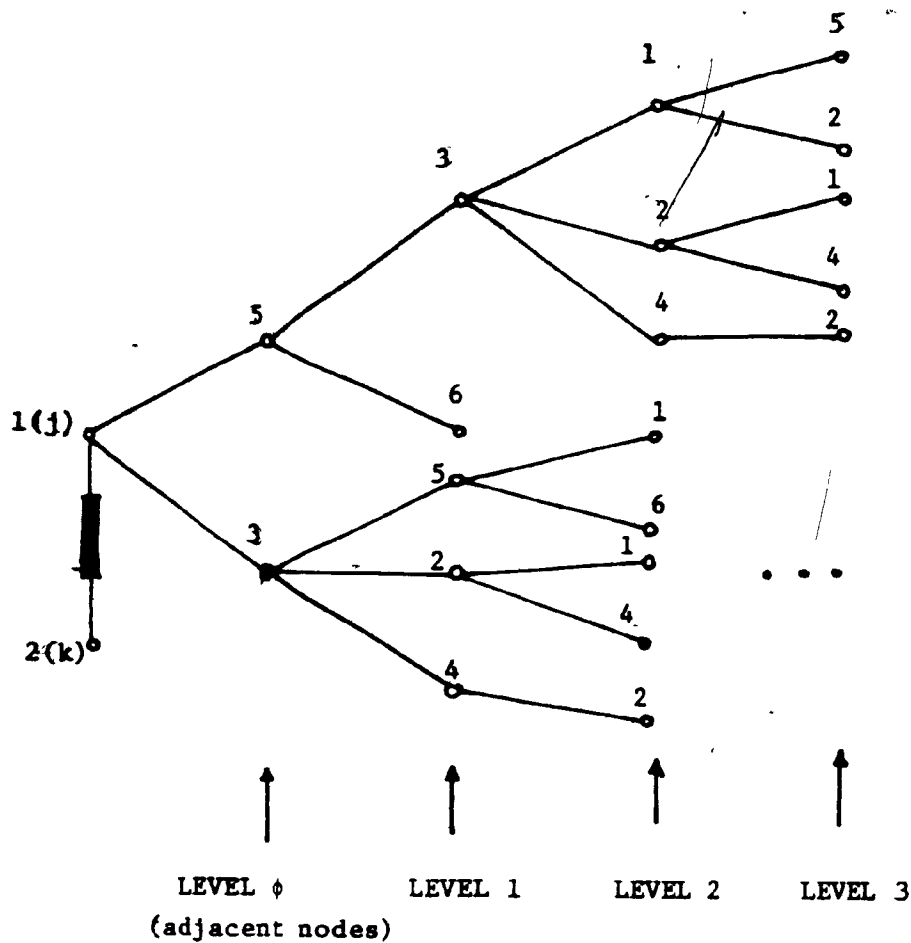


Fig. 3.24 Connection Tree Structure of the 6-node Example Network

Next, consider a tree structure starting from node 1 (j) , which is depicting all the connections from node 1 to the rest of the system. The nodes which are directly connected to node 1 are called the 'adjacent nodes' and the connection level is denoted as 'LEVEL ϕ ' as shown in Figure 3.24, e.g., nodes 5 and 3 in this case. LEVEL 1 is the collection of all the nodes directly connected to the 'adjacent nodes'. LEVEL 2 is the collection of all the nodes directly connected to the nodes in LEVEL 1 and so on.

The algorithm is thus to find a match between node 2 (k) and a node in LEVEL 1 or beyond. The node which is being checked with node 2 (k) is called a 'checking node'. Assuming no parallel lines, the smallest loop will possibly be obtained if there is a match between node 2 (k) and a node in LEVEL 1. Table 3.4 shows the procedures of checking in LEVEL 1. Note that the 'linkage node' is defined as the node which provides the link between the 'checking node' and an ending node of the outaged branch (e.g., node 1 (j) in this case).

Table 3.4

Checking Procedures of the Automatic Loop Searcher, Example 1

	Linkage Node	Checking Node	Result
Check # 1	5	3	Not matched
Check # 2	5	6	Not matched
Check # 3	3	5	Not matched
Check # 4	3	2	Matched
Check # 5	3	4	Not matched

In check #1, the 'linkage node' is node 5 and no match is found. The checking therefore proceeds to the next node connected to node 5 (i.e., node 6) . Again, the matching fails. Since all nodes connected to node 5 have been evaluated at this level, the checking moves to node 3 which is at the same level. At the fourth case shown in Table 3.4, a match is found (i.e., loop 1, 3, 2) . The linkage node 3 is now named as a 'loop node' and then stored for later usage (i.e., for the Retained Network Builder (RNB)).

Should no closed loop be found after all the nodes in LEVEL 1 have been checked, or more closed loops be required, the checking can be extended to LEVEL 2 . Table 3.5 shows the checking procedures at LEVEL 2 . Notice that two closed loops, namely (1, 5, 3, 2) and (1, 3, 4, 2), have been located which are exactly the same as those obtained from the inspection method.

A few points are necessary to be mentioned :-

(1) Even though it seems that an exponential type of memory spaces are required in order to handle the data shown in Figure 3.24 at the first glance, actually only very little storage is necessary. That is because only the 'linkage nodes' are required to be retained in each checking.

Table 3.5Checking Procedures of the Automatic Loop Searcher, Example 2

	Linkage Node	Checking Node	Result
Check # 1	5.3	1	Not matched
Check # 2	5.3	2	Matched
Check # 3	5.3	4	Not matched
Check # 4	5.6	-	Not matched
Check # 5	3.5	1	Not matched
Check # 6	3.5	6	Not matched
Check # 7	3.2	1	Not matched
Check # 8	3.2	4	Not matched
Check # 9	3.4	2	Matched

Each 'checking node' is identified from the outermost 'linkage node' by the Link List at the time such a node is required. For example, the nodes connected to node 3 at LEVEL ϕ can easily be identified through a Link List as 1, 2, 4, 5. By excluding node 1, which is the node giving us node 3 at the first place, the remaining nodes will become the 'checking nodes'. They are identified and checked sequentially (i.e., one node after the other) so that no memory space is needed to store each one of them.

(2) Should any 'checking node' be equal to any one of the preceding 'linkage nodes' or the ending node of the outaged branch (in this case it is node $l(j)$), such a 'checking node' is automatically excluded from further checking. This is because it will otherwise lead to a backward search and eventually locate a faulty loop. For instance, the link (1, 5, 3, 1, 2) in Figure 3.24 will lead to such a faulty loop because one of the 'linkage nodes', i.e., node 1, is equal to an ending node of the outaged line. Apparently such a sequence does not form a closed loop from inspection.

(3) By performing the checking level by level as shown above, the algorithm will always search for a loop with the least number of 'linkage nodes'. Any further loops obtained will always have the same or more number of 'linkage nodes'.

Theoretically, the search can be expanded until all nodes in the system are covered. The process need not be performed level by level as shown in these examples. Rather the stopping criterion can be set to stop after one closed loop or after two closed loops have been found. The resulting information (i.e., the 'loop nodes') are thus transferred to the Retained Network Builder, to be described later, in order to construct the bounds on x_{jk} .

In this thesis, the highest level of searching (checking) is set at 7. In other words, the maximum numbers of linkage nodes

completing one closed loop is also 7. Should no closed loop be found at LEVEL 7, the outaged line is labelled as a 'no-closed-loop' line and some contingency filters are not applicable for this line. In general, this kind of situation is rare and such a line may actually be an 'islanding' line. To verify whether such a 'no-closed-loop' line is an 'islanding' line or not, a DC load flow is required. If the exact x_{jk} calculated from a DC load flow is very close to the value $1/y_{jk}$ and hence the LODF becomes infinite, it is indeed an 'islanding' line.

A special case of an 'islanding' effect is the so-called 'semi-independent' line defined previously. It can be detected by this loop searching technique very easily. Should any one of the ending nodes of the outaged branch (j,k) show that there is no other connection to the system beside the only connection to the other node through the outaged branch (j,k), the line is a 'semi-independent' line.

3.5.3 Retained Network Builder

The Retained Network Builder (RNB) has two functions, namely :-

(1) Constructing the conductance matrix of the retained network N1 : After the Automatic Loop Searcher, a group of nodes are obtained. These nodes will include the ending nodes of the outaged

branch, the 'loop nodes' and the 'adjacent nodes'. Note that all the 'adjacent nodes', which are the nodes directly connected to the ending nodes of the outaged branch, are also included here. The reason will become apparent later.

In this study, an algorithm is built to assemble the conductance matrix of the retained network taking into account of all possible connections between all nodes in the retained network. Hence, if any adjacent node has a direct link to any one of the 'loop nodes', additional loop will be added to the retained network. This is the reason why the 'adjacent nodes' are included, because they may increase the accuracy of the result without too much effort.

(2) Solving (3.47) and (3.48) to obtain the bounds on x_{jk} : After the conductance matrix is available, (3.47) can be solved by deleting the row and the column of the conductance matrix corresponding to node k . On the other hand (3.48) can be solved by restoring the row and column values to the conductance matrix and replacing the diagonal elements by the corresponding diagonal elements of the DC Jacobian matrix in order to account for the tie-line conductances. (3.47) and (3.48) are therefore solved separately using the LU factorization and backward- forward substitution methods in order to give the upper and lower bounds of x_{jk} respectively.

3.5.4 Computation Algorithm

The following depicts the algorithm of the computer program written for testing in this study.

- Part A :
- (1) Read in system data.
 - (2) Construct system Link List.
 - (3) Invoke 'SPARSPACK' .
 - (4) Solve the base case DC load flow.
 - (5) Calculate base case line flows.

- Part B :
- For each single line contingency case execute the following:
- (1) Call Automatic Loop Searcher (ALS) .
 - (2) Identify whether the contingency is a 'semi-independent' line or a 'no-closed-loop' line.
If the answer is yes, label the contingency accordingly.
 - (3) If closed loop can be found, call the Retained Network Builder (RNB) .
 - (4) Record the x_{jk} bounds obtained from the RNB .

- Part C :
- For each contingency, execute the following :
- (1) Call Filter # 0(CF⁰) .
 - (2) If no uncertain flow is left, proceed to evaluate the next contingency.
 - (3) Check whether such a contingency is a 'semi-independent' line. If yes, record it as critical.

- (4) Check whether it is a 'no-closed-loop' line. If yes, send the contingency to Filter # 4 (~~CF~~).
- (5) Call Filter # 1 (CF^1).
- (6) If no uncertain flow is left, proceed to evaluate the next contingency.
- (7) Call Filter # 2 (CF^2).
- (8) If no uncertain flow is left, proceed to evaluate the next contingency.
- (9) Call Filter # 3 (CF^3).
- (10) If no uncertain flow is left, proceed to evaluate the next contingency.
- (11) Call Filter # 4 (CF^4).
- (12) Proceed to the next contingency case.

CHAPTER IVCONTINGENCY FILTERING USING LINEARIZED FLOW BOUND ESTIMATES :NUMERICAL EXPERIENCE4.0 Introductory Remarks

In the preceding chapter, the theory of contingency filtering using linearized flow bound estimates has been derived. Different types of bounds have been developed using either a circuit interpretation or an analytical interpretation of the values of x_{jk} and $x_{lm/jk}$. However, the actual conservativeness of such bounds, i.e., whether they are tight enough for any practical use, still remains to be determined. This chapter is intended to report on an investigation of the efficiencies and practicalities of the contingency filters using these derived bounds.

The objectives of the following simulations are summarized as follows, i.e.,

- (1) Examining the numerical conservativeness of various bounds derived from the preceding chapter.
- (2) Testing and evaluating the performances of various filters and different filtering schemes.
- (3) Investigating the performances of the two new contingency selection methods proposed in section 3.4.
- (4) Comparing the DC flow results with the AC load flow results.

Five IEEE test systems, i.e., the 14, 24, 30, 57, 118 bus systems, are used in this thesis in order to provide different system sizes and configurations for the simulations. A heavily and a lightly loaded case for each system are also simulated in order to provide different loading levels for this study. The bus data, their real power injections and the necessary modifications of the five testing systems are depicted in Appendix B. It is cited here that all parallel lines in the systems are replaced by their equivalent models.

4.1 Numerical Results of Different Bound Estimates on x_{jk}

This section illustrates the performance of the Automatic Loop Searcher (ALS) and the Retained Network Builder (RNB) described in section 3.5. It is intended to demonstrate the efficiencies of these algorithms and the accuracy of the x_{jk} bounds obtained. It is important to remember here that for NTC single line outage contingencies, there are at most $2 \times \text{NTC}$ x_{jk} bounds (upper and lower) to be evaluated.

Recall from 3.5.2 that once given the ending nodes of an outaged line, the ALS can search for one or more closed loops which will include the outaged line with the smallest number of nodes. In this study, the highest number of "linkage nodes" (refer to section 3.5.2) is limited to 7. Therefore the maximum number of nodes forming a closed loop is 9 (including the ending nodes of the outaged line).

For the RNB, the maximum number of retained nodes in this thesis is limited to 25 at most. These nodes include the ending nodes of the outaged line, the loop nodes and the adjacent nodes (i.e., nodes directly connected to the ending nodes of the outaged line). The Retained Network Builder will use these retained nodes to construct the necessary retained conductance matrix. The x_{jk} upper and lower bounds for each single outaged case are thus calculated by solving (3.47) and (3.48) using the LU factorization and the backward-forward substitution methods.

Even their nature and functions are different, the ALS and the RNB are regarded as a series process which evaluates the bounds on x_{jk} . They should be viewed as inseparable in the following presentation unless for some special cases, i.e., the "semi-independent" lines or the "no-closed loop" lines where the RNB step is waived.

4.1.1 Results from the IEEE 24-Bus System. An Example

Table 4.1 shows some selected results from the ALS and the RNB performing on the IEEE 24-bus system. The system data are shown in Appendix D. A system one-line diagram is also accompanied in order to allow the reader to trace the loop found from the ALS. Only one closed loop is shown for each case here, however the ALS algorithm can indeed identify two, three or more loops on request. The adjacent nodes, to which the ending nodes of the outaged line are directly connected, are

Table 4.1

Selected Results of the Calculated Bounds of x_{jk} on the IEEE 24-bus System

Line No.	From	To	Closed Loop	Adjac. Node	Total Node	$\tilde{x}_{jk} \times 10^{-1}$	$\hat{x}_{jk} \times 10^{-1}$	$x_{jk} \times 10^{-1}$	\bar{x}_{jk} (%)
1	1	2	1,5,10,6,2	3,4	7	.133	.137	.133	2.63
3	1	5	1,2,6,10,5	3	6	.590	.705	.614	13.1
6	3	9	3,1,2,4,9	24,12,11,8	9	.614	.975	.665	29.3
7	3	24	3,9,11,14,16,15,24	1	8	.546	.680	.612	16.0
11	7	8	semi-indep.	-	-	-	-	-	-
12	8	9	8,10,12,9	7,11,4,3	8	.962	1.02	.983	3.47
15	9	12	9,11,13,12	8,4,3,23,10	9	.384	.484	.415	12.0
19	11	14	11,13,23,20,19,16,14	10,19	9	.276	.356	.321	18.9
21	12	23	12,13,23	10,9,20	6	.331	.566	.429	24.1
23	14	16	14,11,13,23,20,19,16	17,15	9	.267	.335	.305	17.4
25	15	21	15,16,17,22,21	24,18	7	.179	.181	.180	.537
27	16	17	16,15,21,22,17	19,14,18	8	.185	.187	.186	.988
28	16	19	16,14,11,13,23,20,19	17,15	9	.188	.213	.204	10.6
29	17	18	17,22,21,18	16	5	.116	.135	.117	13.1
33	20	23	20,19,16,14,11,13,23	12	8	.100	.104	.103	3.48

also shown and included in the retained network because they may add additional loops to the already defined loop. This will happen if there are direct connections between the adjacent nodes and the loop nodes (e.g., see lines 12,15,25,27,33) . It can be verified by the reader by tracing these connections.

The upper and lower bounds of x_{jk} obtained from the RNB are also shown in Table 4.1 . The exact values of all the x_{jk} , computed separately from a DC load flow, are also depicted in the table for comparison purposes. The \bar{x}_{jk} shown in the last column is defined as the interval enclosed by the upper and lower bounds, normalized by its line reactance. This value is intended to be used as a measurement of the tightness of the x_{jk} bounds obtained from the RNB .

It is noted that at least one closed loop can be found for all the lines in this system except one, i.e., line # 11 . From Figure 4.1, line # 11 is apparently a "semi-independent" line as defined in section 3.2.5 .

The average number of retained nodes of this system is 7 . The maximum number of retained nodes is 9 and the minimum is 5 . The average \bar{x}_{jk} , over all lines excluding the semi-independent case, is found to be 18.8% . The maximum \bar{x}_{jk} is 29.3% and the minimum is 0.537% . The computational time, that is the total elapsed time for locating the closed loops and evaluating the upper and lower bounds for all lines, is 41.4 ms (based on the CPU time on the AMDAHL 5850 computer).

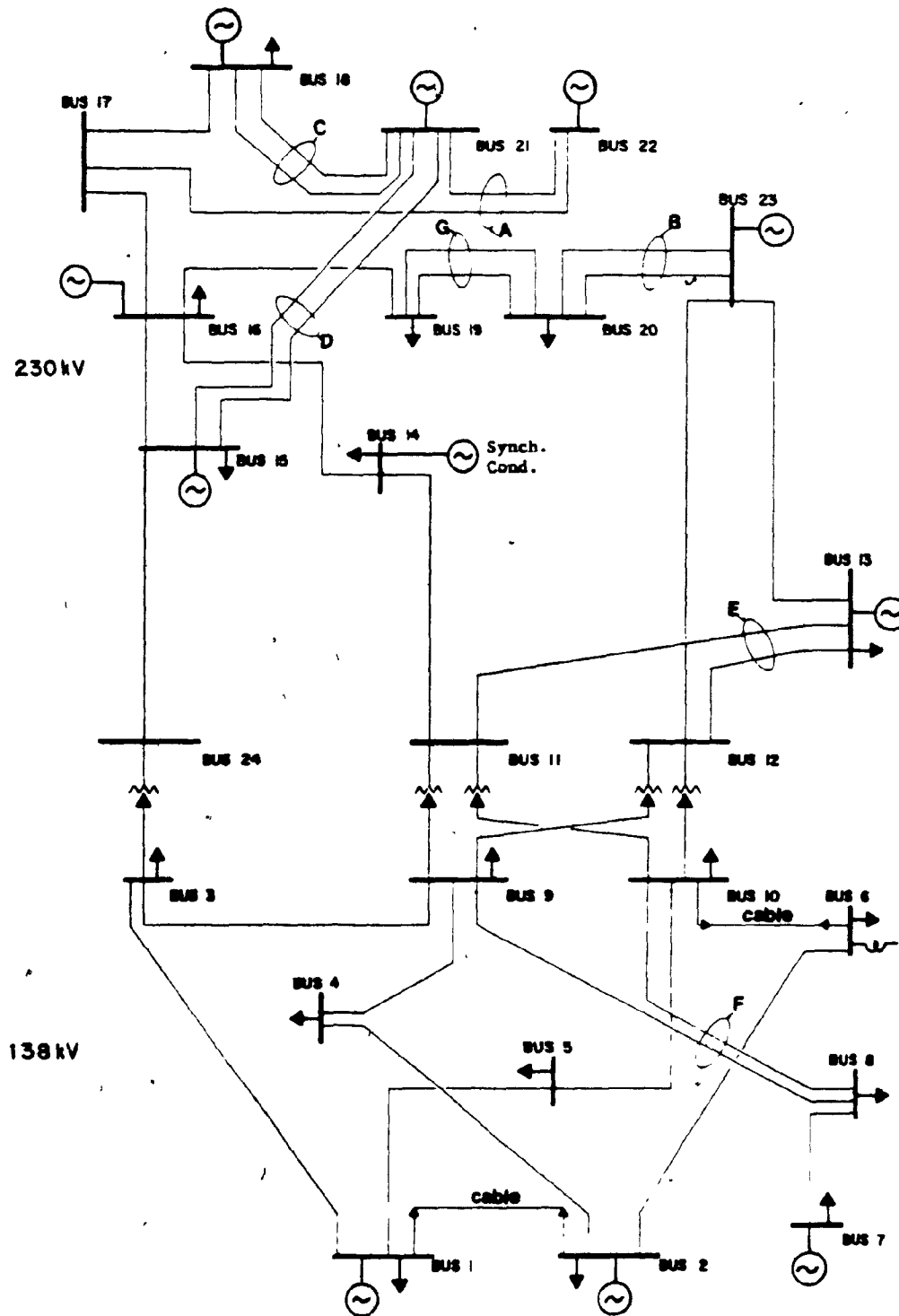


Fig. 4.1 IEEE 24-bus One-line Diagram

4.1.2 Results of the x_{jk} Bounds Based on One Closed Loop

Table 4.2 depicts the performances of the Automatic Loop Searcher (ALS) and the Retained Network Builder (RNB) applied to the five IEEE test systems. The type 1 bounds on x_{jk} described in (3.50) to (3.52) are used, i.e., only one closed loop is requested for each retained network. The average, maximum and minimum number of retained nodes, as well as the average normalized bound interval measurements (\bar{x}_{jk}) are displayed for each system. The timing shown in the table represents the total CPU time required to execute the ALS and RNB for all single line outage contingencies for each system.

Notice that the special cases detected by the ALS, i.e., the "semi-independent" lines and the "no-closed-loop" lines defined in Chapter III, are also shown in Table 4.2. The "islanding lines" are also shown here. However, it has to be mentioned here that the islanding lines are actually detected by DC load flow simulations. ALS cannot identify this. The reason for showing these islanding lines here is for comparison purposes (i.e., how many "no-closed-loop" lines are actually islanding lines).

Notice that in the 57 bus system, 19 lines are found that no closed loop can be established within the specified 7 linkage nodes. After inspecting the system configuration, it is found that in a certain area of the network a lot of lines are connected in series. Hence, a closed loop will usually have to retain more than 7 linkage nodes. Therefore, the ALS fails to locate the necessary nodes. Actually none

Table 4.2Results of x_{jk} Bounds for the IEEE Testing Systemswith One Closed Loop

Bus/Line	14/20	24/34	30/41	57/78	118/179
Average number of retained nodes	7	7	8	8	8
Maximum number of retained nodes	9	9	12	13	15
Minimum number of retained nodes	4	5	3	5	4
Average \bar{x}_{jk} (%)	8.002	11.82	10.36	13.66	14.20
Maximum \bar{x}_{jk} (%)	25.04	29.31	34.99	51.37	58.88
Minimum \bar{x}_{jk} (%)	0.0514	0.5368	0.0	0.9771	0.076
Elapsed time (ms)	20.18	41.41	57.72	103.9	282.8
Number of semi-independent lines	1	1	3	1	7
Number of no-closed-loop lines	0	0	0	19	3
Number of islanding lines	0	0	0	0	2

of them is an islanding line as shown from the DC load flow results, i.e., the LODF is finite. This special system configuration therefore is ill-suited for such bounding analysis. On the other hand, in a larger system, such as the 118-bus system, only 3 lines can a closed loop not be found by the ALS and eventually only two of them turn out to be islanding lines.

4.1.3 Results of the x_{jk} Bounds Based on Two Closed Loops

Table 4.3 depicts the performance of another set of x_{jk} bound results obtained from the same systems but the type 2 bounds described in (3.53) to (3.55) are used, i.e., two closed loops are requested. The ALS in this case searches for an additional loop including the outaged line after the first loop is identified. Generally, the two loops share some common nodes. The following show some examples of the second closed loop detected by the ALS on the 24-bus system, i.e.,

Line 1(1,2) : 1,3,9,4,2

Line 3(1,5) : 1,3,9,12,10,5

Line 6(3,9) : 3,1,5,10,12,9

Line 15(9,12) : 9,11,10,12

Line 27(16,17): 16,15,21,18,17

Line 28(16,19): 16,14,11,13,12,23,20,19

The results of the special cases, e.g., the number of semi-independent lines are the same as the preceding one.

Table 4.3Results of x_{jk} Bounds for the IEEE Testing SystemsWith Two Closed Loops

Bus/Line	14/20	24/34	30/41	57/78	118/179
Average number of retained nodes	8	9	10	9	9
Maximum number of retained nodes	11	12	14	16	16
Minimum number of retained nodes	5	6	3	5	5
Average \bar{x}_{jk} (%)	4.389	7.902	7.477	9.637	10.93
Maximum \bar{x}_{jk} (%)	16.54	23.36	29.06	43.08	58.59
Minimum \bar{x}_{jk} (%)	0.0514	0.5561	0.0	0.4658	0.059
Elapsed time (ms)	27.88	57.3	98.78	185.0	427.8

4.1.4 Discussion

From Tables 4.2 and 4.3, it is found that the ALS performs very well. Even for a large system like the 118-bus, only 3 lines could not be found with at least one closed loop using up to 7 linkage nodes. For all the smaller systems, except the 57-bus, at least one closed loop is found for each retained network. Besides, all the "semi-independent lines" are identified. The problem in the 57-bus system, i.e., 19 "no-closed-loop" lines, can be resolved by increasing the level of searching, e.g., up to 8 or more linkage nodes. However, such a practice may soon become time-consuming and inefficient as the searching level is increased. Therefore, it is recommended to select either the retained nodes by inspection or simply to submit such contingencies to a DC load flow directly. In this study, the later approach is used.

It is observed that the average number of retained nodes in all systems does not increase with the system size, i.e., 8 nodes on average. The range of the number of retained nodes varies from 3 to 16 at most. This phenomenon illustrates that the dimensionality of the equations used to evaluate the x_{jk} bound, i.e., (3.47) and (3.48), are generally small. This is important because the main idea of evaluating these bounds is to reduce the computational burden of solving the exact solution, e.g., solving the exact x_{jk} by (3.21) required to solve a system of equations as large as the total number of nodes.

The average \bar{x}_{jk} values obtained from each one of the five systems show that the bounds obtained from the ALS and RNB are generally very tight, e.g., the average \bar{x}_{jk} ranges from 4.4% to 14.2% (using only one loop or two loops). The average \bar{x}_{jk} value for each system is depicted in a graphical form in Figure 4.2. It is shown that by increasing one additional loop to the first found loop, the average \bar{x}_{jk} value decreases about 3%, i.e., the bounds are tighter in general. The time performances of the ALS and RNB together, using one or two loops, are also shown in Figure 4.3.

By comparing Figures 4.2 and 4.3, it is found that the improvement of accuracy does not change significantly by including more loops. Therefore, it is not worthwhile to include more loops for tighter bound estimates on the expenses of more time-consuming operation. This observation explains the reason why the filtering schemes mentioned in the preceding chapter use only one type of x_{jk} bounds throughout the whole filtering process. The performance between using type 1 and type 2 of the x_{jk} bounds in the filtering process will be demonstrated in a later section.

4.2 Numerical Results of Bound Estimates on $x_{lm/jk}$, LODF and Contingency Flows

4.2.0 Introductory Remarks

According to the filtering scheme designed in 3.3, with a pre-calculated set of x_{jk} bounds, bounds on the LODF and subsequently

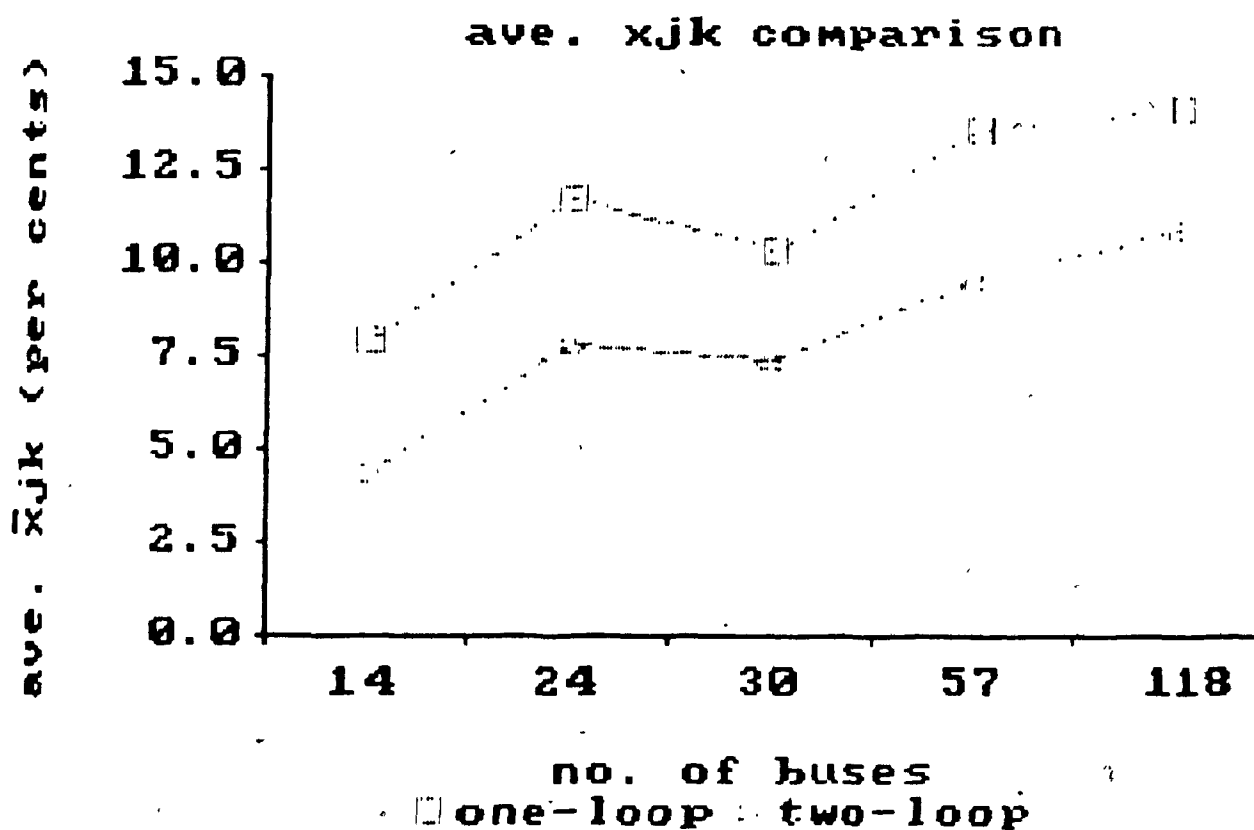


Fig. 4.2 Average \bar{x}_{jk} values for the Five IEEE Systems Based on One and Two Closed Loops.

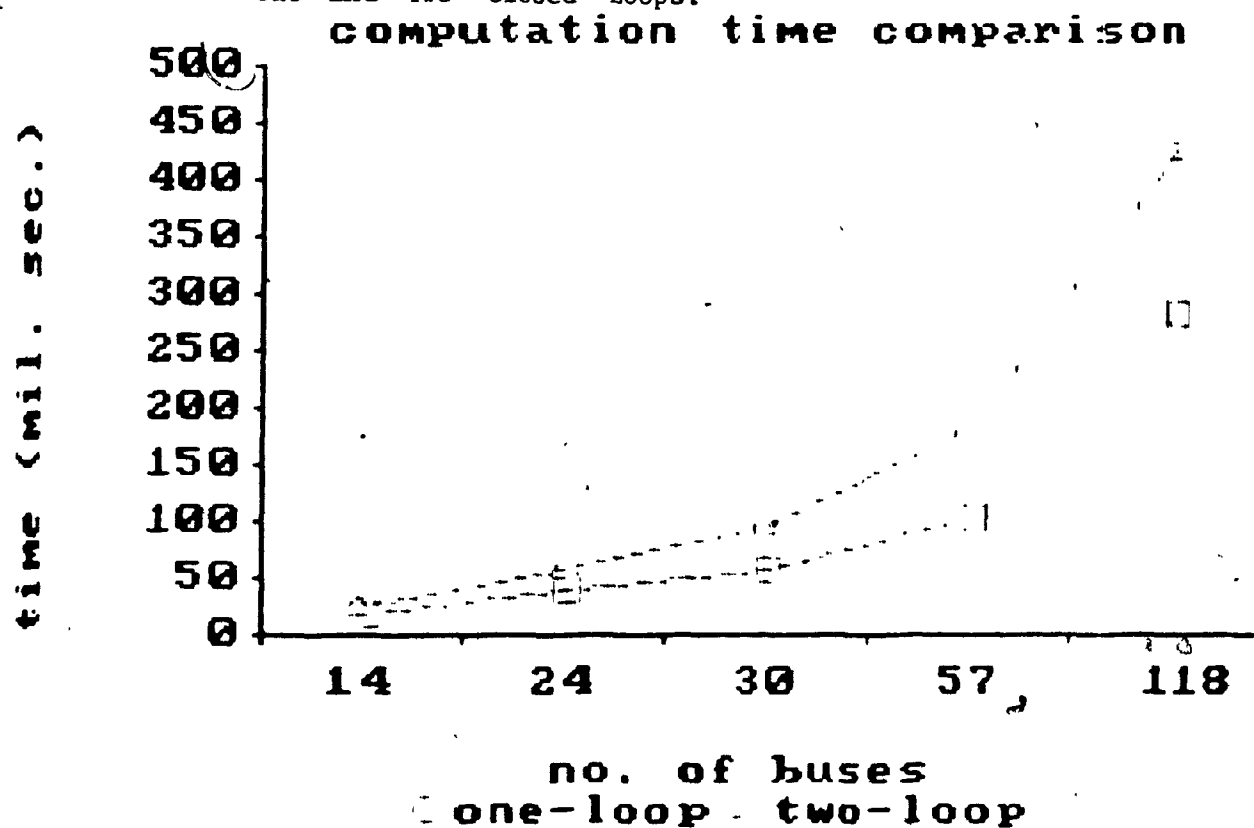


Fig. 4.3 Time Comparison of Evaluating the \bar{x}_{jk} Bounds for the IEEE Systems Based on One and Two Closed Loops.

the contingency flows are constricted from filter to filter numerically and how the load level can affect the tightness of the contingency flow bounds.

The IEEE 30-bus, 41-line system is used in both examples for demonstration. The two examples differ only by their loading levels, i.e., the first one is a normal load and the second one is a light load. The contingency to be studied in both examples is chosen as the outage of line # 7 which is connecting buses 4 and 6 (see Appendix B) . Two DC load flow simulations for the same contingency under the two loading conditions have indicated that line # 6 will be overloaded under the conditions specified in the first example, and no violation for the second case.

4.2.1 Example 1

The loading conditions, i.e., generations and loads, of this example are based on the optimal load flow results given by Alsac and Stott [Alsac et al. 1974] . The real power injections are shown in Appendix B . This loading level is regarded as a "normal" load here. The MVA ratings of the lines are used as the security limits [Alsac et al. 1974] . The pre-contingency flow on line # 7 is 0.354 p.u. (MVA rating : 0.9 p.u.) . Some selected contingency flows with their bound estimates are depicted in Table 4.4 .

In Table 4.4 , it is shown how the bound estimates are gradually constricted from filter to filter. The type 2 x_{jk} bounds, given by (3.53) to (3.55), are used for all filters here. Recall from 3.3 that Filter # 0 (CF^0) uses the extreme bounds of the LODF , i.e., -1 and 1 ; Filter # 1 (CF^1) uses the extreme bounds of $x_{lm/jk}$; Filter # 2 (CF^2) employs the type 1 $x_{lm/jk}$ bounds (i.e., direct links are considered explicitly) ; Filter # 3 (CF^3) uses the type 2 $x_{lm/jk}$ bounds (i.e., exploiting the characteristics of the remote lines) and finally Filter # 4 (CF^4) is the DC load flow simulation which exploits the sparsity of the network and simulates outage by the matrix inversion lemma. The pre-contingency flows, denoted by PCF , as well as the line security limits, denoted by SL , are also depicted besides the line numbers. The status of each contingency flow is determined by comparing the calculated bounds with the security limits (i.e., both upper and lower limits) . The definitions of different types of contingency flows can be referred to section 3.1.3 .

For line # 1, Filter # 3 was called upon because the previous filters have failed to identify the contingency flow. However, filter # 3 is found not applicable in this case. This is because the retained network associated with line # 1 includes nodes 1,2,3,4, 5,6 . On the other hand, the retained network associated with line # 7 contains nodes 1,2,3,4,6,7,8,9,10,12,28 . Both retained networks share 5 common nodes together therefore Filter # 3 cannot be employed. Hence it is denoted as Not Applicable (N.A.) in Table 4.4 and the bounds

Table 4.4

Selected Results on the Bound Estimates of Example 1

	$x_{lm/jk}$ $\times 10^{-1}$	$\rho_{lm/jk}$	$P_{lm/jk}$ (p.u.)	Status
<hr/>				
Line # 1	PCF = 1.198 p.u., SL = \pm 1.3 p.u.			
Fil # 0	-	(-1,1)	(0.844,1.55)	Uncertain
Fil # 1	(-0.41,0.41)	(-1,1)	(0.844,1.55)	Uncertain
Fil # 2	(-0.092,0.088)	(-0.51,0.488)	(1.02,1.37)	Uncertain
Fil # 3	N.A.	Ibid	Ibid	Uncertain
Fil # 4	0.0714	0.283	1.298	Safe*
<hr/>				
Line # 6	PCF = 0.502 p.u., SL = \pm 0.65 p.u.			
Fil # 0	-	(-1,1)	(0.148,0.856)	Uncertain
Fil # 1	(-0.751,0.751)	(-1,1)	(0.148,0.856)	Uncertain
Fil # 2	(0.169,0.636)	(0.203,1)	(0.574,0.856)	Uncertain
Fil # 3	N.A.	Ibid	Ibid	Uncertain
Fil # 4	0.392	0.507	0.681	Unsafe
<hr/>				
Line # 17	PCF = 0.0790 p.u., SL = \pm 0.32 p.u.			
Fil # 0	-	(-1,1)	(-0.275,0.433)	Uncertain
Fil # 1	(-0.873,0.873)	(-1,1)	(-0.275,0.433)	Uncertain
Fil # 2	(-0.279,0.454)	(-0.331,0.538)	(-0.038,0.269)	Safe
<hr/>				
Line # 37	PCF = 0.0607 p.u., SL = \pm 0.16 p.u.			
Fil # 0	-	(-1,1)	(-0.293,0.414)	Uncertain
Fil # 1	(-0.993,0.993)	(-0.712,0.712)	(-0.191,0.312)	Uncertain
Fil # 2	(-0.464,0.464)	(-0.332,0.332)	(-0.057,0.178)	Safe
Fil # 3	(-0.095,0.095)	(-0.068,0.068)	(0.0366,0.085)	Safe
<hr/>				

* marginally safe contingency flow

on the LODF and the contingency flow remain the same as in the previous case. A DC load flow is finally required in order to determine the status of line # 1 . Note that the result is very close to the limit (i.e., 1.29 p.u., compared to 1.3 p.u.) . Therefore, an "*" is marked besides the status to indicate that this line is only marginally safe.

For the contingency flow analysis of line # 6 , only the final DC load flow filter is capable of identifying it and it is found to be overloaded after the contingency. Note that this is a triangular case described in 3.2.6, i.e., line # 6 and line # 7 have node 6 in common. Since these two lines are very close to each other, Filter # 3 cannot be applied either.

For line # 17 , the contingency flow bounds are found to lie within the security limits after Filter # 2 . For line # 37 , contingency flow bounds are found to be safe after Filter # 3 . Note that the retained network for line # 37 is composed of nodes 29,27,30, 28,25 . Comparing these nodes and the previously stated retained nodes for line # 7 , although both retained network share a common node 28 , there is no line overlapping. Hence, Filter # 3 is still applicable here and this filter indeed identifies the contingency.

It has to be noted that for those lines whose base case flows are already close to their limits, they are more likely to become an uncertain flow in the filtering process. For example, line # 1 and

line # 6 in Table 4.4 are fairly heavily loaded in the base case, both of them eventually require a DC load flow to determine their status. On the other hand, line # 17 and line # 37 are initially lightly loaded and finally none of them uses the higher order filters.

The overall performance of all the filters for the outage of line # 7 in this example is depicted in Table 4.5. One violation is detected, i.e., line # 6 shown in Table 4.5. This indeed agrees with the previous DC load flow result.

Table 4.5

Filter Performances of The Outage of Line # 7
in the 30-Bus, 41-Line System under Normal Load

	Cumulative Safe Flows after Filtering	Overloaded Flows detected after Filtering	Uncertain Flows after Filtering
Fil # 0	12	0	28
Fil # 1	12	0	28
Fil # 2	21	0	19
Fil # 3	23	0	17
Fil # 4	39	1	-

4.2.2 Example 2

This example also uses the optimal load flow results from Alsac and Stott [Alsac et al. 1974], however, the net real power injections are all reduced by 50% . Such a procedure is intended to simulate a light load situation for analysis. The contingency is still the same, i.e., line # 7 is out of service. The pre-contingency flow on line # 7 is 0.177 p.u. In Table 4.6, some selected bound estimates are shown.

Table 4.6Selected Results on the Bound Estimates of Example 2

	$x_{lm/jk}$ $\times 10^{-1}$	$p_{lm/jk}$	$P_{lm/jk}$ (p.u.)	Status
Line # 1	PCF = 0.599 p.u., SL = \pm 1.3 p.u.			
Fil # 0	-	(-1,1)	(0.422,0.76)	Safe
Line # 6	PCF = 0.251 p.u., SL = \pm 0.65 p.u.			
Fil # 0	-	(-1,1)	(0.074,0.428)	Safe
Line # 17	PCF = 0.0395 p.u., SL = \pm 0.32 p.u.			
Fil # 0	-	(-1,1)	(-0.138,0.216)	Safe
Line # 37	PCF = 0.0303 p.u., SL = \pm 0.16 p.u.			
Fil # 0	-	(-1,1)	(-0.147,0.207)	Uncertain
Fil # 1	(-0.993,0.993)	(-0.712,0.712)	(-0.096,0.156)	Safe

Since the network and the contingency being studied are exactly the same, the bounds on $x_{lm/jk}$ and $p_{lm/jk}$ in Table 4.4 and Table 4.6 remain unchanged, e.g., see line # 37 in both tables. However, since the loading has been greatly reduced, i.e., 50%, the base case line flows are also generally reduced in terms of their magnitudes. As a result, the interval enclosed by the real power flow bounds is also tightened and hence the bound estimates are more discriminatory. This can be verified by comparing the intervals of the contingency flows from both Table 4.4 and Table 4.6. For example, consider line # 1, in Table 4.4, the interval enclosed by the contingency flow bounds is 0.706 p.u. However, in Table 4.6, the corresponding interval is 0.338 p.u.

The overall performance of all filters in this light load case is shown in Table 4.7. There is no violation detected, which agrees with the previous DC load flow result. Note that the higher order filters including the DC load flow are not required at all in this condition. Most contingency flows are identified by the most conservative filters. This is indeed one of the great advantages of this filtering method.

Table 4.7

Filter Performances of the Outage of Line # 7
in the 30-Bus, 41-Line System Under Light Load

	Cumulative Safe Flows after Filtering	Overloaded Flows Detected after Filtering	Uncertain Flows after Filtering
Fil # 0	28	0	12
Fil # 1	32	0	8
Fil # 2	40	0	0
Fil # 3	-	-	-
Fil # 4	-	-	-

4.3 Filters Performances

4.3.0 Introductory Remarks

In the preceding sections, the numerical results on different bound types have been presented. The next step would therefore be to combine these different bound types into a series of filters and to observe their performances in the actual classification process. There are two major interests here, i.e., the identification efficiency and computational efficiency of each filter.

The identification efficiency considers the ability of each filter to reduce the number of uncertain flows for each uncertain contingency, e.g., the ability of each filter in identifying critical and non-critical contingencies. Such an ability is directly related to the tightness of the bounds used in each filter.

The computational efficiency focuses on the speed performances of different filters. For example, some filters have good identification efficiencies but poor computational efficiencies because it may be too time-consuming to calculate a set of very tight bounds. Such an efficiency usually is a trade-off with the identification efficiency. In the following demonstration, it is intended to explore these two efficiencies with the different filters proposed previously.

4.3.1 Identification Efficiencies of Filters

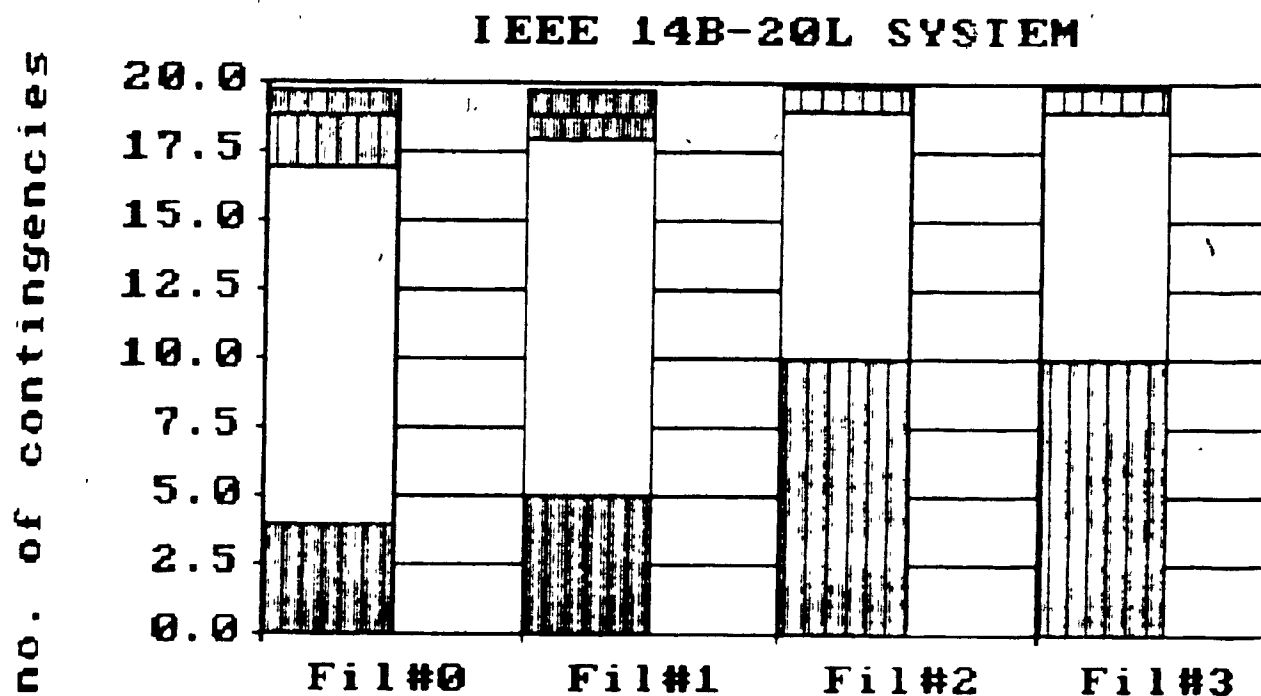
The IEEE systems are used in the following to demonstrate this filtering method applied to different system sizes and configurations. The loading conditions, i.e., real power injections, are depicted in Appendix B. All primary outages in each system are tested, i.e., NL contingencies are evaluated in a system with NL lines.

Results of the two proposed filtering schemes, described in section 3.3, are shown from Figures 4.4 to 4.8. The five IEEE systems are used for testing. All the figures denoted by a subscript "a" show the filtering results obtained by using one closed loop for the

x_{jk} bounds, i.e., scheme 1 in 3.3 . For the figures denoted with the subscript "b", the x_{jk} bounds are based on the two closed loop results, i.e., scheme 2 in 3.3 .

In these figures, each stack bar represents a filter type. The range specified at the bottom (e.g., 0,1-3,4-7,...) represents the type of contingency which has the number of uncertain flows within the specified range (e.g., a contingency with 2 uncertain flows is grouped into the 1-3 range). The "zero" range represents those contingencies classified as either critical or non-critical after each filter. Note that the "zero" range is a cumulative measurement. The height of the stack represents the total number of contingencies. For example, in Figure 4.4.a, Filter # 0 (CF^0) has 4 non-critical contingencies; 13 uncertain contingencies have 1 to 3 uncertain flows after Filter # 0 (CF^0); 2 uncertain contingencies have 4 to 6 uncertain flows and so on.

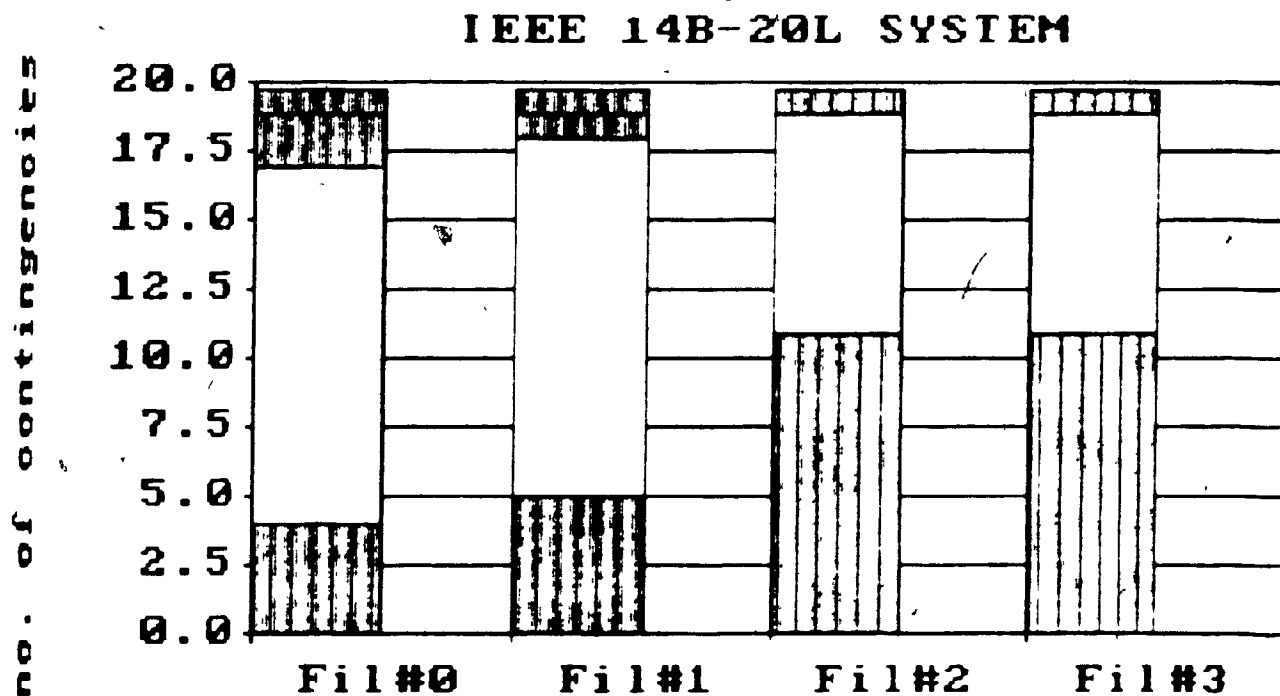
The semi-independent lines are grouped into the "zero" range after Filter # 1 (CF^1) . For those contingencies whose x_{jk} bounds cannot be established, e.g., the "no-closed-loop" lines, (CF^4) , the filters used here are not applicable except Filter # 0 (CF^0) and Filter # 4 . After Filter # 0 (CF^0) , they have to be sent to Filter # 4 (CF^4) directly. In the figures presented, such cases are excluded after Filter # 0 (CF^0) . Note that the 57-bus, 78-line system has 19 such contingencies. In Figure 4.7.a and 4.7.b, the total number



Filter Types (1 closed loop)

■ 0 □ 1-3 ▨ 4-6 □ >7

Fig. 4.4.a Filter Performances on IEEE 14-Bus System
Using Type 1 Bound of x_{jk} .



Filter Types (2 closed loops)

■ 0 □ 1-3 ▨ 4-6 □ >7

Fig. 4.4.b Filter Performances on IEEE 14-Bus System Using
Type 2 Bound of x_{jk} .

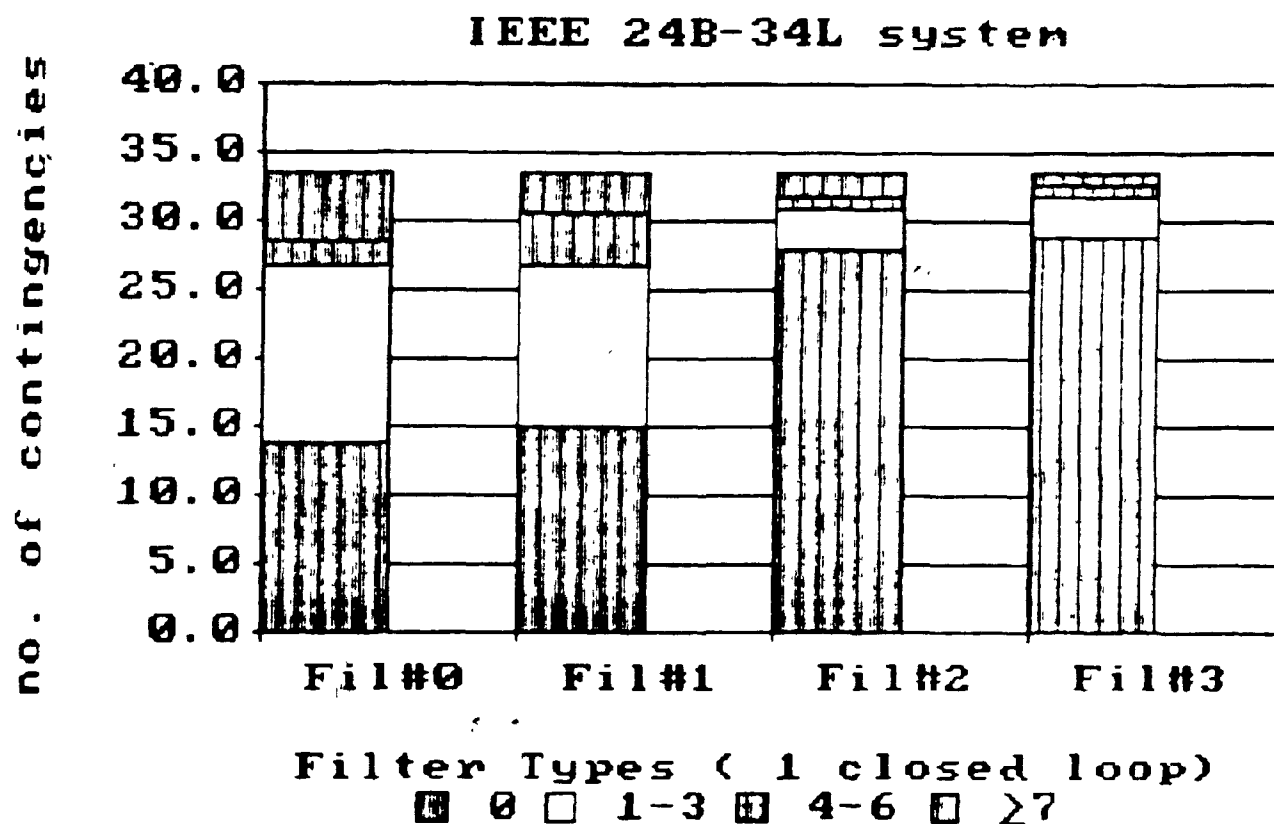


Fig. 4.5.a Filter Performances on IEEE 24-Bus System Using Type 1 Bound of x_{jk} .

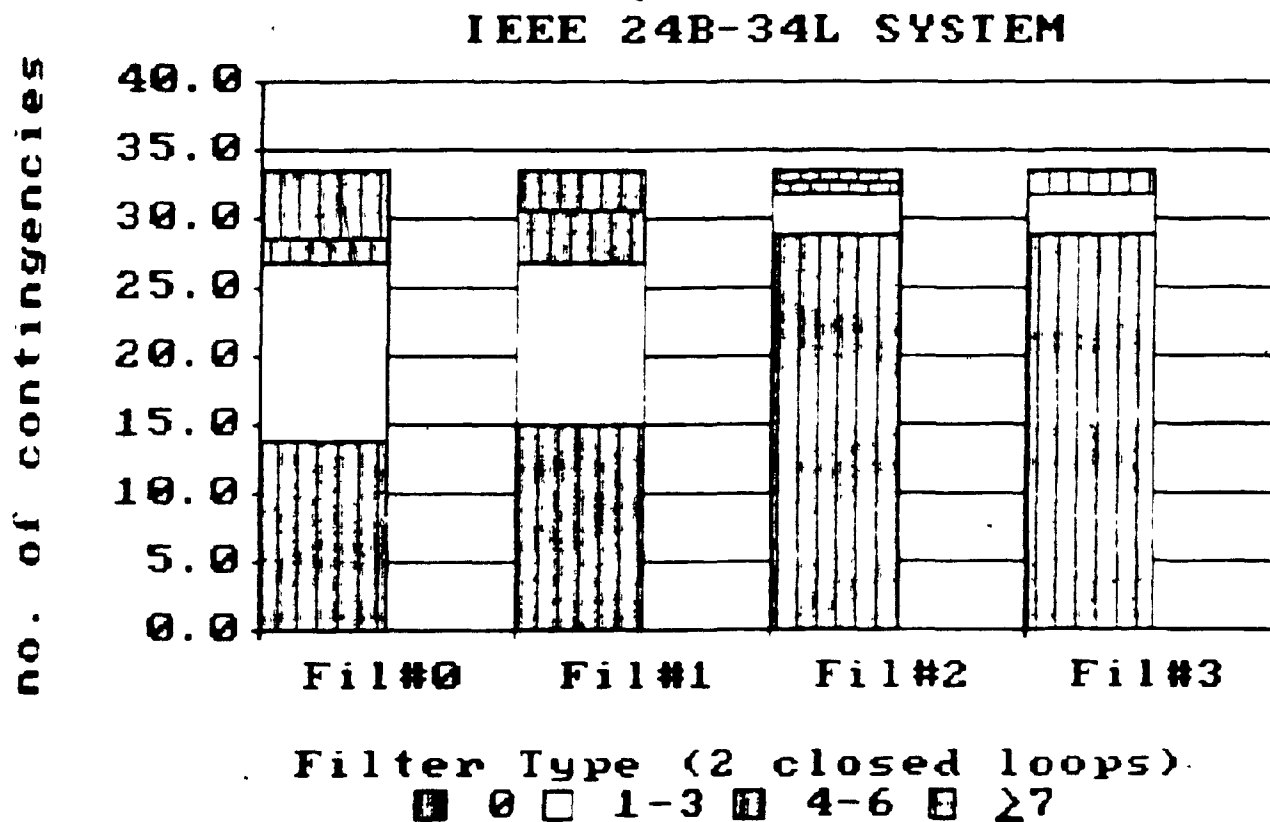
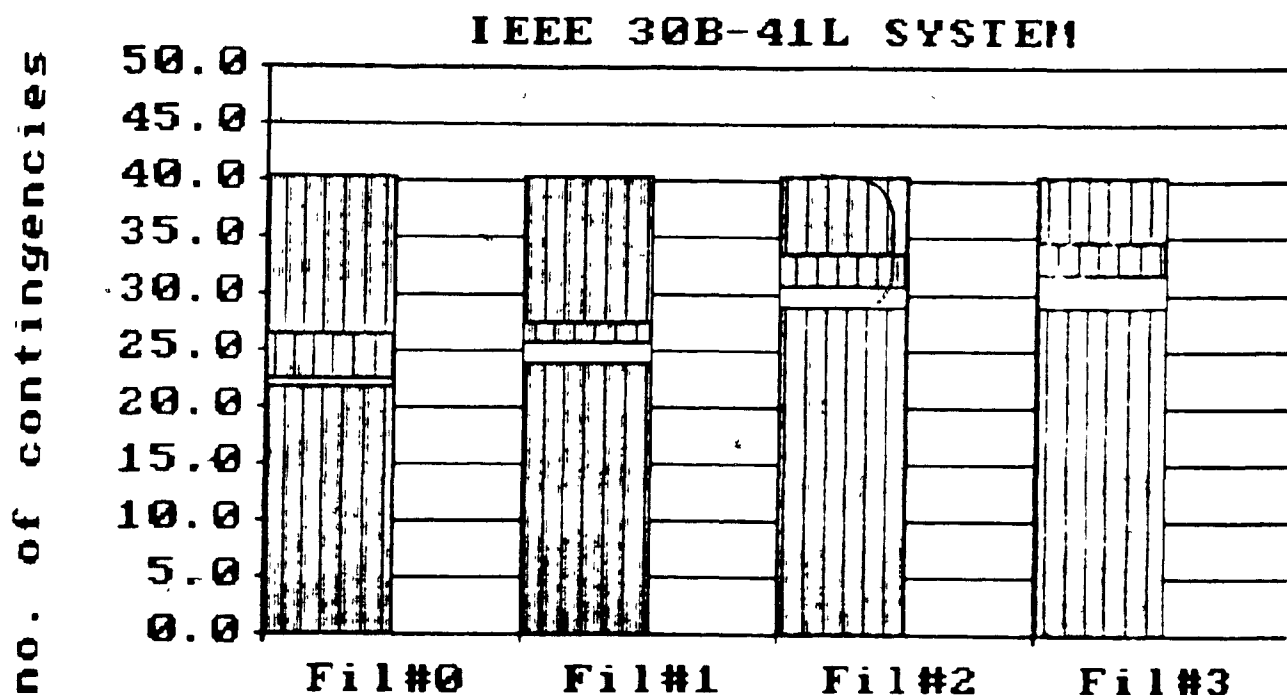


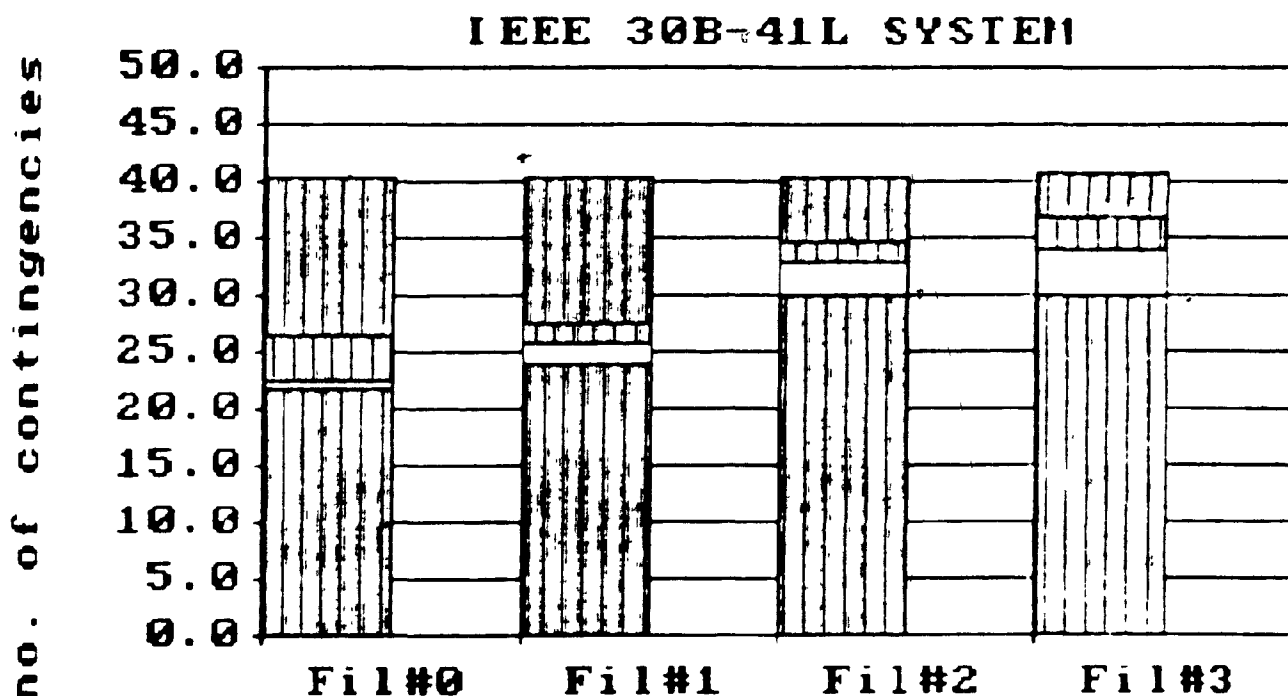
Fig. 4.5.b Filter Performances on IEEE 24-Bus System Using Type 2 Bound of x_{jk} .



Filter Types (1 closed loop)

■ 0 □ 1-7 ■ 8-14 □ ≥15

Fig. 4.6a Filter Performances on IEEE 30-Bus System
Using Type 1 Bound of x_{jk} .



Filter Types (2 closed loops)

■ 0 □ 1-7 ■ 8-14 □ ≥15

Fig. 4.6b Filter Performances on IEEE 30-Bus System
Using Type 2 Bound of x_{jk} .

IEEE 57B-78L SYSTEM

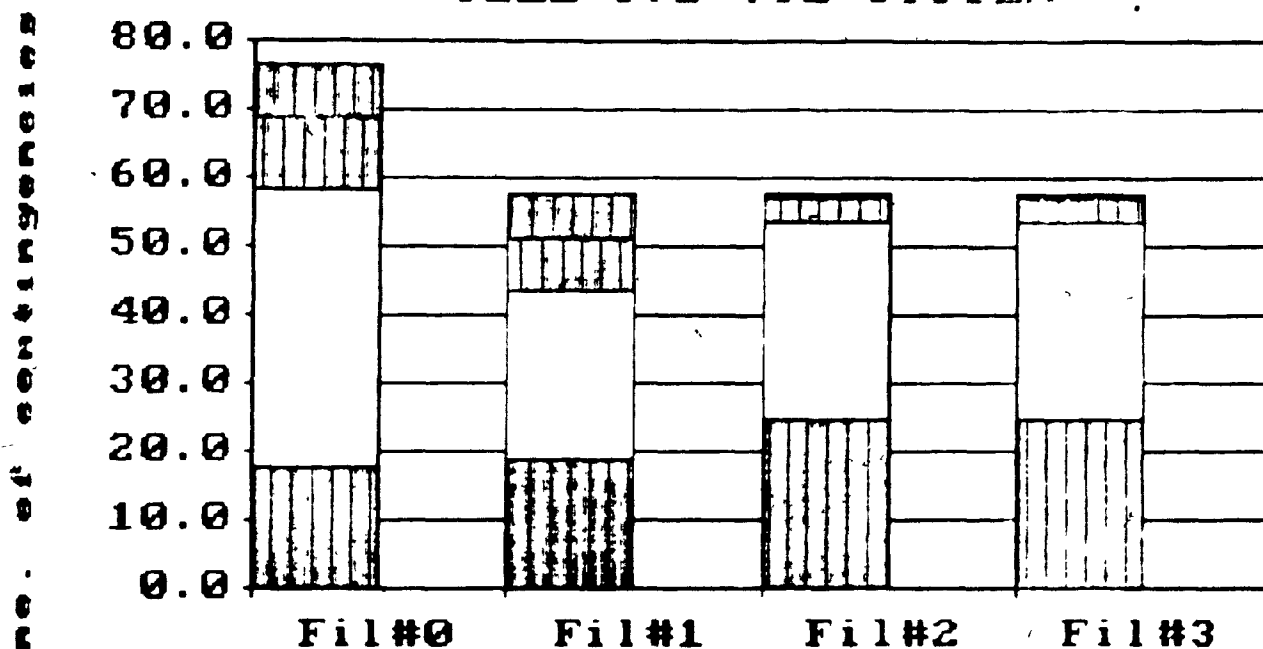


Fig. 4.7a Filter Performances on IEEE 57-Bus System
 Using Type 1 Bound of x_{jk} .

IEEE 57B-78L SYSTEM

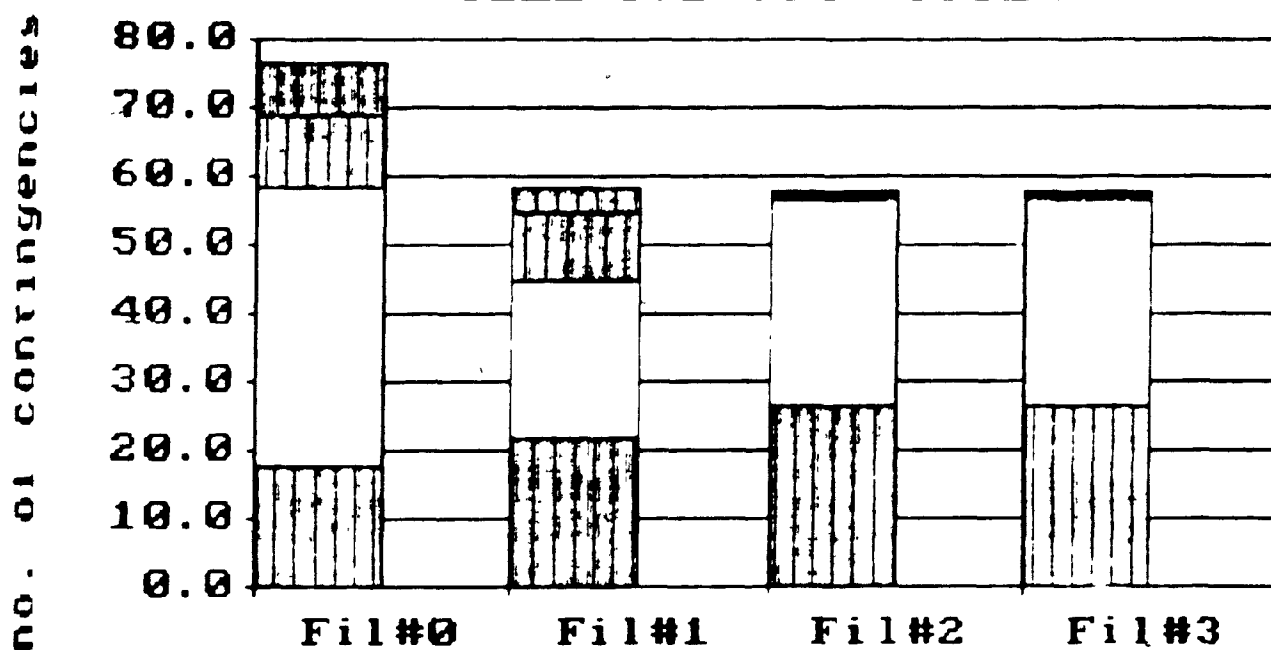
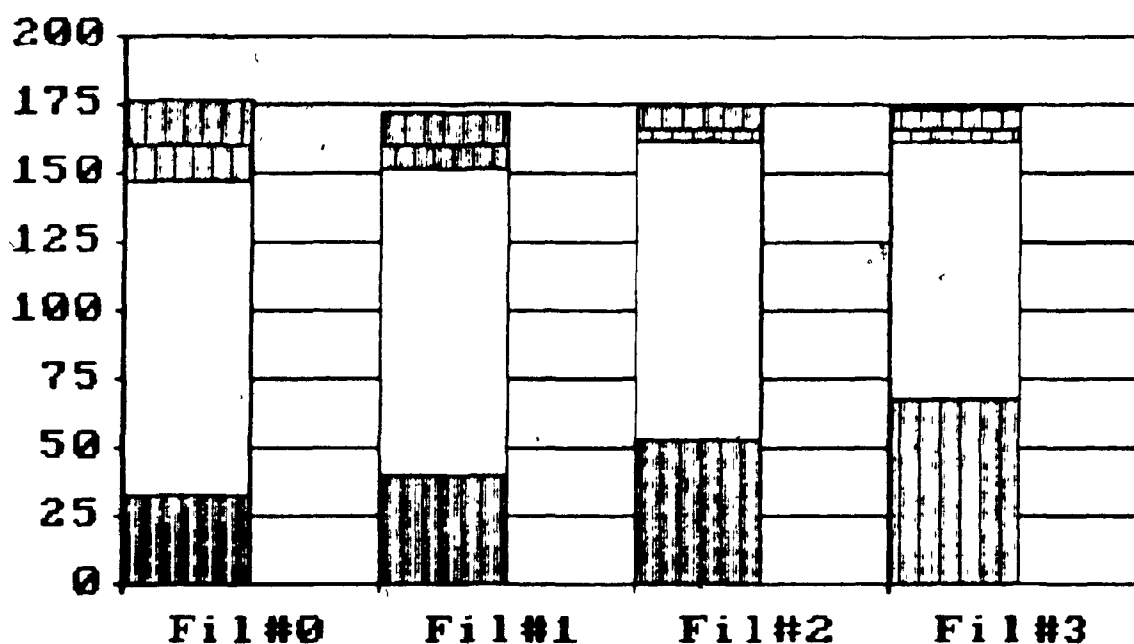


Fig. 4.7b Filter Performances on IEEE 57-Bus System
 Using type 2 Bound of x_{jk} .

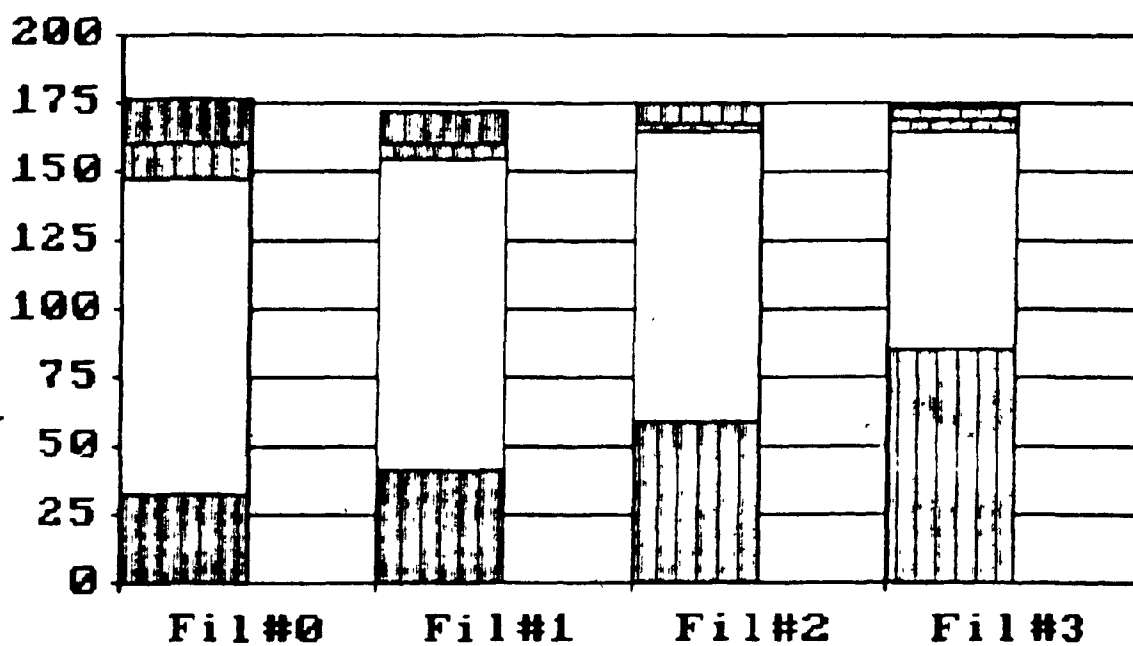
no. of contingencies

IEEE 118B-179L SYSTEM**Filter Types (1 closed loop)**

0
 1-29
 30-58
 >59

Fig. 4.8a Filter Performances on IEEE 118-Bus System
Using Type 1 Bound on x_{jk} .

no. of contingencies

IEEE 118B-179L SYSTEM**Filter Types (2 closed loops)**

0
 1-29
 30-58
 >59

Fig. 4.8b Filter Performances on IEEE 118-Bus System
Using Type 2 Bound on x_{jk} .

of contingencies beyond Filter # 0 (CF^0) is reduced to 59 . The 19 "no-closed-loop" lines are excluded. From the figures, the following observations are noted:-

- (1) The number of the "zero" range contingencies, i.e., contingencies classified as critical or non-critical, grows as the filtering process proceeds. The number of contingencies with uncertain flows also shrink gradually along with the filtering process.
- (2) By using a tighter bound on x_{jk} , namely increasing the number of closed loops for the retained network, the filtering performance is practically unaffected. This can be observed by comparing the "a" and "b" figures.
- (3) Results from Filter # 0 (CF^0) and Filter # 1 (CF^1) are almost exactly the same for all five systems.
- (4) The improvements, in terms of the expansion of the "zero" range, between Filter # 2 (CF^2) and Filter # 3 (CF^3) are not significant in the small systems, e.g., 14, 24, 30-bus systems. However, on the 118-bus system, Filter # 3 (CF^3) reduces significantly the number of uncertain contingencies which have a large number of uncertain flows in the previous filter.
- (5) The IEEE 57-bus system is an exceptional case where 19 contingencies are not able to be analyzed by this filtering method due to its system structure, i.e., a lot of lines connected in series.

Filter # 0 (CF^0), even though it is the most conservative and the easiest to be computed, does classify a lot of contingencies. In the loading conditions specified here, Filter # 0 in general can classify at least 1/3 of the contingencies. From the simulations, it is also shown that the extreme bounds of $x_{lm/jk}$ used in Filter # 1 (CF^1) are not very useful because they usually give the extreme bounds on the $c_{lm/jk}$, which eventually give the same results as Filter # 0.

Filter # 2 (CF^2) performs better in the small systems than the larger ones. Recall that such a filter exploits the direct links characteristics between lines. Thus, in a smaller system, such characteristics are usually more profound. However, for larger systems, most unce-tain line flows are found to be farther away from the outaged line, therefore the bounds it establishes do not seem to be very effective (type 1a bounds of the $x_{lm/jk}$ are mostly used).

It was originally thought that by using only one close loop for the retained network, the performance of Filter # 3 (CF^3) can be improved. This is due to the speculation that if less nodes are retained for each retained network, the possibility of applying Filter # 3 will generally be increase (recall the applicability of Filter # 3 relies on the complete separation of the two retained networks, i.e., one from the outaged line and one from the outaged line and one from the line under consideration). It was also speculated that for a large system, such as the 118-bus system, the "remote line" condi-

tions will be more common and thus Filter # 3 will be useful. However, according to the simulations, it is found that by retaining one or two closed loops, Filter # 3 is usually not applicable in the small systems, e.g., the 14-bus. However, Filter # 3 does reduce the number of uncertain flows in most uncertain contingencies whose initial uncertain flow number is high. On larger systems, where Filter # 3 is usually applicable, the bound estimates using 2 closed loops do seem to be more useful in terms of identifying critical or non-critical contingencies.

4.3.2 Computational Efficiency of Filters

The following filtering schemes are used here to investigate the computational efficiency of each filter, i.e.,

- (1) Scheme 1 : Filters (# 0,1,2,3,4) are used,
- (2) Scheme 2 : Filters (# 0,2,3,4) are used.
- (3) Scheme 3 : Filters (# 0,2,4) are used.
- (4) Scheme 4 : Filters (# 0,4) are used.

(Note that these filter types should be referred to section 3.3) . As seen from these filtering schemes, a particular filter is eliminated from the filtering procedure in each filtering scheme. The total CPU time for processing that particular scheme is then recorded. As a result, the computational efficiency of each filter can be observed by comparing the different CPU processing times.

The timing are presented in Table 4.8 . The CPU times indicated here are based on the AMDAHL 5850 computer at McGill. Each timing represents the total elapsed time for the completion of the filtering procedure, i.e., including the DC load flow (Filter # 4) which classifies all remaining uncertain contingencies as either critical or non-critical. Since the x_{jk} bounds are assumed to be pre-calculated, the time required for the evaluation of the x_{jk} bounds are not included here. All five systems are tested and the results are compared to the corresponding DC load flow simulations which do not have any pre-filtering. Note that in this study all the DC load flow simulations exploits the sparsity properties of the network and also use the matrix inversion lemma in simulating the outages. The loadings of the five test systems are recorded in Appendix B .

Table 4.8

CPU Time (ms) of Different Filtering Schemes

Bus					
Scheme No.	14	24	30	57	118
1	8.70	12.1	61.1	109.	754.
2	8.15	10.5	56.3	84.0	692.
3	7.62	9.53	33.0	98.0	459.
4	7.32	14.1	19.4	96.7	434.
DC load flow without pre- filtering	9.30	24.0	37.6	131.	646.

It is noticed from the table that using all the filters, e.g., in scheme 1, is not always beneficial. For example, the 30-bus and 118-bus systems take more time in using the filtering method than the DC load flow. Even if Filter # 1 (CF^1) is eliminated, the 30-bus and 118-bus systems still takes a longer time than the DC load flow.

However, if Filter # 3 is removed, as in the case of scheme 3, the computational efficiencies for all five systems are shown to be better than the DC load flow without any pre-filtering. If Filter # 2 (CF^2) is also eliminated, as in the case of scheme 3, the processing times are also further reduced.

It is observed that Filter # 3 (CF^3) is generally the most time-consuming filter. Recall from the previous chapter that the applicability of Filter # 3, where the characteristics of the remote lines are exploited, depends on the complete separation of the two retained networks. That is one from the outaged branch (j,k) and the other one from the arbitrary branch (l,m), under consideration. Every time Filter # 3 is called, the program has to check for such separation node by node. The process can easily become time-consuming. Also from the identification efficiency point of view, such a filter is not particularly powerful, therefore its application on the filtering scheme is not very attractive.

It is also noted that the results from scheme 4 are better than those from scheme 3 in general. There is only one case

where the 24-bus system takes more time in scheme 4 than in scheme 3 . This is because Filter # 2 identifies a lot of non-critical contingencies in the 24-bus system in particular. As a result, by including Filter # 2 it reduces the number of uncertain contingencies for the final DC load flow (Filter # 4) hence it also reduces the overall time. However, from the previous section, it is found that Filter # 2 generally does not perform so well as in the other systems. Therefore it can be concluded that the combination of filters shown in scheme 4 is by far the most efficient schedule.

4.3.3 Performances under Different Loading Conditions

It has been pointed out previously that the system loading conditions can affect the filtering process. In a light load case, the pre-contingency branch flows are comparatively smaller in magnitude. Hence the interval of the contingency flow bounds derived is generally narrower. Therefore, the lower order filters can usually identify the contingencies as critical or non-critical and higher order filters are not necessary. As a result, the whole processing time can be reduced if the loading conditions is reduced. This is demonstrated by using the IEEE 118-bus system.

The injections shown in Appendix B is regarded as a heavy load case. A medium load case is simulated by decreasing all the injections to 80% of their original values. A light load case is also

simulated by further reducing the injections to 50% of their original values. The identification efficiencies are depicted in Figures 4.9 and 4.10. The x_{jk} bound used here is obtained from retaining two closed loops. Note that the heavy load case has already been shown in Figure 4.8b. The timing of the medium load is recorded as 440.ms using scheme 2 described previously. The light load case with the same filtering scheme is 183.8 ms. By comparing these CPU times with the timing shown in Table 4.8, it is apparent that such a filtering method can take full advantage of the system loading conditions. For light load case, its processing time is drastically reduced, e.g., more than 300% improvement in speed between the heavy and light loads of the 118-bus system.

4.4 Performance of the Proposed Selection and Ranking Algorithms

4.4.1 Method A : Selection Based on the Number of Uncertain Flows

Results obtained from applying the proposed contingency selection method based on the number of uncertain flows are presented here. The most efficient filtering scheme, i.e., using only Filter # 0 and Filter # 4 (CF^4) is used. The IEEE 30-bus and 118-bus systems are chosen to demonstrate the efficiency of this selection method. The selection is accomplished by assuming a threshold of 8 lines for the 30-bus system and 30 lines for the 118-bus system. Therefore, any uncertain contingency with a number of contingency flows greater than such a threshold will be submitted to the DC load flow (CF^4). Those

no. of contingencies

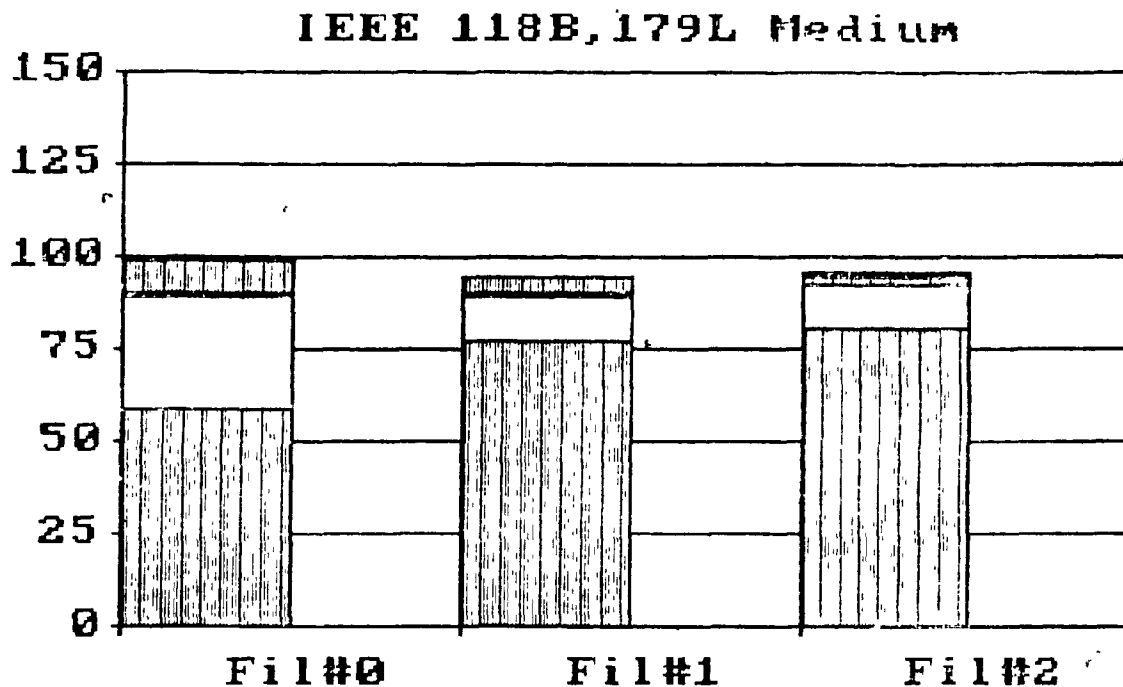


Fig. 4.9 Filter Performances on IEEE 118-bus System Under Light Load.

no. of contingencies

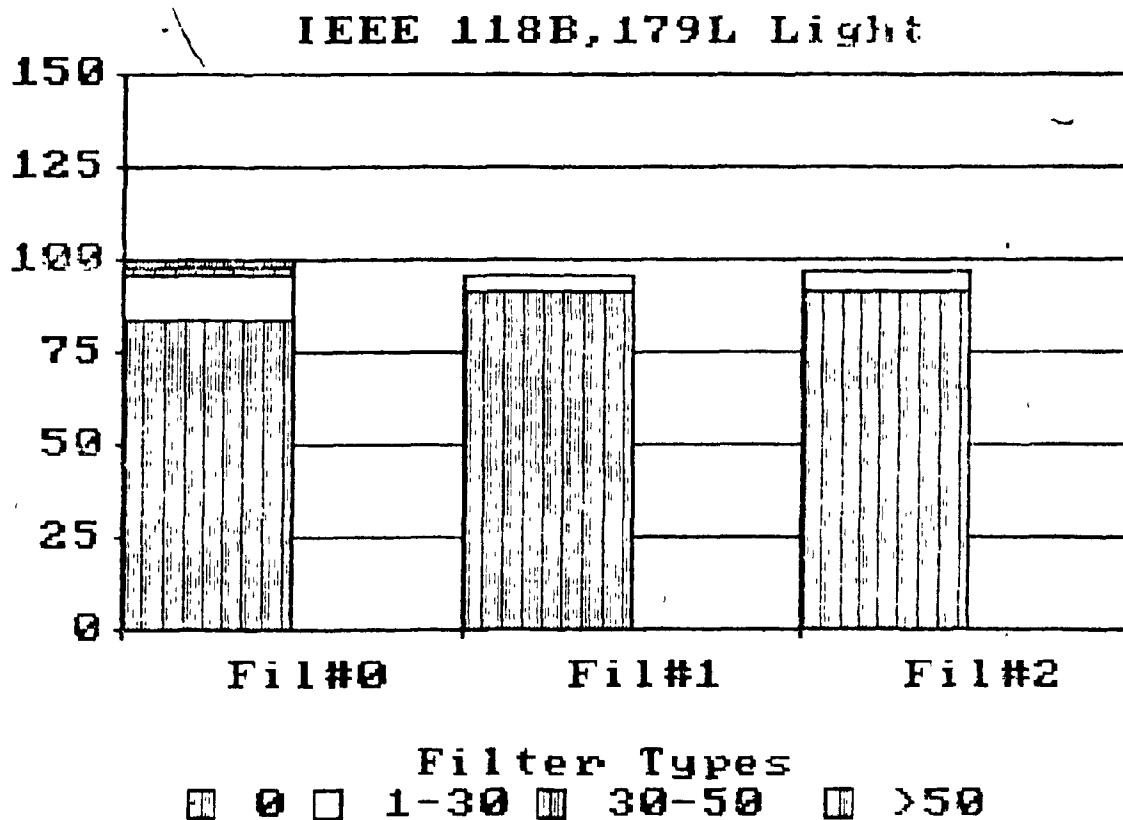


Fig. 4.10 Filter Performances on IEEE 118-bus System Under Medium Load.

whose number of uncertain flows are less than the threshold will be assumed safe and waived from Filter # 4 . With the above specified threshold values, all critical contingencies, obtained from a separated DC load flow simulation without any pre-filtering, are captured. In Table 4.9, the computational efficiencies are shown for the systems under a heavy load case and a light load case.

Table 4.9

Computational Efficiency of Selection Method A

Based on the Total CPU Time (ms)

Bus/Line	30/41	118/179
Heavy Load	17.6	174.5
Light Load	15.2	102.5

4.4.2 Method B : Selection Based on the Relative Overload Expectation

The same systems and same loading conditions are used as in the preceding case. The thresholds of the Relative Overload Expectation (ROE) , defined in section 3.4 , for both systems are set at 5% . Again, all critical contingencies according to a separate DC load flow simulation without any pre-filtering are captured. The recorded CPU timing for the completion of all single outage analysis are depicted in Table 4.10 .

Table 4.10Computational Efficiency of Selection Method BBased on the Total CPU Time (ms)

Bus/Line	30/41	118/179
Heavy Load	19.6	179.4
Light Load	18.7	84.9

4.4.3 Discussion

From the results shown in Tables 4.9 and 4.10, both methods perform almost the same in terms of speed. The improvement is significant compared to those schemes without selection, e.g., in the 118-bus system it is up to 500 % on average (heavy and light loads). It was also found from various simulations that by increasing the threshold the speed can be even further increased. However, it also suffers from some errors where critical contingencies may be missed. In this study, the values of the threshold are selected by a conservative guess, e.g., using 1/3 of the total line number to be a threshold.

In terms of using the number of uncertain flows or the ROE as a scalar performance index for ranking, their performances are discussed in the following. However, note that in this study, ranking is not done before selection. In each single line outage study, as

soon as the contingency whose performance index (i.e., number of uncertain flows or ROE) exceeds the threshold value, it will be automatically submitted to Filter # 4 .

Table 4.11 depicts the 10 highest ranked contingencies according to both indices in the 30-bus system.

Table 4.11
Ranking of Contingencies According to
Methods A and B

Rank	Method A (Line No.)	Method B (Line No.)
1	1 *	1 *
2	5 *	5 *
3	4 *	2 *
4	2 *	6
5	6	4 *
6	9	7 *
7	7 *	15
8	3	9
9	10	14
10	8	3
<hr/>		
Number of missed con- tingencies	1 (line # 36)	1 (line # 36)

* critical contingency

It was observed that in general Method B using the ROE gives a better ranking performance than Method A. For example, in Table 4.11, method B groups the critical contingencies more closely and higher up on the list. Therefore, if the selection is done by only choosing the top N ranked contingencies (e.g., the top 10 or 20). The Method B will be recommended.

4.5 DC and AC Load Flow Simulations Comparison

The 30-bus system is used for comparison of the DC load flow results and the AC load flow results. The AC load flow is simulated on the PTIFLO iterative load flow program installed in the McGill computer system. All primary outages are simulated one by one and the resulting power flows are compared with the power flows obtained from the DC model.

It was found that all the severe contingencies indicated by the AC simulations, i.e., single line outage of line # 1,2,4,5,7 and 36, are all captured according to the DC load flow simulations. There are only two contingency flows which are overloaded in the AC results are not detected by the DC simulation. However, it was found that both contingency flows are marginally safe according to the DC load flow (see Table 4.4, contingency flow of line # 1 during outage of line # 7). Hence, it is concluded that the DC model indeed gives a very good approximation to the AC full model.

CHAPTER V

CONCLUSIONS AND RECOMMENDATIONS

FOR FUTURE RESEARCH

5.1 Conclusions

The major interest of this study was to investigate the numerical performances of a contingency severity analysis technique using the linearized flow bound estimates. In addition, various proposed methods for contingency analysis and contingency selection and ranking were also reviewed. The findings of the study regarding these objectives can be summarized into two parts described as follows : -

Part 1: Review of Contingency Analysis Methods and Contingency Selection Algorithms

(1) Contingency analysis methods can basically be categorized into the point-wise and region-wise approaches. The point-wise approach evaluates the security of a system at one specified operating point. The region-wise approach analyzes the security of a system by investigating the "secure" region of operation.

(2) The point-wise approach contingency analysis methods are the most commonly employed in the industry now because the necessary techniques have been well established, e.g., fast and efficient load flow solution techniques and the compensation methods used for outage simulations. However, such an approach is ill-suited for studies involving uncertainties, massive simulations or global security evaluation, etc.

(3) The region-wise approach contingency analysis methods have stirred up a great deal of interest in recent years. This is mostly due to the advantages associated with such an approach, namely the system uncertainties can more easily be considered in such an analysis; global security evaluation is also possible and massive contingency simulations can be alleviated or avoided. However, the development of these methods are still limited to the approximate system models, e.g., DC load flow or decoupled models, at the present state.

(4) Current practices in contingency analysis usually select a few critical events for detailed analysis in order to meet the stringent time limit or to avoid massive simulations. Such selections are traditionally done by the operator or according to some previous simulation results. However, an adaptive and dynamic contingency selection scheme is more desirable as has been proposed by many authors. Two approaches are generally used, i.e., selection based on a Scalar Performance Index (SPI) and selection based on a Vector Performance Index (VPI) .

(5) The SPI approach uses a scalar quantity to measure the severity of each contingency and subsequently uses such measurements to rank contingencies. The highest ranked events will thus be selected. These methods are generally fast but are occasionally unreliable due to masking problems. Severe contingencies may thus be misranked in some cases.

(6) The VPI approach establishes a vector quantity for each contingency and each element of the vector contributes to the decision of whether the contingency is critical or non-critical.⁴ Selection is then accomplished by choosing only the critical events. Masking problems can be avoided and the decision is more accurate and reliable. The drawback on such an approach is that the evaluation speed is slower, but this disadvantage can be improved by setting up a multi-stage filtering strategy as described in Chapter II.

Part 2: Theory Derivation and Numerical Experience of the Contingency Filtering Technique using Linearized Flow Bound Estimates

- (1) Using the DC load flow model, the post-contingency real power line flows can be bounded by using the base case flows and the Line Outage Distribution Factors (LODF) bounds.
- (2) If the interval enclosed by such bounds lies within the security limits, the flow is safe. If the interval lies completely outside the limits, the flow is unsafe. For any other conditions, the flow is said to be uncertain.
- (3) If all the line flows after a contingency are found to be safe from the bounding method, the contingency is non-critical. If there is one or more unsafe flows, the contingency is said to be critical. Those contingencies which have uncertain flows will be classified as uncertain contingencies.

(4) The bound estimates are developed by establishing bounds on the LODF, a quantity which is independent of the loading conditions. A resistive network interpretation is developed in order that some network topological characteristics can be exploited to bound the LODF.

(5) Different types of bounds are established and various combinations of these bounds are used to build a series of filters. Each filter evaluates a set of bounds of the LODF for the incoming uncertain contingencies flows and subsequently calculates the bounds for their contingency flows. After filtering, the incoming contingencies are classified into three groups, namely critical, non-critical and uncertain contingencies. The uncertain contingencies are then submitted to the next filter where a tighter set of bounds are evaluated for those uncertain flows remaining. The final filter is a DC load flow simulation which calculates the exact values and clarifies any uncertainties remaining.

(6) Different filter types were studied in detail in order to examine their identification and computational efficiencies. It is found that some filters are not very useful in terms of their identification or computational efficiencies.

(7) Filter # 3 (referred to in section 3.3) which exploits the characteristics of the remote lines is found to be computationally in-

efficient. It is due to the fact that checking the applicable conditions for such a filter is too time-consuming.

(8) Filter # 2 is found to perform only fairly in terms of its identification efficiency. Especially on larger systems like the IEEE 118-bus system, the bound estimates that it provides are generally still too conservative and the improvements in terms of the reduction of the number of uncertain flow are small.

(9) Filter # 1 most of the time gives the same bound estimates as the preceding Filter # 0 hence Filter # 0 is not very useful at all. It is shown in this study that in general the combined use of Filter # 0 and the DC load flow simulation gives the best performance among all other combinations.

(10) It is also observed that the flow bound estimates developed in this study are strongly dependent on the system loading level. If the system is heavily loaded, the obtained flow bounds will be more conservative and hence it is more difficult to classify the contingencies in general. However, if the system is lightly loaded, the filtering performance is greatly enhanced because the flow bounds are less conservative then.

(11) Two newly proposed contingency selection methods using results from the filtering were tested. The two methods are basically two dif-

ferently defined scalar performance indices. It is found that with any one of the two selection methods, the computational efficiency is greatly increased to almost 5 times faster without sacrificing any identification accuracy, e.g., missing critical contingencies. Furthermore, by using the values of these performance indices to ranking contingencies, the ranking list is shown to be very reliable, i.e., all the overloaded cases are ranked very high on the list.

(12) The DC load flow results on the IEEE 30-bus system are validated with the AC load flow simulations. All contingencies causing overloads in the AC results are captured in the DC results.

5.2 Recommendations for Further Research

The following interests are considered worthwhile in pursuing further research :-

(1) In this study, the bounds on the LODF are derived based on the most primitive estimates and the network interpretation approach, however, deriving the LODF bounds based on other analytical approach, e.g., bounding the LODF using the partitioned matrices of the DC Jacobian [Galiana 1984], should also be investigated in a more detailed manner.

(2) In practice, the bus voltage violations or generator reactive power violations after a contingency should also be considered. How-

ever, the DC model employed in this study can only solve for the real power flows problem. To establish a similar filtering scheme for the voltage-reactive power evaluation is highly desirable. For example, using the decoupled load flow model, the voltage-reactive power relationship can be linearized to form a system similar to the DC model and a similar factor like the LODF can be established, e.g.,

$$v_i = v_i + \sigma(v_j - v_k) \quad (5.1)$$

where v_i is the post-contingency voltage; v_i, v_j, v_k are the pre-contingency voltages; σ is defined as a factor only dependent on the system structure.

(3) Using the LODF or other factors (e.g., σ in previous case) for bounding the post-contingency conditions are by no means the only viable methods. Other approaches like exploiting the characteristics of the non-linear power flow formulation have also shown some similar bounding results [Kaye et al. 1982 ; Ilic-Spong et al. 1984] . However, numerical experience with these analytical bounds still remains to be explored.

(4) The linearized contingency severity analysis method proposed in this thesis can very well serve as a filter for the AC contingency analysis process. However, the error between the DC model and the AC model is still not explicitly derived in general. Should such a re-

relationship be developed, e.g., an error range around the DC solution where the true AC solution will lie, by bounding the DC model, one can also bound the exact AC model directly as well.

BIBLIOGRAPHY AND REFERENCES

- Aboytes, F., 'Stochastic Contingency Analysis,' IEEE Trans. on PAS, Vol. PAS-97, No. 2, pp.335-341, March 1978.
- Albuyeh, F., 'Automatic Contingency Selection by Sensitivity Matrices,' Paper no. A 80 060-4, IEEE Winter Power Meeting, New York, N.Y., February 1980.
- Albuyeh, F., Bose, A., Heath, B., 'Reactive Power Considerations in Automatic Contingency Selection,' IEEE Trans. on PAS, Vol. PAS-101, No. 1, pp. 107-112, January 1982.
- Alsac, O., Stott, B., 'Optimal Load Flow with Steady State Security,' IEEE Trans. on PAS, Vol. PAS-93, No. 3, pp. 745-751, May/June 1974.
- Arafteh, S.A., 'Real-time Security Assessment with Fast Optimum Generation Shift Control,' PICA Proc., Toronto, Ontario, Canada, pp.360-368, May 1977.
- Banakar, M.H., Galiana, F.D., 'Power System Security Corridors Concept and Computation,' IEEE Trans. on PAS, Vol. PAS-100, No. 11, pp.4524-4532, November 1982.
- Billinton, R., Power System Reliability Evaluation, Gordon and Breach, 1970.
- Brown, H.E., 'Contingencies Evaluated by a Z-matrix Method,' IEEE Trans. on PAS, Vol. PAS-88, pp. 409-412, April 1969.
- Brown, H.E., 'Interchange Capability and Contingency Evaluation by a Z-matrix Method,' IEEE Trans. on PAS, Vol. PAS-91, pp. 1827-1832, September 1972.

- Chamorro, R.S., Anderson, M.D., Richards, E.F., 'Fast Transient Contingency Evaluation in Power Systems,' IEEE Trans. on PAS, Vol. PAS-100, No. 4, pp.1796-1805, April 1981.
- Cheng, W.M.J., Galiana, F.D., 'Contingency Severity Selection Based on Flow Bounds : Numerical Experience,' Power System Computation Conference Proceeding, Helsinki, Finland, August 1984.
- Debs, A.S., Benson, A.R., 'Security Assessment of Power Systems,' System Engineering for Power : Status and Prospects Conference Proc., Henniker, New Hampshire, pp. 144-176, August 1975.
- Dersin, P., Levis, A.H., 'Feasibility Sets for Steady-state Loads in Electric Power Networks,' IEEE Trans. on PAS, Vol. PAS-101, No. 1, pp. 60-70, January 1982.
- Dhar, R.N., Computer Aided Power System Operation and Analysis, McGraw-Hill, 1982.
- Dommel, H.W., Sato, N., 'Fast Transient Stability Solutions,' IEEE Trans. on PAS, Vol. PAS-91, No. 4, pp. 1643-1650, July/August 1972.
- Dy Liacco, T.E., 'The Adaptive Reliability Control of Power System,' IEEE Trans. on PAS, Vol. PAS-86, pp. 517-531, May 1967.
- Dy Liacco, T.E., 'The Emergency Concept of Security Control,' Proc. 1970 Symp. Power Systems, (Purdue University, Lafayette, Ind.), May 1970.
- Ejebe, G.C., Wollenberg B.F., 'Automatic Contingency Selection,' IEEE Trans. on PAS, Vol. PAS-98, No. 1, pp. 97-109, January/February 1979.

El-Abiad, A.H., 'Digital Calculation of Line to Ground Short Circuits by Matrix Methods,' AIEE Trans., Vol. 79, Pt III, pp. 333, 1960.

El-Abiad, A.H., Stagg, G.W., 'Automatic Evaluation of Power System Performance--Effects of Line and Transformer Outages,' AIEE Trans. on PAS, Vol. PAS-81, pp. 712-716, 1962.

Elgerd, O.I., Electric Energy System Theory, An Introduction, McGraw-Hill, 1982.

Enns, M.K., Quada, J.J., Sackett, B., 'Fast Linear Contingency Analysis,' IEEE Trans. on PAS, Vol. PAS-101, No. 4, pp. 783-791, April 1982.

Erisman, A.M., Neves, K.W., Dwarakanath, M.H., ed. Electric Power Problems : The Mathematical Challenge, SIAM, 1980.

Farghal, S.A., Tantawy, M.A., Abou Hussien, M.S., Hassan, S.A., Abu Elela, A.A., 'Fast Technique for Power System Security Assessment Using Sensitivity Parameters of Linear Programming,' IEEE Trans. on PAS, Vol. PAS-103, No. 5, pp. 946-953, May 1984.

Fischl, R., Ejebe, G.C., Demaio, J.A., 'Identification of Power System Steady-state Security Regions under Load Uncertainty,' Paper no. A 76 495-2, IEEE Power Summer Meeting, Portland, OR., July 1976.

Galiana, F.D., Schweppe, F.C., Glavitsch, H., 'Synthesis of Security Monitoring Schemes in Power Systems,' IFAC/IFIP Conference Proc., Zurich, March 1974.

Galiana, F.D., Glavitsch, H., Fiechter, A., 'A General Compensation Method for the Study of Line Outages in Load Flow Problems,' PSCC Conference Proc., London, September 1975.

Galiana, F.D., 'Bound Estimates of the Severity of Line Outages in Power System Contingency Analysis and Ranking,' Paper no. 84 WM 043-6, IEEE Winter Power Meeting, Dallas, Texas, January 1984.

George, A., Liu, J.W., Computer Solution of Large Sparse Positive Definite Systems, Prentice-Hall, 1981.

Hajdu, L.P., Podmore, R., 'Security Enhancement for Power Systems,' System Engineering for Power : Status and Prospects Conference Proc., Henniker, New Hampshire, pp. 177-195, August 1975.

Hakimashhadi, H., Heydt, G.T., 'Fast Transient Security Assessment,' IEEE Trans. on PAS, Vol. PAS-102, No. 12, pp. 3816-3824, December 1983.

Halpin, T.F., 'Contingency Selection Theory for Steady-state Security Assessment of Power Systems,' Ph.D. Thesis, Drexel University, Philadelphia, P.A., 1982.

Halpin, T.F., Fischl, R., Fink, R., 'Analysis of Automatic Contingency Selection Algorithms,' IEEE Trans. on PAS, Vol. PAS-103, No. 5, pp. 938-945, May 1984.

Handschin, E., ed. Real-time Control of Electric Power Systems, Elsevier Publishing Company, 1972.

Hanson, S.O., Bose, A., 'Input-output Processing of On-line Contingency Analysis,' PICA Conference Proc., pp. 58-63, 1979.

Hinkel, R.O., Keglovitz, F.J., Daumer, M.F., 'Security Monitoring and Security Analysis for Pennsylvania Power and Light Company's Power Control Center,' PICA Conference Proc., Toronto, Ontario, Canada, pp. 83-86, May 1977.

Hnyilicza, E., Lee, S.I.Y., Schweppe, F.C., 'Steady-state Security Regions : Set-theoretic Approach,' PICA Conference Proc., pp. 347-355, 1975.

'IEEE Reliability Test System,' IEEE Trans. on PAS, Vol. PAS-98, No. 6, pp. 2047-2055, November/December 1979.

Ilic-Spong, M., Thorp, J.S., Schulz, D., 'Existence and Uniqueness of a Solution to the Reactive Power Problem for an Electric Power Network,' International Symposium on Circuits and Systems Proc., Montreal, Quebec, Canada, May 1984.

Irisarri, G., Levner, D., Sasson, A.M., 'Automatic Contingency Selection for On-line Security Analysis--- Real-time Test,' IEEE Trans. on PAS, Vol. PAS-98, No. 5, pp. 1552-1559, September/October 1979.

Irisarri, G.D., Sasson, A.M., 'An Automatic Contingency Selection Method for On-line Security Analysis,' IEEE Trans. on PAS, Vol. PAS-100, No. 4, pp. 1838-1844, April 1981.

Kamagai, S., Wu, F.F., 'Existence of Solutions of Decoupled Power Flow Equations with Security Constraints,' ISCS Proc., pp. 63-65, 1980.

Kaye, R.J., Wu, F.F., 'Analysis of Linearized Decoupled Power Flow Approximations for Steady State Security Assessment,' Memorandum No. UCB/ERL M82/71, Electronics Research Lab., College of Engineering, University of California, Berkeley, CA., November 1982.

Khu, K.T., Lauby, M.G., Bowen, D.W., 'A Fast Linearization Method to Evaluate The Effects of Circuit Contingencies Upon System Load-bus Voltages,' IEEE Trans. on PAS, Vol. PAS-101, No. 10, pp. 3926-3932, October 1982.

Lauby, M.G., Mikolinnas, T.A., Reppen, N.D., 'Contingency Selection of Branch Outages Causing Voltage Problems,' IEEE Trans. on PAS, Vol. PAS-102, No. 12, pp. 3899-3904, December 1983.

Limmer, H.C., 'Techniques and Applications of Security Calculations Applied to Dispatching Computers,' PSCC Proc., Rome, Italy, 1969.

Ma., K.T., Kusic, G.L., 'Tie Line Contingency Studies Based Upon Partial Information,' IEEE Trans. on PAS, Vol. PAS-102, No. 6, pp. 1838-1842, June 1983.

MacArthur, C.A., 'Transmission Limitations Computed by Superposition,' AIEE Trans. on PAS, Vol. 57, pp. 827-831, December 1961.

Mamandur, K.R.C., Berg, G.J., 'Efficient Simulation of Line and Transformer Outages in Power Systems,' IEEE Trans. on PAS, Vol. PAS-101, No. 10, October 1982.

Mescua, J., Fischl, R., 'On the Determination of a Secure Voltage Profile for an Electric Power System,' International Symposium on Circuits and Systems Proc., 80CH1564-4, Vol. 3 of 3, April 1980.

Medicherla, T.K.P., Rastogi, S.C., 'A Voltage-criterion Based Contingency Selection Technique,' IEEE Trans. on PAS, Vol. PAS-101, No. 9, pp. 3523-3531, September 1982.

Mikolinnas, T.A., Wollenberg, B.F., 'An Advanced Contingency Selection Algorithm,' IEEE Trans. on PAS, Vol. PAS-100, No. 2, pp. 608-617, February 1981.

Pai, M.A., Computer Techniques in Power System Analysis, Tata McGraw-Hill.

Pang, C.K., Prabhakara, F.S., El-Abiad, A.H., Koivo, A.J., 'Security Evaluation in Power Systems Using Pattern Recognition,' IEEE Trans. on PAS, Vol. PAS-93, pp. 969-976, May/June 1974.

Peterson, N.M., Tinney, W.F., Bree, D.W., 'Iterative Linear AC Power Flow Solution for Fast Approximate Outage Studies,' IEEE Trans. on PAS, Vol. PAS-91, pp. 2048-2056, September/October, 1972.

Sachdev, M.S., Ibrahim, S.A., 'A Fast Approximate Technique for Outage Studies in Power System Planning and Operation,' IEEE Trans. on PAS, Vol. PAS-93, pp. 1133-1142, 1974.

Stagg, G.W., El-Abiad, A.H., Computer Methods in Power System Analysis, McGraw-Hill, 1968.

Stott, B., 'Decoupled Newton Load Flow,' IEEE Trans. on PAS, Vol. PAS-91, pp. 1955-1957, September/October 1972.

Stott, B., Alsac, O., 'Fast Decoupled Load Flow,' IEEE Trans. on PAS, Vol. PAS-93, pp. 859-869, May/June 1974.

Stott, B., 'Review of Load-flow Calculation Methods,' IEEE Proc., Vol. 62, No. 7, pp. 916-929, July 1974.

Subramanian, A.K., Wilbur, J., 'Power System Security Functions of the Energy Control Center at the Orange and Rockland Utilities,' IEEE Trans. on PAS, Vol. PAS-102, No. 12, pp. 3825-3834, December 1983.

Sullivan, R.L., Power System Planning, McGraw-Hill, 1977.

Tinney, W.F., Hart, C.E., 'Power Flow Solution by Newton's Method,' IEEE Trans. on PAS, Vol. PAS-86, No. 11, pp. 1449-1460, November 1967.

Tinney, W.F., 'Compensation Methods for Network Solutions by Optimally Ordered Triangular Factorization,' IEEE Trans. on PAS, Vol. PAS-91, No. 1, pp. 123-127, January/February 1972.

Uemura, K., 'Power Flow Solution by a Z-matrix Type Method and Its Application to Contingency Evaluation,' PICA Conference Proc., Boston, Mass., pp. 386-390, May 1971.

Uemura, K., Matsuki, J., 'Contingency Evaluation Methods of Power Systems by Partial Correction of Z-matrix,' PICA Conference Proc., Minneapolis, Minnesota, pp. 397-401, June 1973.

Vemuri, S., Usher, R.E., 'On-line Automatic Contingency Selection Algorithms,' IEEE Trans. on PAS, Vol. PAS-102, No. 2, pp. 346-354, February 1983.

Wasley, R.G., Daneshdoost, M., 'Identification and Ranking of Critical Contingencies in Dependent Variable Space,' IEEE Trans. on PAS, Vol. PAS-102, No. 4, pp. 881-892, April 1983.

Wood, A.J., Wollenberg, B.F., Power Generation Operation and Control,
John Wiley and Sons, 1984.

Zaborszky, J., Whang, K.W., Prasad, K., 'Fast Contingency Evaluation
Using Concentric Relaxation,' IEEE Trans. on PAS, Vol. PAS-99,
No. 1, pp. 28-36, January/February 1980.

APPENDIX A

DERIVATION OF A DC LOAD FLOW MODEL

The following assumptions are required in order to derive the DC load flow model, i.e.,

(Assum. A.1) All branch resistances are neglected.

(Assum. A.2) Bus voltage magnitudes are all unity.

(Assum. A.3) The bus phase angle difference between the ending buses of a branch are relatively small, hence :

$$\sin(\delta_i - \delta_j) \approx \delta_i - \delta_j \quad (A.1)$$

(Assum. A.4) All reactive powers are neglected.

The DC load flow model is now derived from the full AC model. It is commonly known that the net complex power injection (S_i) at bus i can be expressed in terms of the bus voltage (V_i) and the bus current injection (I_i), i.e.,

$$S_i = V_i I_i^* \quad (A.2)$$

or

$$S_i^* = V_i^* I_i \quad (A.3)$$

where * denotes the conjugate value. From the nodal equations of the network, i.e.,

$$\underline{I} = \underline{Y} \underline{V} \quad (\text{A.4})$$

where :

\underline{I} \triangleq bus current injection vector.

\underline{V} \triangleq bus voltage vector.

\underline{Y} \triangleq admittance matrix.

hence, (A.3) can be expressed in terms of (A.4), i.e.,

$$S_i^* = V_i^* \sum_{j=1}^{n+1} Y_{ij} V_j \quad (\text{A.5})$$

where :

Y_{ij} \triangleq the admittance of the branch connecting buses i and j.

$n+1$ \triangleq total number of buses in the system.

Using the polar form, (A.5) can be expanded into the real and reactive parts :

$$S_i^* = P_i - jQ_i \quad (\text{A.6})$$

where :

$$P_i = \sum_{j=1}^{n+1} |V_i Y_{ij} V_j| \cos (\theta_{ij} - \delta_i + \delta_j) \quad (\text{A.7})$$

$$Q_i = - \sum_{j=1}^{n+1} |V_i Y_{ij} V_j| \sin (\theta_{ij} - \delta_i + \delta_j) \quad (\text{A.8})$$

From (Assum. A.4), (A.4) is neglected in the following. Also from the assumptions, i.e. (Assum. A.1) and (Assum. A.3), the trigonometric function in (A.7) can be approximated as follows, i.e.,

$$\begin{aligned} \cos(\theta_{ij} - \delta_i + \delta_j) &= \sin(\delta_i - \delta_j) \\ &= (\delta_i - \delta_j) \end{aligned} \quad (\text{A.9})$$

If the admittance Y_{ij} is replaced by the susceptance B_{ij} and (A.9) is substituted into (A.7), the net real power injection at bus i can be expressed as :

$$P_i = \sum_{j=1}^{n+1} B_{ij} (\delta_i - \delta_j) \quad (\text{A.10})$$

or in a matrix form :

$$\underline{P}' = \underline{B}' \underline{\delta}' \quad (\text{A.11})$$

where :

$$B'_{ii} \triangleq \sum_{j=1}^{n+1} \frac{1}{B_{ij}}$$

$$B'_{ij} \triangleq -\frac{1}{B_{ij}}$$

$$\underline{P}' \triangleq [P_1, P_2, \dots, P_{n+1}]^T$$

$$\underline{\delta}' \triangleq [\delta_1, \delta_2, \dots, \delta_{n+1}]^T$$

However, \underline{B}' in (A.11) is singular, therefore the row and column corresponding to the reference bus, denoted as the $(n+1)^{\text{th}}$

bus, are deleted from (A.11). Finally, the DC load flow model can be expressed as follows, i.e.,

$$\underline{P} = \underline{B} \underline{\delta} \quad (\text{A.12})$$

where :

$$\underline{P} \triangleq [P_1, P_2, \dots, P_n]^T$$

$$\underline{\delta} \triangleq [\delta_1, \delta_2, \dots, \delta_n]^T$$

$\underline{B} \triangleq$ 'DC load flow Jacobian; its elements are the same as \underline{B}' defined in (A.11) but the $(n+1)^{\text{th}}$ row and column are deleted.

$$\delta_{n+1} = 0$$

It should be reminded here that the P_i used above is indeed the following :

$$P_i = P_{gi} - P_{di} \quad (\text{A.13})$$

where :

$P_{gi} \triangleq$ net real power generation at bus i .

$P_{di} \triangleq$ net real power demand at bus i .

APPENDIX B

DATA OF FIVE IEEE TESTING SYSTEMS

The following pages display the system data of the five IEEE testing systems used in this study, i.e., 14, 24, 30, 57, 118 - bus systems. Each one of these systems is stored as a separate file in the MUSIC A system at McGill. The interpretations of the numbers in each file are as follows, i.e.,

- (1) Line # 1 : total number of buses (NB), total number of lines (NL), slack bus number, optional variable (no significance in this research).
- (2) Line # 2 to line # $NL + 1$:
Line number from bus-to-bus Resistance (p.u.) ,
Reactance (p.u.) , Rating (p.u.) .
- (3) Line # $(NL + 2)$ to $*(NL + NB + 2)$:
Bus number Real Power Injection (MW)
(+ve = generation, -ve = load) .
- (4) Note that all parallel lines are replaced by their equivalent models.
- (5) All ratings are calculated based on $1/5$ of the reciprocal of the impedance value of the line except those whose ratings are already given in the references.

IEEE 14-BUS

DISPLAY WCD14A

*IN PROGRESS

0001	14	20	1	0			
0002	1	1	2		0.01938	0.05917	3.38009
0003	2	2	3		0.04699	0.19797	1.01025
0004	3	2	4		0.05811	0.17632	1.13430
0005	4	1	5		0.05403	0.22304	0.89670
0006	5	2	5		0.05695	0.17388	1.15022
0007	6	3	4		0.06701	0.17103	1.16939
0008	7	4	5		0.01335	0.04211	4.74947
0009	8	5	6		0.00000	0.25202	0.79359
0010	9	4	7		0.00000	0.20912	0.95639
0011	10	7	8		0.00000	0.17615	1.13540
0012	11	4	9		0.00000	0.55618	0.35960
0013	12	7	9		0.00000	0.11001	1.81802
0014	13	9	10		0.03181	0.08450	2.36686
0015	14	6	11		0.09498	0.19890	1.00553
0016	15	6	12		0.12291	0.25581	0.78183
0017	16	6	13		0.06615	0.13027	1.53527
0018	17	9	14		0.12711	0.27038	0.73970
0019	18	10	11		0.08205	0.19207	1.04129
0020	19	12	13		0.22092	0.19988	1.00060
0021	20	13	14		0.17093	0.34802	0.57468
0022			1		1.00000		
0023			2		232.39990		
0024			3		2.00000		
0025			4		18.30000		
0026			5		3.00000		
0027			6		-94.20000		
0028			7		4.00000		
0029			8		-47.80000		
0030			9		5.00000		
0031			10		-7.60000		
0032			11		6.00000		
0033			12		-11.20000		
0034			13		7.00000		
0035			14		0.00000		

*END

*GO

IEEE 24-BUS

DISPLAY WCD24A

*IN PROGRESS

0001	24	34	1	1			
0002	1	1	2		0.00260	0.01390	2.00000
0003	2	1	3		0.05460	0.21120	2.20000
0004	3	1	5		0.02180	0.08450	2.20000
0005	4	2	4		0.03280	0.12670	2.20000
0006	5	2	6		0.04970	0.19200	2.20000
0007	6	3	9		0.03080	0.11900	2.20000
0008	7	3	24		0.00230	0.08390	6.00000
0009	8	4	9		0.02680	0.10370	2.20000
0010	9	5	10		0.02280	0.08830	2.20000
0011	10	6	10		0.01390	0.06050	2.00000
0012	11	7	8		0.01590	0.06140	2.20000
0013	12	8	9		0.04270	0.16510	2.20000
0014	13	8	10		0.04270	0.16510	2.20000
0015	14	9	11		0.00230	0.08390	6.00000
0016	15	9	12		0.00230	0.08390	6.00000
0017	16	10	11		0.00230	0.08390	6.00000
0018	17	10	12		0.00230	0.08390	6.00000
0019	18	11	13		0.00610	0.04760	6.25000
0020	19	11	14		0.00540	0.04180	6.25000
0021	20	12	13		0.00610	0.04760	6.25000
0022	21	12	23		0.01240	0.09660	6.25000
0023	22	13	23		0.01110	0.08650	6.25000
0024	23	14	16		0.00500	0.03890	6.25000
0025	24	15	16		0.00220	0.01730	6.25000
0026	25	15	21		0.00320	0.02450	12.50000
0027	26	15	24		0.00670	0.05190	6.25000
0028	27	16	17		0.00330	0.02590	6.25000
0029	28	16	19		0.00300	0.02310	6.25000
0030	29	17	18		0.00180	0.01440	6.25000
0031	30	17	22		0.01350	0.10530	6.25000
0032	31	18	21		0.00170	0.01300	12.50000
0033	32	19	20		0.00260	0.01980	12.50000
0034	33	20	23		0.00140	0.01080	12.50000
0035	34	21	22		0.00870	0.06780	6.25000
0036			1			42.00000	
0037			2			53.00000	
0038			3			-180.00000	
0039			4			-74.00000	
0040			5			-71.00000	
0041			6			-136.00000	
0042			7			125.00000	
0043			8			-171.00000	
0044			9			-175.00000	
0045			10			-195.00000	
0046			11			0.00000	

0047	12	0.00000
0048	13	235.00000
0049	14	-194.00000
0050	15	-167.00000
0051	16	0.00000
0052	17	0.00000
0053	18	-33.00000
0054	19	-181.00000
0055	20	-128.00000
0056	21	400.00000
0057	22	300.00000
0058	23	550.00000
0059	24	0.00000
*END		

*60

IEEE 30-BUS

DISPLAY WCD30A

*IN PROGRESS

0001	30	41	1	0			
0002	1	1	2		0.01920	0.05750	1.3
0003	2	1	3		0.04520	0.18520	1.3
0004	3	2	4		0.05700	0.17370	0.65
0005	4	3	4		0.01320	0.03790	1.3
0006	5	2	5		0.04720	0.19830	1.3
0007	6	2	6		0.05810	0.17630	0.65
0008	7	4	6		0.11900	0.04140	0.9
0009	8	5	7		0.04600	0.11600	0.7
0010	9	6	7		0.02670	0.08200	1.3
0011	10	6	8		0.01200	0.04200	0.32
0012	11	6	9		0.00000	0.20800	0.65
0013	12	6	10		0.00000	0.55600	0.32
0014	13	9	11		0.00000	0.20800	0.65
0015	14	9	10		0.00000	0.11000	0.65
0016	15	4	12		0.00000	0.25600	0.65
0017	16	12	13		0.00000	0.14000	0.65
0018	17	12	14		0.12310	0.25590	0.32
0019	18	12	15		0.06620	0.13040	0.32
0020	19	12	16		0.09450	0.19870	0.32
0021	20	14	15		0.22100	0.19970	0.16
0022	21	16	17		0.08240	0.19320	0.16
0023	22	15	18		0.10700	0.21850	0.16
0024	23	18	19		0.06390	0.12920	0.16
0025	24	19	20		0.03400	0.06800	0.32
0026	25	10	20		0.09360	0.20900	0.32
0027	26	10	17		0.03240	0.08450	0.32
0028	27	10	21		0.03480	0.07490	0.32
0029	28	10	22		0.07270	0.14990	0.32
0030	29	21	22		0.01160	0.02360	0.32
0031	30	15	23		0.10000	0.20200	0.16
0032	31	22	24		0.11500	0.17900	0.16
0033	32	23	24		0.13200	0.27000	0.16
0034	33	24	25		0.18850	0.32920	0.16
0035	34	25	26		0.25440	0.38000	0.16
0036	35	25	27		0.10930	0.20870	0.16
0037	36	28	27		0.00000	0.39600	0.65
0038	37	27	29		0.21980	0.41530	0.16
0039	38	27	30		0.32020	0.60270	0.16
0040	39	29	30		0.23990	0.45330	0.16
0041	40	8	28		0.06360	0.20000	0.32
0042	41	6	28		0.01690	0.05990	0.32
0043			1		140.00000		
0044			2		27.14000		
0045			3		-2.40000		
0046			4		-7.60000		
0047			5		-72.69000		

0048	6	0.00000
0049	7	-22.80000
0050	8	-7.85000
0051	9	0.00000
0052	10	-5.80000
0053	11	12.14000
0054	12	-11.20000
0055	13	12.00000
0056	14	-6.20000
0057	15	-8.20000
0058	16	-3.50000
0059	17	-9.00000
0060	18	-3.20000
0061	19	-9.50000
0062	20	-2.20000
0063	21	-17.50000
0064	22	0.00000
0065	23	-3.20000
0066	24	-8.70000
0067	25	0.00000
0068	26	-3.50000
0069	27	0.00000
0070	28	0.00000
0071	29	-2.40000
0072	30	-10.60000

*END

*GO

IEEE 57-BUS

DISPLAY WCD57A

*IN PROGRESS

0001	57	78	1	0			
0002	1	1	2		0.00830	0.02800	6.84831
0003	2	2	3		0.02980	0.08500	2.22044
0004	3	3	4		0.01120	0.03660	5.22530
0005	4	4	5		0.06250	0.13200	1.36940
0006	5	4	6		0.04300	0.14800	1.29769
0007	6	6	7		0.02000	0.10200	1.92414
0008	7	6	8		0.03390	0.17300	1.13449
0009	8	8	9		0.00990	0.05050	3.88642
0010	9	9	10		0.03690	0.16790	1.16342
0011	10	9	11		0.02580	0.08480	2.25637
0012	11	9	12		0.06480	0.29500	0.66218
0013	12	9	13		0.04810	0.15800	1.21095
0014	13	13	14		0.01320	0.04340	4.40888
0015	14	13	15		0.02690	0.08690	2.19857
0016	15	1	15		0.01780	0.09100	2.15693
0017	16	1	16		0.04540	0.20600	0.94812
0018	17	1	17		0.02380	0.10800	1.80846
0019	18	3	15		0.01620	0.05300	3.60877
0020	19	4	18		0.00000	0.49250	0.40609
0021	20	5	6		0.03020	0.06410	2.82255
0022	21	7	8		0.01390	0.07120	2.75694
0023	22	10	12		0.02770	0.12620	1.54794
0024	23	11	13		0.02230	0.07320	2.61365
0025	24	12	13		0.01780	0.05800	3.29652
0026	25	12	16		0.01800	0.08130	2.40186
0027	26	12	17		0.03970	0.17900	1.09081
0028	27	14	15		0.01710	0.05470	3.48976
0029	28	18	19		0.46100	0.68500	0.24222
0030	29	19	20		0.28300	0.43400	0.38601
0031	30	20	21		0.00000	0.77670	0.25750
0032	31	21	22		0.07360	0.11700	1.44692
0033	32	22	23		0.00990	0.01520	11.02552
0034	33	23	24		0.16600	0.25600	0.65550
0035	34	24	25		0.00000	1.20600	0.16584
0036	35	24	26		0.00000	0.04730	4.22833
0037	36	26	27		0.16500	0.25400	0.66031
0038	37	27	28		0.06180	0.09540	1.75951
0039	38	28	29		0.04180	0.05870	2.77539
0040	39	7	29		0.00000	0.06480	3.08642
0041	40	25	30		0.13500	0.20200	0.82318
0042	41	30	31		0.32600	0.49700	0.33649
0043	42	31	32		0.50700	0.75500	0.21992
0044	43	32	33		0.03920	0.03600	3.75780
0045	44	32	34		0.00000	0.95300	0.20986
0046	45	34	35		0.05200	0.07800	2.13346
0047	46	35	36		0.04300	0.05370	2.90721

0048	47	36	37	0.02900	0.03660	4.28298
0049	48	37	38	0.06510	0.10090	1.66558
0050	49	37	39	0.02390	0.03790	4.46364
0051	50	36	40	0.03000	0.04660	3.60870
0052	51	22	38	0.01920	0.02950	5.68216
0053	52	11	41	0.00000	0.74900	0.26702
0054	53	41	42	0.20700	0.35200	0.48977
0055	54	41	43	0.00000	0.41200	0.48544
0056	55	38	44	0.02890	0.05850	3.06517
0057	56	15	45	0.00000	0.10420	1.91939
0058	57	14	46	0.00000	0.07350	2.72109
0059	58	46	47	0.02300	0.06800	2.78612
0060	59	47	48	0.01820	0.02330	6.76460
0061	60	48	49	0.08340	0.12900	1.30198
0062	61	49	50	0.08010	0.12800	1.32453
0063	62	50	51	0.13860	0.22000	0.76917
0064	63	10	51	0.00000	0.07120	2.80899
0065	64	13	49	0.00000	0.19100	1.04712
0066	65	29	52	0.14420	0.18700	0.84695
0067	66	52	53	0.07620	0.09840	1.60701
0068	67	53	54	0.18780	0.23200	0.67005
0069	68	54	55	0.17320	0.22650	0.70143
0070	69	11	43	0.00000	0.15300	1.30719
0071	70	44	45	0.06240	0.12420	1.43891
0072	71	40	56	0.00000	1.19500	0.16736
0073	72	56	41	0.55300	0.54900	0.25666
0074	73	56	42	0.21250	0.35400	0.48440
0075	74	39	57	0.00000	1.35500	0.14760
0076	75	57	56	0.17400	0.26000	0.63928
0077	76	38	49	0.11500	0.17700	0.94752
0078	77	38	48	0.03120	0.04820	3.48330
0079	78	9	55	0.00000	0.12050	1.65975
0080			1	423.00000		
0081			2	-3.00000		
0082			3	-1.00000		
0083			4	0.00000		
0084			5	-13.00000		
0085			6	-75.00000		
0086			7	0.00000		
0087			8	300.00000		
0088			9	-121.00000		
0089			10	-5.00000		
0090			11	0.00000		
0091			12	-67.00000		
0092			13	-18.00000		
0093			14	-10.50000		
0094			15	-22.00000		
0095			16	-43.00000		
0096			17	42.00000		
0097			18	-27.20000		
0098			19	-3.30000		

0099	20	-2.30000
0100	21	0.00000
0101	22	0.00000
0102	23	-6.30000
0103	24	0.00000
0104	25	-6.30000
0105	26	0.00000
0106	27	-9.30000
0107	28	-4.60000
0108	29	-17.00000
0109	30	-3.60000
0110	31	-5.80000
0111	32	-1.60000
0112	33	-3.80000
0113	34	0.00000
0114	35	-6.00000
0115	36	0.00000
0116	37	0.00000
0117	38	-14.00000
0118	39	0.00000
0119	40	0.00000
0120	41	-6.30000
0121	42	-7.10000
0122	43	-2.00000
0123	44	-12.00000
0124	45	0.00000
0125	46	0.00000
0126	47	-29.70000
0127	48	0.00000
0128	49	-18.00000
0129	50	-21.00000
0130	51	-18.00000
0131	52	-4.90000
0132	53	-20.00000
0133	54	-4.10000
0134	55	-6.80000
0135	56	-7.60000
0136	57	-6.70000

*END

*GO

IEEE 118-BUS

DISPLAY WCD118B

*IN PROGRESS

0001	118	179	69	0			
0002	1	1	2		0.03030	0.09990	2.00000
0003	2	1	3		0.01290	0.04240	4.71000
0004	3	4	5		0.00176	0.00798	25.06000
0005	4	3	5		0.02410	0.10800	1.85000
0006	5	5	6		0.01190	0.05400	3.70000
0007	6	6	7		0.00459	0.02080	9.62000
0008	7	8	9		0.00244	0.03050	6.56000
0009	8	5	8		0.00000	0.02670	7.49000
0010	9	9	10		0.00258	0.03220	6.21000
0011	10	4	11		0.02090	0.06880	2.91000
0012	11	5	11		0.02030	0.06820	2.93000
0013	12	11	12		0.00595	0.01960	10.20000
0014	13	2	12		0.01870	0.06160	3.25000
0015	14	3	12		0.04840	0.16000	1.25000
0016	15	7	12		0.00862	0.03400	5.88000
0017	16	11	13		0.02225	0.07310	2.74000
0018	17	12	14		0.02150	0.07070	2.83000
0019	18	13	15		0.07440	0.24440	0.82000
0020	19	14	15		0.05950	0.19500	1.03000
0021	20	12	16		0.02120	0.08340	2.40000
0022	21	15	17		0.01320	0.04370	4.58000
0023	22	16	17		0.04540	0.18010	1.11000
0024	23	17	18		0.01230	0.05050	3.96000
0025	24	18	19		0.01119	0.04930	4.06000
0026	25	19	20		0.02520	0.11700	1.71000
0027	26	15	19		0.01200	0.03940	5.08000
0028	27	20	21		0.01830	0.08490	2.36000
0029	28	21	22		0.02090	0.09700	2.06000
0030	29	22	23		0.03420	0.15900	1.26000
0031	30	23	24		0.01350	0.04920	4.07000
0032	31	23	25		0.01560	0.08000	2.50000
0033	32	25	26		0.00000	0.03820	5.24000
0034	33	25	27		0.03180	0.16300	1.50536
0035	34	27	28		0.01913	0.08550	2.34000
0036	35	28	29		0.02370	0.09430	2.12000
0037	36	17	30		0.00000	0.03880	5.15000
0038	37	8	30		0.00431	0.05040	3.97000
0039	38	26	30		0.00799	0.08600	2.89451
0040	39	17	31		0.04740	0.15630	1.28000
0041	40	29	31		0.01080	0.03310	6.04000
0042	41	23	32		0.03170	0.11530	1.73000
0043	42	31	32		0.02980	0.09850	2.03000
0044	43	27	32		0.02290	0.07550	2.65000
0045	44	15	33		0.03800	0.12440	1.61000
0046	45	19	34		0.07520	0.24700	0.81000
0047	46	35	36		0.00224	0.01020	12.61000

0048	47	35	37	0.01100	0.04970	4.02000
0049	48	33	37	0.04150	0.14200	1.41000
0050	49	34	36	0.00871	0.02680	7.46000
0051	50	34	37	0.00256	0.00940	21.28000
0052	51	37	38	0.00000	0.03750	5.33000
0053	52	37	39	0.03210	0.10600	1.89000
0054	53	37	40	0.05930	0.16800	1.19000
0055	54	30	38	0.00464	0.05400	3.70000
0056	55	39	40	0.01840	0.06050	3.31000
0057	56	40	41	0.01450	0.04870	4.11000
0058	57	40	42	0.05550	0.18300	1.09000
0059	58	41	42	0.04100	0.13500	1.48000
0060	59	43	44	0.06080	0.24540	0.81000
0061	60	34	43	0.04130	0.16810	1.19000
0062	61	44	45	0.02240	0.09010	2.22000
0063	62	45	46	0.04000	0.13560	1.47000
0064	63	46	47	0.03800	0.12700	1.57000
0065	64	46	48	0.06010	0.18900	1.06000
0066	65	47	49	0.01910	0.06250	3.20000
0067	66	42	49	0.03575	0.16150	1.51140
0068	67	45	49	0.06840	0.18600	1.08000
0069	68	48	49	0.01790	0.05050	3.96000
0070	69	49	50	0.02670	0.07520	2.66000
0071	70	49	51	0.04860	0.13700	1.46000
0072	71	51	52	0.02030	0.05880	3.40000
0073	72	52	53	0.04050	0.16350	1.22000
0074	73	53	54	0.02630	0.12200	1.64000
0075	74	49	54	0.03993	0.14507	1.32921
0076	75	54	55	0.01690	0.07070	2.83000
0077	76	54	56	0.00275	0.00955	20.94000
0078	77	55	56	0.00488	0.01510	13.25000
0079	78	56	57	0.03430	0.09660	2.07000
0080	79	50	57	0.04740	0.13400	1.49000
0081	80	56	58	0.03430	0.09660	2.07000
0082	81	51	58	0.02550	0.07190	2.78000
0083	82	54	59	0.05030	0.22930	0.87222
0084	83	56	59	0.04070	0.12243	1.55021
0085	84	55	59	0.04739	0.21580	0.92678
0086	85	59	60	0.03170	0.14500	1.38000
0087	86	59	61	0.03280	0.15000	1.33000
0088	87	60	61	0.00264	0.01350	14.81000
0089	88	60	62	0.01230	0.05610	3.57000
0090	89	61	62	0.00824	0.03760	5.32000
0091	90	59	63	0.00000	0.03860	5.18000
0092	91	63	64	0.00172	0.02000	10.00000
0093	92	61	64	0.00000	0.02680	7.46000
0094	93	38	65	0.00901	0.09860	2.02840
0095	94	64	65	0.00269	0.03020	6.62000
0096	95	49	66	0.00900	0.04595	4.27140
0097	96	62	66	0.04820	0.21800	0.91743
0098	97	62	67	0.02580	0.11700	1.71000

0099	98	65	66	0.00000	0.03700	5.41000
0100	99	66	67	0.02240	0.10150	1.97000
0101	100	65	68	0.00138	0.01600	12.50000
0102	101	47	69	0.08440	0.27780	0.71994
0103	102	49	69	0.09850	0.32400	0.61728
0104	103	68	69	0.00000	0.03700	5.41000
0105	104	69	70	0.03000	0.12700	1.57480
0106	105	24	70	0.10221	0.41150	0.49000
0107	106	70	71	0.00882	0.03550	5.63000
0108	107	24	72	0.04880	0.19600	1.02000
0109	108	71	72	0.04460	0.18000	1.11000
0110	109	71	73	0.00866	0.04540	4.41000
0111	110	70	74	0.04010	0.13230	1.51000
0112	111	70	75	0.04280	0.14100	1.42000
0113	112	69	75	0.04050	0.12200	1.63934
0114	113	74	75	0.01230	0.04060	4.93000
0115	114	76	77	0.04440	0.14800	1.35000
0116	115	69	77	0.03090	0.10100	1.98000
0117	116	75	77	0.06010	0.19990	1.00000
0118	117	77	78	0.00376	0.01240	16.13000
0119	118	78	79	0.00546	0.02440	8.20000
0120	119	77	80	0.01088	0.03321	5.72323
0121	120	79	80	0.01560	0.07040	2.84000
0122	121	68	81	0.00175	0.02020	9.90000
0123	122	80	81	0.00000	0.03700	5.41000
0124	123	77	82	0.02980	0.08530	2.34000
0125	124	82	83	0.01120	0.03665	5.46000
0126	125	83	84	0.06250	0.13200	1.52000
0127	126	83	85	0.04300	0.14800	1.35000
0128	127	84	85	0.03020	0.06410	3.12000
0129	128	85	86	0.03500	0.12300	1.63000
0130	129	86	87	0.02828	0.20740	0.96000
0131	130	85	88	0.02000	0.10200	1.96000
0132	131	85	89	0.02390	0.17300	1.16279
0133	132	88	89	0.01390	0.07120	2.81000
0134	133	89	90	0.01638	0.06517	2.97640
0135	134	90	91	0.02540	0.08360	2.39000
0136	135	89	92	0.00799	0.03829	5.11291
0137	136	91	92	0.03870	0.12720	1.57233
0138	137	92	93	0.02580	0.08480	2.36000
0139	138	92	94	0.04810	0.15800	1.26582
0140	139	93	94	0.02230	0.07320	2.73000
0141	140	94	95	0.01320	0.04340	4.61000
0142	141	80	96	0.03560	0.18200	1.09890
0143	142	82	96	0.01620	0.05300	3.77000
0144	143	94	96	0.02690	0.08690	2.30000
0145	144	80	97	0.01830	0.09340	2.14000
0146	145	80	98	0.02380	0.10800	1.85000
0147	146	80	99	0.04540	0.20600	0.97087
0148	147	92	100	0.06480	0.29500	0.67797
0149	148	94	100	0.01780	0.05800	3.45000

0150	149	95	96	0.01710	0.05470	3.66000
0151	150	96	97	0.01730	0.08850	2.26000
0152	151	98	100	0.03970	0.17900	1.12000
0153	152	99	100	0.01800	0.08130	2.46000
0154	153	100	101	0.02770	0.12620	1.58000
0155	154	92	102	0.01230	0.05590	3.58000
0156	155	101	102	0.02460	0.11200	1.79000
0157	156	100	103	0.01600	0.05250	3.81000
0158	157	100	104	0.04510	0.20400	0.98039
0159	158	103	104	0.04660	0.15840	1.26000
0160	159	103	105	0.05350	0.16250	1.23000
0161	160	100	106	0.06050	0.22900	0.87336
0162	161	104	105	0.00994	0.03780	5.29000
0163	162	105	106	0.01400	0.05470	3.66000
0164	163	105	107	0.05300	0.18300	1.09000
0165	164	105	108	0.02610	0.07030	2.84000
0166	165	106	107	0.05300	0.18300	1.09000
0167	166	108	109	0.01050	0.02880	6.94000
0168	167	103	110	0.03906	0.18130	1.10314
0169	168	109	110	0.02780	0.07620	2.62000
0170	169	110	111	0.02200	0.07550	2.65000
0171	170	110	112	0.02470	0.06400	3.13000
0172	171	17	113	0.00913	0.03010	6.64000
0173	172	32	113	0.06150	0.20300	0.99000
0174	173	32	114	0.01350	0.06120	3.27000
0175	174	27	115	0.01640	0.07410	2.70000
0176	175	114	115	0.00230	0.01040	19.23000
0177	176	68	116	0.00034	0.00405	49.38000
0178	177	12	117	0.03290	0.14000	1.43000
0179	178	75	118	0.01450	0.04810	4.16000
0180	179	76	118	0.01640	0.05440	3.68000
0181			1	-51.		
0182			2	-20.		
0183			3	-39.		
0184			4	-39.		
0185			5	0.		
0186			6	-52.		
0187			7	-19.		
0188			8	-28.		
0189			9	0.		
0190			10	450.		
0191			11	-70.		
0192			12	38.		
0193			13	-34.		
0194			14	-14.		
0195			15	-90.		
0196			16	-25.		
0197			17	-11.		
0198			18	-60.		
0199			19	-45.		
0200			20	-18.		

0201	21	-14.
0202	22	-10.
0203	23	-7.
0204	24	-13.
0205	25	220.
0206	26	314.
0207	27	-71.
0208	28	-17.
0209	29	-24.
0210	30	0.
0211	31	-36.
0212	32	-59.
0213	33	-23.
0214	34	-59.
0215	35	-33.
0216	36	-31.
0217	37	0.
0218	38	0.
0219	39	-27.
0220	40	-66.
0221	41	-37.
0222	42	-96.
0223	43	-18.
0224	44	-16.
0225	45	-53.
0226	46	-9.
0227	47	-34.
0228	48	-20.
0229	49	117.
0230	50	-17.
0231	51	-17.
0232	52	-18.
0233	53	-23.
0234	54	-65.
0235	55	-63.
0236	56	-84.
0237	57	-12.
0238	58	-12.
0239	59	-122.
0240	60	-78.
0241	61	160.
0242	62	-77.
0243	63	0.
0244	64	0.
0245	65	391.
0246	66	353.
0247	67	-28.
0248	68	0.
0249	69	516.4
0250	70	-66.
0251	71	0.

0252	72	-12.
0253	73	-6.
0254	74	-68.
0255	75	-47.
0256	76	-68.
0257	77	-61.
0258	78	-71.
0259	79	-39.
0260	80	347.
0261	81	0.
0262	82	-54.
0263	83	-20.
0264	84	-11.
0265	85	-24.
0266	86	-21.
0267	87	4.
0268	88	-48.
0269	89	607.
0270	90	-163.
0271	91	-10.
0272	92	-65.
0273	93	-12.
0274	94	-30.
0275	95	-42.
0276	96	-38.
0277	97	-15.
0278	98	-34.
0279	99	-42.
0280	100	215.
0281	101	-22.
0282	102	-5.
0283	103	17.
0284	104	-38.
0285	105	-31.
0286	106	-43.
0287	107	-50.
0288	108	-2.
0289	109	-8.
0290	110	-39.
0291	111	36.
0292	112	-68.
0293	113	-6.
0294	114	-8.
0295	115	-22.
0296	116	-184.
0297	117	-20.
0298	118	-33.

*END

*GO